

https://dspace.org/

Performance of filter drains under large embankment loads

Rumpelt, Thomas Karl

2015-09-09
http://hdl.handle.net/10539/18591

Downloaded from a DSpace repository. https://dspace.org/

PERFORMANCE OF FILTER DRAINS

UNDER LARGE EMBANKMENT LOADS

THOMAS KARL RUMPELT

A dissertation submitted to the Faculty of Engineering, University of the Witwatersrand, Johannesburg, in partial fulfillmen for the Degree of Master of Science in Engineering.

Johannesburg, 1983

D E C L A R A T I O N

I, Thomas Karl Rumpelt hereby declare that this is my own unaided work and I have not submitted this dissertation to any other University for degree purposes.

T. Rumpelt

20th day of September 1983

ABSTRACT

A testing apparatus was developed for the determination of the change in permeability of coarse porous media subjected to a decrease in porosity and degradation of the grain skeleton as a result of large loads. A literature survey was conducted to establish the design criteria for the flow and loading tests. The mathematical model describing flow through coarse porous media was further developed on a theoretical basis by postulating the layered medium model. This model is a means by which the variability of the particle sizes in the medium is taken into account.

The design, construction and operation of the testing apparatus is described. The specimen tested was loaded up to 3,45 MPa; consequently the permeability of the specimen decreased considerably. Nevertheless, the Forcheimer equation in the form of $K = C_1/R + C_2$ was found to yield repeatable values for the turbulent friction factor C_2, thus providing a means of predicting the change in permeability if the change in porosity and effective particle diameter are known.

TABLE OF CONTENTS

Section	Description	Page
1	INTRODUCTION	1
2	LITERATURE REVIEW	7
	2.1 Introduction	7
	2.2 Flow equations	7
	2.2.1 Formation of concepts	7
	2.2.2 Comparison of flow equations and conclusions	20
	2.3 Mechanical properties of filter drains	25
	2.3.1 Description of the grain skeleton	25
	2.3.2 Particle forces	28
	2.3.3 Particle breakage	31
	2.3.4 Factors which influence particle breakage	32
	2.3.5 Grading and grain breakage	34
	2.3.6 Particle size and grain breakage	37
	2.3.7 Stress level and particle breakage	38
	2.3.8 Quantitative description of particle breakage	39
3	THEORETICAL DEVELOPMENT OF THE FLOW EQUATION	41
	3.1 Introduction	41
	3.2 Flow equation applied to stratified media	42
	3.3 Development of the layered model	43
	3.4 Parallel layered model	44
	3.4.1 Laminar flow	45
	3.4.2 Turbulent flow	46
	3.4.3 Transitional flow	47
	3.5 Series layered model	48
	3.5.1 Laminar flow	49
	3.5.2 Turbulent flow	50

TABLE OF CONTENTS (Cont.)

Section	Description	Page
	3.5.3 Transitional flow	51
	3.6 Application of effective particle diameter equations	52
	3.6.1 Effect of grading on permeability	53
	3.6.2 Vector notation applied to layered media	56
	3.6.3 Randomly layered model	61
4	DESIGN AND CONSTRUCTION OF EQUIPMENT	64
	4.1 Introduction	64
	4.2 Design criteria	65
	4.2.1 General	65
	4.2.2 Testing cylinder as loading cylinder	66
	4.2.3 Testing cylinder as permeameter	67
	4.3 Design and construction	68
	4.3.1 Equipment required for flow tests	68
	4.3.2 Equipment required for loading tests	73
	4.4 Cylinder wall effects	76
	4.4.1 Introduction	76
	4.4.2 Hydraulic considerations	76
	4.4.3 Mechanical considerations	79
	4.4.4 Possible solutions	80
5	EXPERIMENTAL PROCEDURE	82
	5.1 Introduction	82
	5.2 Sample preparation	83
	5.3 Calibration of measuring instruments	84
	5.4 Flow tests	84
	5.5 Loading tests	86
6	TEST RESULTS	91
	6.1 Introduction	91
	6.2 Sample properties	91
	6.3 Particle size analysis	92
	6.4 Porosities	95

TABLE OF CONTENTS (Cont.)

Section	Description	Page
	6.5 Flow tests	100
	6.6 Suitability of lining	108
	6.7 Conclusions	109
7	CONCLUSIONS	111
	7.1 Literature review	111
	7.2 Theoretical development of the flow equation	111
	7.3 Experimental procedure	112
	7.4 Test results	113
	7.5 Design and construction of equipment	114
	7.6 Practical considerations	115
8	REFERENCES	116

TABLE OF CONTENTS (Cont.)

APPENDICES		PAGE
A	Estimation of magnitude of wall effects	120
B	Griffith criterion for failure of brittle materials applied to cylinders and spheres	122
C	Schedule of equipment items and working drawing of equipment	126
D	Calibration curves	135
E	HP 41C listings of programs	138

LIST OF FIGURES

Figure No	Description	Page
CHAPTER 1		
1.1	Illustration of drains in dams and tailings dams	1
1.2	Consequences of decrease in effective drainage	2
1.3	Alternatives to graded gravel filters under large embankments	4
CHAPTER 2		
2.1	Determination of exponent b from flow tests	13
2.2	Plot of friction factor vs Reynolds number for various roughness values	16
2.3	Models of porous media with voids	18
2.4	Definition of stone shape and size	19
2.5	Friction factor vs Reynolds number generalised plot	26
2.6	Structurally idle particles	27
2.7	Movement of particles relative to interparticle friction	30
2.8	Comparison of degree of grain breakage for different failure conditions	34
2.9	Degradation of filter and soil under load	35
2.10	Degradation of single sized rock under progressively increasing stress compared with degradation of graded rock	36
2.11	Particle breakage as a function of grain diameter	37
2.12	Comparison of crushing of soils with different initial grain size	38
2.13	Changes in porosity and particle size under progressively increasing stress for single sized and graded rock	38
2.14	Relative crushing of gravels at various stress levels	39
CHAPTER 3		
3.1	Orthogonal components of the hydraulic gradient vector in stratified media	42
3.2	Parallel layered model	44
3.3	Series layered model	48

LIST OF FIGURES (Cont.)

Figure No	Description	Page
	CHAPTER 3	
3.4	Grading curves for various rockfill samples	54
3.5	Flow through inclined layers	58
3.6	Variation of flow velocity and effective particle diameter	60
3.7	Variation of effective particle diameter	62
	CHAPTER 4	
4.1	Flow test circuit diagram	69
4.2	Cylinder during flow test	70
4.3	Suggested alternative piezometer tap	71
4.4	Piezometer tubes on mounting board	73
4.5	Cylinder during load test	75
4.6	Velocity distribution across an unlined permeameter	77
	CHAPTER 5	
5.1	Flow test set-up	85
5.2	Manoeuvering cylinder in and out of press	88
5.3	Load test set-up	90
	CHAPTER 6	
6.1	Grading curves of sample before and after loading	93
6.2a	Change in effective particle diameter - parallel layer model	94
6.2b	Change in effective particle diameter - series layer model	94
6.3	Plot of load and pressure vs deflection and porosity for load test No 1	96
6.4	Plot of load vs deflection for both load tests	97
6.5	Comparison of changes in porosity	99
6.6	Test No 1: plot of velocity against hydraulic gradient	101

LIST OF FIGURES (Cont.)

Figure No	Description	Page
6.7	Test No. 2: Plot of velocity against hydraulic gradient	102
6.8	Test No. 3: Plot of velocity against hydraulic gradient	103
6.9	Test No. 1: Plot of friction factors	105
6.10	Test No. 2: Plot of friction factors	106
6.11	Test No. 3: Plot of friction factors	107
APPENDIX A		
A1	Definition of cross sectional areas in an unlined permeameter	120
APPENDIX B		
B1	(a) Cylinder compressed between concentrated line loads	
	(b) Stress distribution on loaded diameter	123
B2	Typical fractures resulting from loading shown i Figure B1	123
B3	(a) Cylinder compressed by diametral load p distributed over arc 2	124
	(b) Stress distribution on loaded diameter	124
APPENDIX C		
C1	Layout of pipes to permeameter	128
C2	Details of loading plates and pedestal	129
C3	Details of loading plates and pedestal	130
C4	Detail of screen and supporting frame	131
C5	Manometer board and fittings	132
C6	Tee square for manometr board	133
C7	Details and application of lifting harness at Macklow-Smith press	134

LIST OF TABLES

Table No	Description	Page
2.1	Data from previous investigations	24
3.1	Equations for the particle diameter	52
3.2	Comparison of effective particle diameters	53
3.3	Expressions f(d) for equation 3.20	57
3.4	Results of simplified calculation of effective particle diameter for the random model	63
5.1	Physical properties of rockfill tested	83
6.1	Sample description	92
6.2	Effective particle diameters of crushed material	92
6.3	Deflection (after rebound) and porosities of sample for the flow tests	99

PREFACE AND ACKOWLEDGEMENTS

Preliminary investigations into the effect of large loads on the permeability of rockfill were undertaken by Blight and Caldwell (1980) for the design of the stone underdrainage required for a 300 m high tailings impoundment at Mt. Tolman Mine in Washington State USA.

The purpose of the present investigational project was to design and test a permeameter which could double as a oedometer so that both the flow and loading characteristics of rockfill could be investigated without disturbing the sample.

A literature survey on flow through rockfill and particle breakage under loads was undertaken and submitted to the University as part of the proposal for this project. Stephenson (1979) had done previous research and correlation of results available in the literature on the flow behaviour through rockfill. Further theoretical development of the flow equation was undertaken under the guidance of Professor Stephenson, leading to the publication of a co-authored paper entitled "Stratification of Rockfill Embankments and the effect on Permeability".

I would like to express my appreciation to the following people and institutions.

My supervisors, Professor G E Blight and Professor D Stephenson, whose assistance, inspiration and advice I gratefully acknowledge.

The academic and workshop staff of the Civil Engineering Department, particularly Vincent Newey and Charley Cooper, whose constructive criticisms, advice and ideas I appreciated.

The University of the Witwatersrand and the Council for Scientific and Industrial Research whose financial support I acknowledge with thanks.

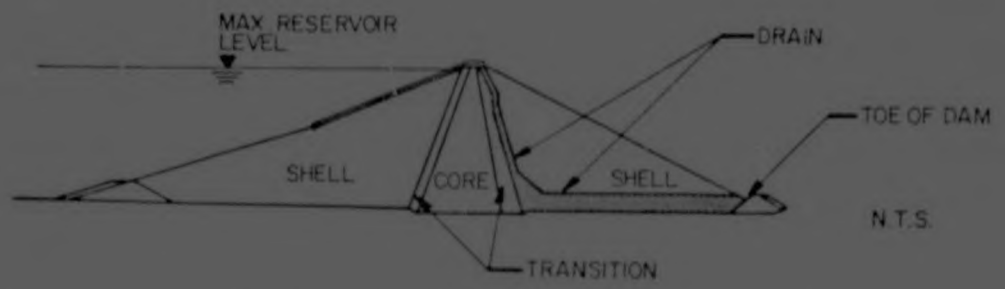
Steffen, Robertson and Kirsten Inc for their assistance in the preparation of this dissertation, in particular Gordon McPhail, who saw to it that it was written. A special thank you goes to Anne Melhuish and Julie Kemack for their patient typing and to Linda Woodgate for tracing the figures.

My colleagues at the University, Gary Bentel and Mark Axelrod, for their friendship, encouragement and useful discussions.

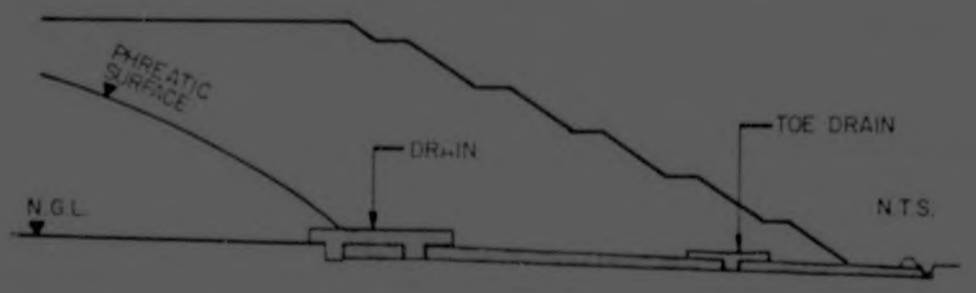
My family and Mary for the much appreciated moral support, encouragement and patience.

1 INTRODUCTION

With the construction of tailings impoundments and embankment dams to unprecedented heights the need has arisen to make use of cobbles or gravel, rather than sand, as the underdrainage medium to accommodate the large seepage quantities (Fig 1.1).



a) CROSS SECTION OF A TYPICAL ROCK OR EARTH DAM (APPROXIMATELY 300m HIGH)



b) CROSS SECTION OF A HIGH TAILINGS IMPOUNDMENT (MAXIMUM 300m HIGH)

FIGURE 1.1 ILLUSTRATION OF DRAINS IN DAMS & TAILINGS DAMS

This requirement for an efficient filter drain calls for grading and particle size distribution criteria which are in conflict with the requirements for effective load bearing capacity without excessive particle breakage. Cedergren (1977) has pointed out the inadequacy of blends of sands and gravels to function as drains and emphasises the need for highly permeable open-graded aggragates. On the other hand it has been shown (Blight and Caldwell, 1980 and Marsal, 1973) that single sized gravels will degrade more than graded gravels under the applied stresses they will have to bear under high embankments. This degradation then results in a decrease

in permeability and hence effectiveness of the drainage medium. The consequence of a loss in permeability in the drainage medium of a large embankment is that the operation and stability of the facility could be seriously affected. The phreatic surface rises in the region of the toe, reducing the stability of the embankment or dam because of the increase in water pressure within the critical failure zone. Uncontrolled seepage through the face of an earth or tailings dam may precipitate erosion, piping and subsequent local sloughing of the wall and possible overall failure of the dam. In tailings dams the loss of clear seepage water represents a substantial loss in "return" water which could otherwise be re-utilised at the plant.

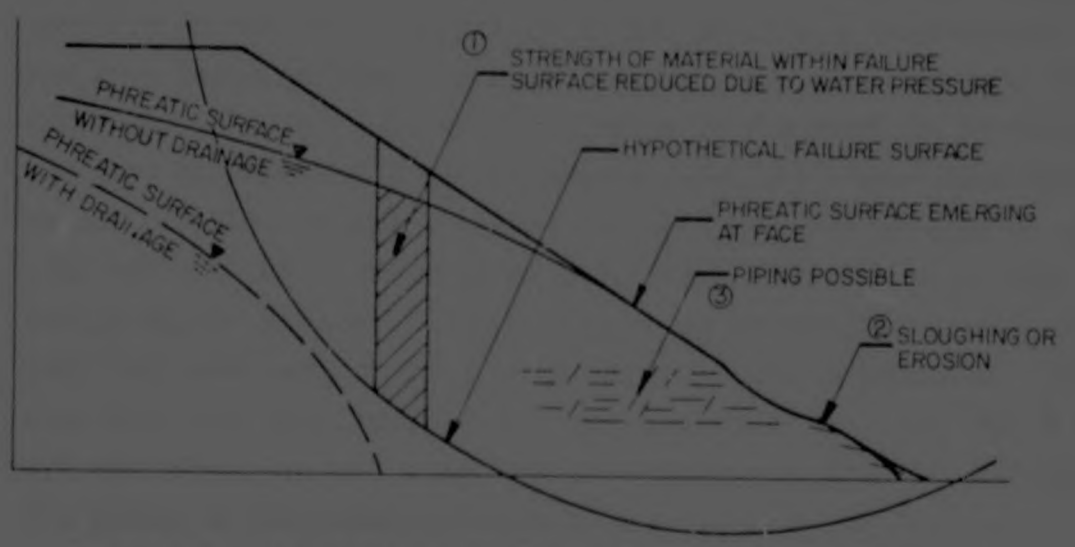


FIGURE I.2 CONSEQUENCES OF DECREASE IN EFFECTIVE DRAINAGE OF DAMS OR EMBANKMENTS: ① STRENGTH REDUCTION, ② SLOUGHING, ③ PIPING

Traditionally the flow of water through porous media has been analysed by means of the Darcy equation which is applicable to laminar flow. Research on the flow through gravel and rockfill (almost exclusively single sized) was initiated with the advent of rockfill dams and throughflow rockfill dams without spillways which were used as coffer dams. In all cases non-Darcy flow is described by means of:

. exponential formulas such as

$$v = ai^b \qquad \text{.....(1.1)}$$

in permeability and hence effectiveness of the drainage medium. The consequence of a loss in permeability in the drainage medium of a large embankment is that the operation and stability of the facility could be seriously affected. The phreatic surface rises in the region of the toe, reducing the stability of the embankment or dam because of the increase in water pressure within the critical failure zone. Uncontrolled seepage through the face of an earth or tailings dam may precipitate erosion, piping and subsequent local sloughing of the wall and possible overall failure of the dam. In tailings dams the loss of clear seepage water represents a substantial loss in "return" water which could otherwise be re-utilised at the plant.

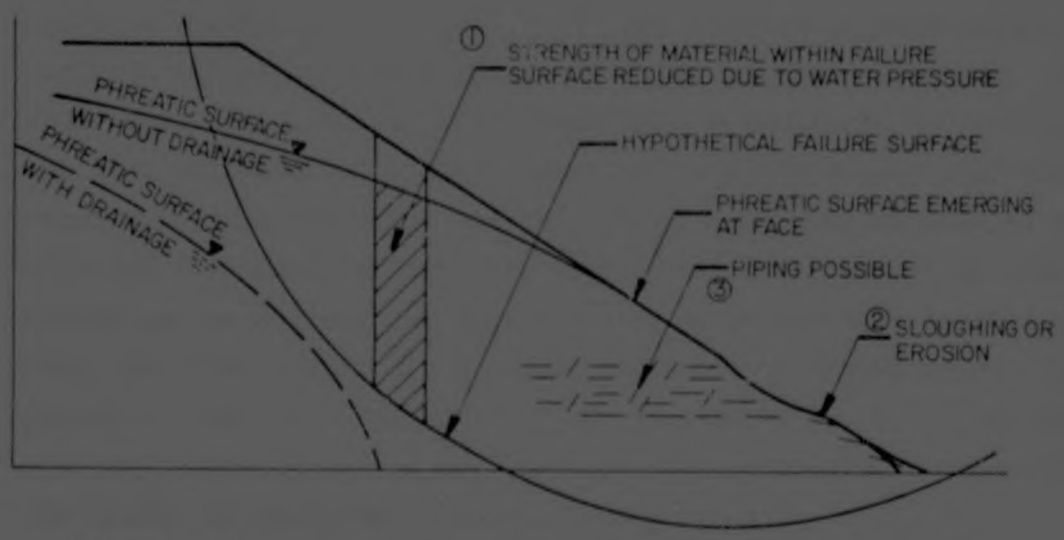


FIGURE I.2 CONSEQUENCES OF DECREASE IN EFFECTIVE DRAINAGE OF DAMS OR EMBANKMENTS: ① STRENGTH REDUCTION, ② SLOUGHING, ③ PIPING

Traditionally the flow of water through porous media has been analysed by means of the Darcy equation which is applicable to laminar flow. Research on the flow through gravel and rockfill (almost exclusively single sized) was initiated with the advent of rockfill dams and throughflow rockfill dams without spillways which were used as coffer dams. In all cases non-Darcy flow is described by means of:

. exponential formulas such as

$$v = ai^b \qquad \text{.....(1.1)}$$

. or the Forcheimer equation and modifications in the form of

$$i = c\,v + d\,v^2 + \ldots\ldots \qquad \ldots\ldots(1.2)$$

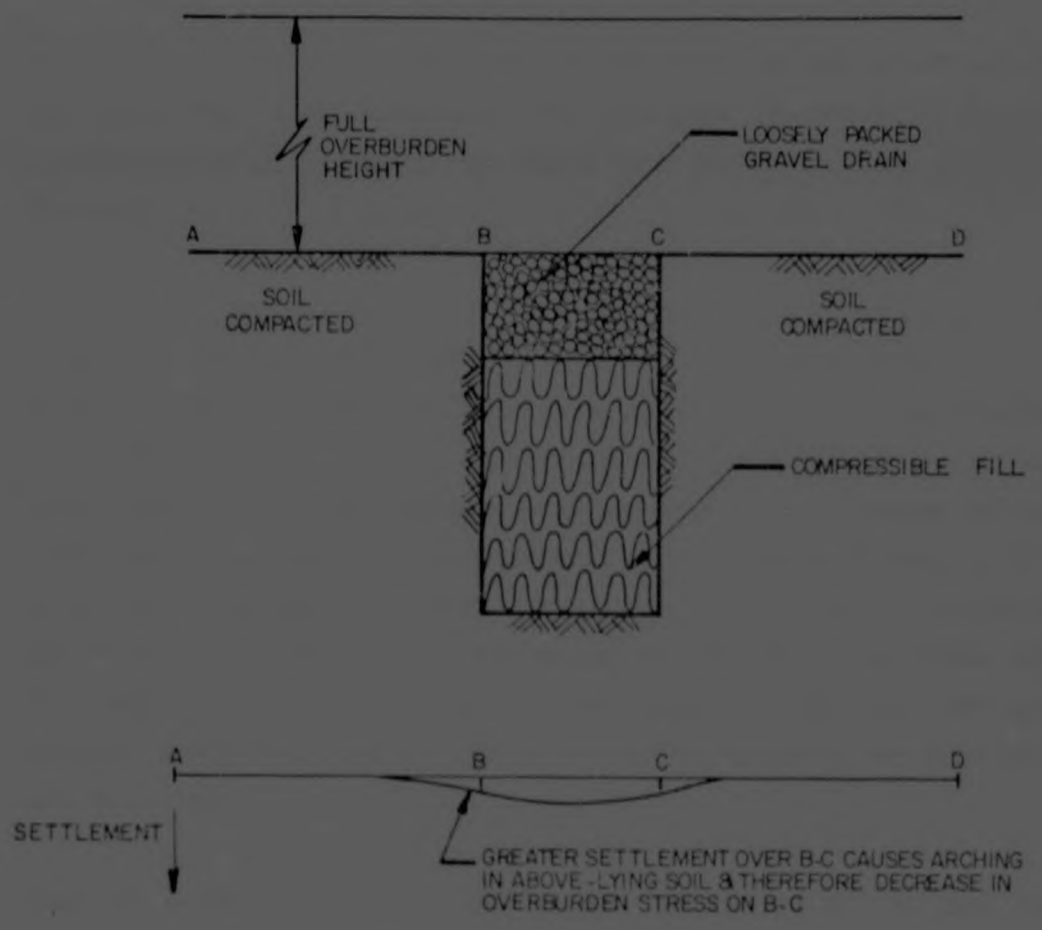
where v = average seepage velocity
i = hydraulic gradient
a,b,c,d = empirical constants

Difficulties and differences arise in defining the pertinent parameters required to describe the flow through rockfill or gravels. The empirical constants derived in numerous tests have been found to be dependent on various material properties. Because the tests were invariably undertaken with uniformly sized particles, the effect of particle grading on permeability is not positively established. It has been indicated that a graded material degrades relatively little under applied loads. It would therefore be desirable to investigate the flow behaviour of a graded material with its higher load bearing capacity. Alternatively, a single sized stone may be used to begin with and the effect of crushing under load investigated so that the drains may be designed in such a way as to be serviceable even after they had been subjected to large stresses and degradation. Where possible, the "null option" may be considered in which the drains are positioned in such a way that the overburden load is shed around the drain, or decreased altogether, see Fig 1.3.

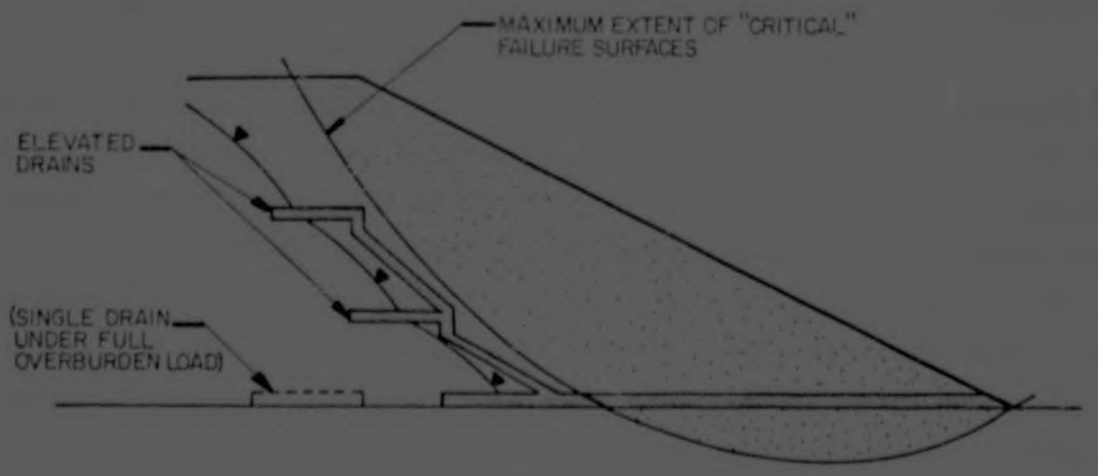
The study of flow through graded or degraded gravel will also find application in throughflow rockfill dams. As the various lifts are placed and compacted, particle crushing and layering of fines takes place.

The method of investigation and scope of this dissertation is best described by means of a summary of the following chapters:

Chapter 2 consists of a comparative literature review dealing with flow through uniformly graded rockfills and gravels, mechanics of particle breakage subject to load and the design of various testing apparatus. The most important conclusion to emerge from this review



a) SHEDDING OVERBURDEN STRESS



b) ELEVATED DRAINS OR SLOPING DRAINS

FIGURE 1.3 ALTERNATIVES TO GRADED GRAVEL FILTERS UNDER LARGE EMBANKMENTS

is that particle size and porosity are the most important parameters for both the flow equation and particle breakage. There only remains a rational means by which the particle size ought to be defined.

Chapter 3 deals with the theoretical development of a flow velocity-headloss relationship applied to graded materials. The parallel layer and series layer models are postulated as representative extreme situations of graded particle disposition. The assumption is made that the layered medium consists of layers of various sized particles parallel and perpendicular to the direction of flow. An effective particle diameter is obtained for laminar, transitional and turbulent flow. This dimension represents a weighted mean of the particle sizes by taking the layering of the medium into account. Applications of these models to randomly orientated media are discussed.

Chapter 4 describes the design and construction of the testing equipment. The criteria for testing the flow properties were partially incompatible with those for testing the amount of particle breakage under load. Because of the large particle size of the gravel used, the experiments had to be conducted on a correspondingly large scale. The permeameter, 1,8 m high and 0,6 m in diameter, can take a sample of stone weighing 186 kg. The permeameter could then double as an oedometer, though not simultaneously, with a capacity of having a load of 712 kN (or 3,45 MPa on the cross section) applied to the sample. It would have been desirable to conduct the flow tests with the simulated overburden loads applied to the specimen at the same time. However, it was found that the amount of rebound upon unloading, even after large loads, was small. Therefore, the tests were considered to be representative of simulating flow under large embankment loads. The cylinder was lined to overcome wall effects during the flow and loading tests.

The experimental procedure, which consists of calibrations, particle size analyses, repeated loading and flow tests is described in

Chapter 5. The number of tests performed was sufficient to establish that the equipment can be used to conduct a more thorough study on the particle breakage characteristics and resulting influence on the through flow characteristics of various types of rockfill or gravels.

The test results in Chapter 6 illustrate the fact that:

(i) The Forcheimer equation in its form $I = C_1/R + C_2$ provides a better means than an exponential equation of describing the flow through porous media of different particle sizes and porosities, and

(ii) it is possible to predict the reduction in throughflow characteristics of a rockfill subjected to large stresses and degradation from the change in particle size and porosity, taking the layering and arrangement of particles into account.

2 LITFRATURE REVIEW

2.1 Introduction

The effect of particle breakage or gradation on the through-flow characteristics of rockfill has to the knowledge of the author not been documented in the literature. The literature survey is therefore divided into two sections, namely the development of various flow equations for rockfill and the mechanical properties of rockfill. The latter subject was found in the literature to be approached mainly from the construction point of view: Particle breakage and compaction was investigated in order to establish design and quality control criteria for the construction of rockfill dams to the correct densities for the stability of the structures.

2.2 Flow equations

With the advent of throughflow rockfill dams approximately twenty-five years ago interest was shown in the development of flow equations for coarse porous media. It was recognised that the Darcy equation was of limited use as it applied to laminar flow only. This lead to the derivation of equations of an empirical and semi-empirical nature. Often it was engineering judgement rather than theoretical deduction which influenced the choice of parameters and eventual forms of various flow equations. In almost all instances single sized rock or cobbles were used, and comparisons were drawn in many cases with ideal particles, such as cubes or spheres.

2.2.1 Formation of concepts

Traditionally Darcy's linear relation between flow velocity and headloss has been used to solve problems involving the flow of water through porous media, ie:

$$v = -k \frac{\partial H}{\partial l} \qquad \text{.....(2.1a)}$$

or

$$v = -k\, i \qquad \text{.....(2.1b)}$$

Where

v = average seepage velocity

k = permeability, a dimensional term and a function of the fluid and the aquifer

H = total potential head of the fluid

l = distance measured in the direction of the resultant velocity

i = total head gradient = $\frac{\partial H}{\partial l}$

The Darcy equation is valid for laminar flow, that is where either the pore spaces are small (as in clays, silts and sands) or the flow velocity is low. The significance of these two criteria will become apparent with the definition of the Reynolds number aplied to flow through porous media, discussed in Section 2.2.2. The Hazen formula (equation 2.2) has long been in use to estimate the permeability of sands (Cedergren, 1977). The permeability is proportional to the square of a representative particle dimension, ie

$$k = C\ d_{10}^2 \qquad \text{.....(2.2)}$$

Where

C = empirical constant

d_{10} = effective grain size (10 percent of the total weight of the sand is smaller than this dimension).

Leps (1973) describes the pioneering work in the flow through rockfill, beginning with the intuitive approach adopted by Weiss and the earliest laboratory data

obtained by Escande in 1953. It was recognised that the Darcy law did not generally hold for coarse granular media. Escande concluded from his experiments that the flow was turbulent and obeyed the equation:

$$v^2 = Bi \qquad \text{.....(2.3)}$$

where

v = apparent velocity of the water at any location along a flow path
i = the hydraulic gradient at any location along a flow path
B = an empirical constant for a given rockfill and varies with gradation in accord with the Reynolds number (which at that stage was not clearly defined).

Later laboratory tests performed by Wilkins (1956) gave rise to an equation of the form:

$$v_v = C \eta^a m^b i^c \qquad \text{.....(2.4)}$$

Where

v_v = velocity through voids
η = viscosity
m = hydraulic mean radius
= e (void ratio)/S_v (surface area per unit volume)
C,a,b,c = constants

Having performed extensive tests on stone of various gradings and shapes, a relationship between S_v and particle diameter was arrived at resulting in the following equations:

For stone, $v_v = 32{,}9\ m^{0{,}5}\ i^{0{,}54}$ .....(2.5a)
marbles, $v_v = 46{,}5\ m^{0{,}5}\ i^{0{,}50}$ .....(2.5b)

Where
V_v and m are in imperial units (inches and seconds).

While e, the void ratio, is an indirect function of the grading and is included in the above equations, no explicit relationship between grading, stone size and flow velocity is indicated. Since the surface areas of the particles were measured directly the investigations did take surface roughness and shape into account. (Hence the different values for C and c).

Similar equations were obtained by Olivier (1967). The relationship between surface area per unit volume S_v and $1/d_s$, the reciprocal of the effective particle diameter, was established for crushed granite and compared to idealised shapes.

$$S_v = \phi_s/d_s \qquad \text{.....(2.6)}$$

The ϕ_s values for various shaped particles are as follows:

spheres: 6,0
cubes: 7,46
hexahedrons: 7,81

while measurements of crushed granite yielded a ϕ_s value of 8,29.

The importance of this result will become apparent in Chapter 3 where the theoretical development of the flow equation makes use of the particle diameter to take account of grading and layering of various sized stone in the flow equation.

Ward (1964) recognised the need for research into the calculation of the permeability of a porous medium from the results of a sieve analysis using both size and size distribution parameters. Using dimensional analysis in

which v (velocity), k (permeability) and (kinematic viscosity of the fluid) were chosen as parameters, the constants a and b in the Forcheimer equation:

$$i = av + bv^2 \qquad \text{.....(2.7)}$$

were evaluated. This equation was fitted to results obtained in tests conducted at various flow rates ranging from laminar, transitional to turbulent. To plot the equation it was transformed into a log-log relationship between a Fanning friction factor and Reynolds number. Silberman (1965) however suggested that this type of analysis had resulted in the velocity square term becoming a second order one describing linear and non-linear laminar flow. Ward (1966) goes on to redefine the constants. This time in terms of n (porosity), d (particle diameter), and $_s$ (a particle shape factor), substantiating their applicability by means of dimensional analysis. In addition to that he presents a statistical relationship defining the particle shape factor in terms of the geometric mean size of the porous medium (as with previous investigations) and the corresponding geometric standard deviation of the size distribution.

Parkin et al (1966), Leps (1973) and Cedergren (1977) felt that at that stage no satisfactory understanding of non-Darcy flow had been evolved, and that it was found to be more convenient to base their work on an empirical law such as:

$$i = av^b \qquad \text{.....(2.8)}$$

In which a = a dimensional coefficient dependent on the particular medium and b = an exponent which, although varying with rock and flow characteristics,

satisfactorily approximates 1,85 for most practical flows in materials composed of convex particles coarser than 12,5 mm diameter. This equation can be compared directly to Wilkins' formula (equation 2.5a). The coefficient a is assumed to be principally a function of the hydraulic radius (void ratio/surface area per unit volume) and shape factor. Parkin et al (1966) prepared a nomogram for the determination of a using the parameters e (void ratio) and S_v (surface area per unit volume).

Dudgeon (1966) utilised the same form of equation but devised a different method of determining the values of the coefficient and exponent. The gradient i is plotted against velocity v on a log-log graph. The exponent b is determined from the slope of the curve for a particular flow regime. Substitution then yields the coefficient a. The results obtained indicate clearly the complex transitions from laminar to completely turbulent flow. Figure 2.1 shows a typical set of results obtained by Dudgeon.

An attempt was also made to present a generalised friction factor versus Reynolds number plot, ie

$$f = \frac{2gdi}{v^2} \quad \text{vs} \quad R = \frac{vd}{\nu} \qquad \text{.....(2.9)}$$

Where

f = friction factor
g = gravitational acceleration
d = representative grain diameter size
i = hydraulic gradient
v = flow velocity in the voids
R = Reynolds number
ν = viscosity of fluid

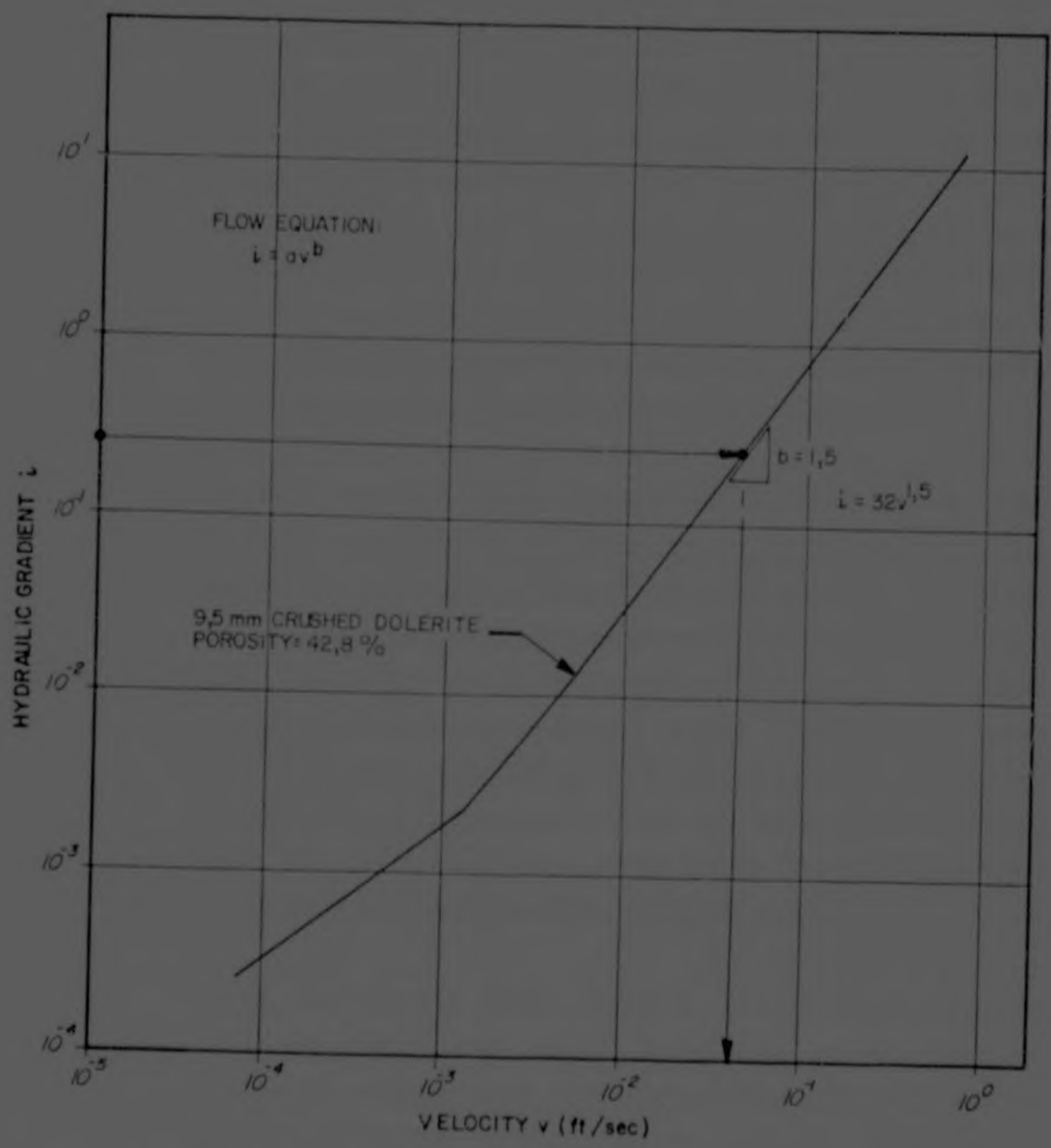


FIGURE 2.1 DETERMINATION OF EXPONENT b FROM FLOW TESTS (AFTER DUDGEON, 1966)

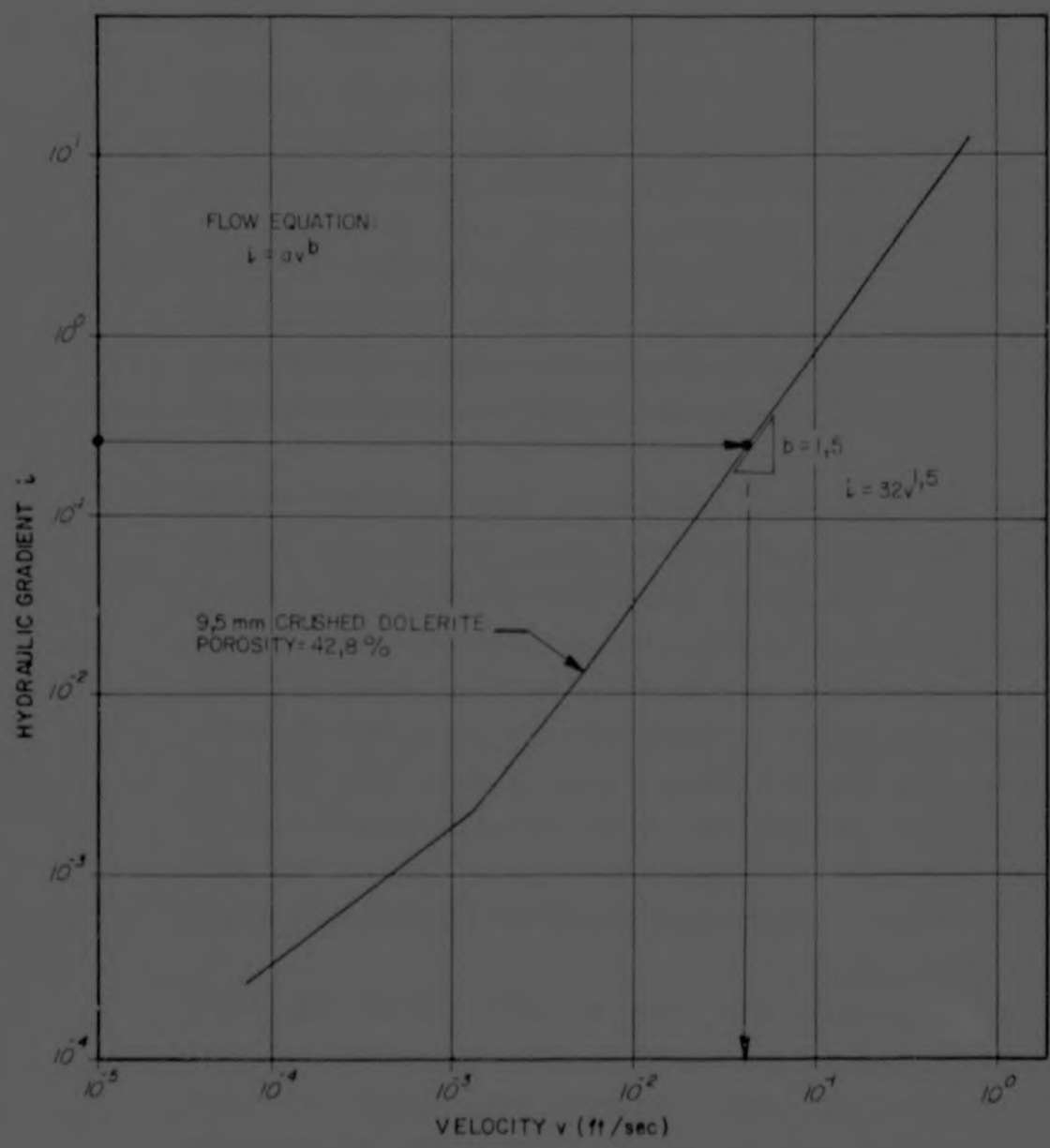


FIGURE 2.1 DETERMINATION OF EXPONENT b FROM FLOW TESTS (AFTER DUDGEON, 1966)

Dudgeon commented that the only likely solution to the problem of a generalised plot is to deal with a set of graphs for each family of geometrically similar porous media in a form similar to the Moody diagram for pipes.

A coefficient analogous to the e/D factor in the Moody Diagram, which separates one curve from another, needs to be found. In dealing with the interrelationship between the Moody Diagram and exponential formulae, Moore (1959) presented a Modified Moody diagram with lines of constant exponent b in the formula $i = av^b$, the exponential type resistance formula applicable to a particular pipe for a limited range of Reynolds numbers. The investigators using the exponential formula for the flow through rockfill have adopted a similar approach together with the abovementioned restrictions.

Hubbert (Wright, 1968) showed the limitations of pipe analogy arguments by pointing out that in pipe flow the motion is along rectilinear paths at constant velocity, whereas in flow through granular media the fluid undergoes continual cycles of acceleration and deceleration while following curvilinear paths. Deductions based purely on pipe flow analyses therefore cannot be applied to flow through granular media, and thus it is unlikely that the failure of the linear Darcy law signifies the onset of turbulence in flow through granular media.

Ahmed and Sunada (1969) support this view by showing that the energy loss due to turbulence is much smaller than the energy loss resulting from the convective accelerations due to the tortuous path the fluid has to follow in the pores, particularly in the transitional flow regime at low Reynolds numbers. Detailed tests on turbulence had indicated that with gradually increasing flow velocities fluid from one channel mixes with the

fluid of another, indicating that the departure from Darcy's law could be the result of convective accelerations rather than turbulent flow. Dimensional analysis was employed to derive the quadratic Forcheimer relationship (equation 2.7) beginning with the Navier-Stokes equations. This equation was found to fit numerous results of tests performed on sands. The advantage of the quadratic equation is that the constants are dependent upon a particular medium whereas the variables in the exponential formula (Equations 2.4 or 2.8) are velocity dependent.

Investigations into the existence of a unique relationship between the Fanning friction factor and Reynolds number common to all types of porous media resulted in the development of a third dimensionless parameter by Arbhabhirama and Dinoy (1973). This parameter, a function of the ratio of the particle mean diameter to the average hydraulic radius of the pore spaces, can be considered analogous to the relative roughness parameter used in the Moody diagram. Investigations to date had prodced transformations of the Forcheimer equation of the form:

$$K = C_1/R + C_2 \qquad \text{.....(2.10)}$$

Arbhabhirama and Dinoy had established an empirical relationship between C_2 and the relative roughness parameter based on dimensional analyses so that equation 2.10 became:

$$K = C_1/R + f(d/m) \qquad \text{.....(2.11)}$$

K = Fanning friction factor
R = Reynolds number
C_1, C_2 = constants for particular medium
d = representative particle diameter
m = hydraulic radius of pore spaces

The resulting plot of the empirical relationship between Friction factor and Reynolds number is shown schematically in Figure 2.2. The characteristic length chosen by the authors for the parameters was the square root of the permeability. This introduces difficulties in the application of their curves, since either permeability or test data will have to be available to predict the flow behaviour of a certain medium.

A similar, simpler approach was adopted by Stephenson (1979). The various curves of the friction factor plot were drawn for media having differently shaped particles, and fitted the equation:

$$K = 800/R + K_t \qquad \text{.....(2.12)}$$

Where

K_t - 1 (smooth polished marbles)
2 (semi rounded stone)
4 (angular stone)

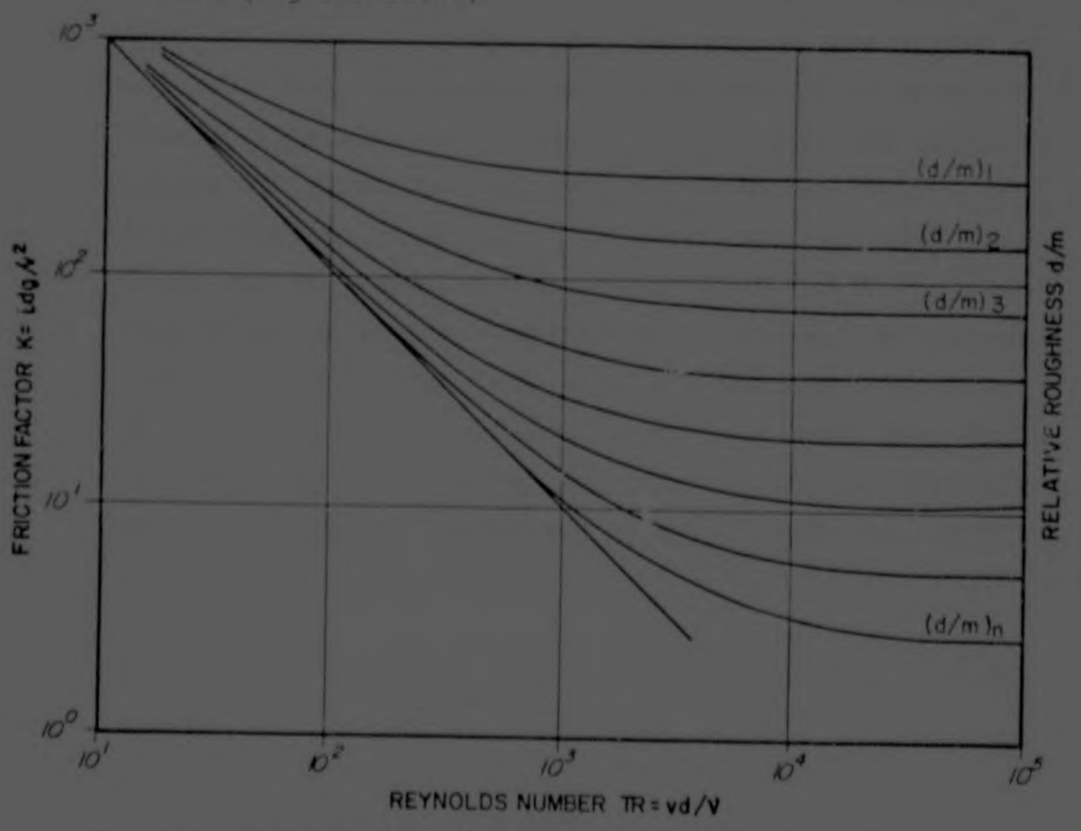


FIGURE 2.2 PLOT OF FRICTION FACTOR vs. REYNOLDS NUMBER FOR VARIOUS ROUGHNESS VALUES (AFTER ARBHABHIRAMA & DINOY, 1973)

For laminar flow

$K \simeq 800/R$ .....(2.13)

and turbulent flow

$K \simeq K_t$ .....(2.14)

the parameters K and R are redefined in terms of the velocity of fluid in the pores (rather than the apparent velocity v which equals the flow rate Q divided by the gross cross sectional area of the medium A), and a representative particle diameter d.

The reasoning behind these definitions was reviewed by Rumpelt and Stephenson (1982). For any hydraulic gradient, flow through granular media is dependent on the geometry and structure of the porous matrix, fluid properties and flow characteristics.

The porosity of a granular medium is a function of the packing of the grains, their shape, arrangement and size distribution and is defined as the ratio of volume of the void space to the bulk volume of the granular medium. Only interconnected pores are of interest to flow considerations. Idealised models of the availability of voids to the flow in a porous medium are illustrated in Figure 2.3. The true void velocity of a fluid may be shown to be between $v/n^{2/3}$ and v/n, but this velocity is not necessarily in the general direction of flow. The flow path is tortuous and consequently the directional head loss is higher than that indicated by a velocity of $v/n^{2/3}$ and is probably more nearly due to a velocity of v/n (Stephenson, 1979), ie

$v_v = v/n$ .....(2.15)

Where

v_v = real velocity in voids

v = apparent velocity = Q/A

n = porosity

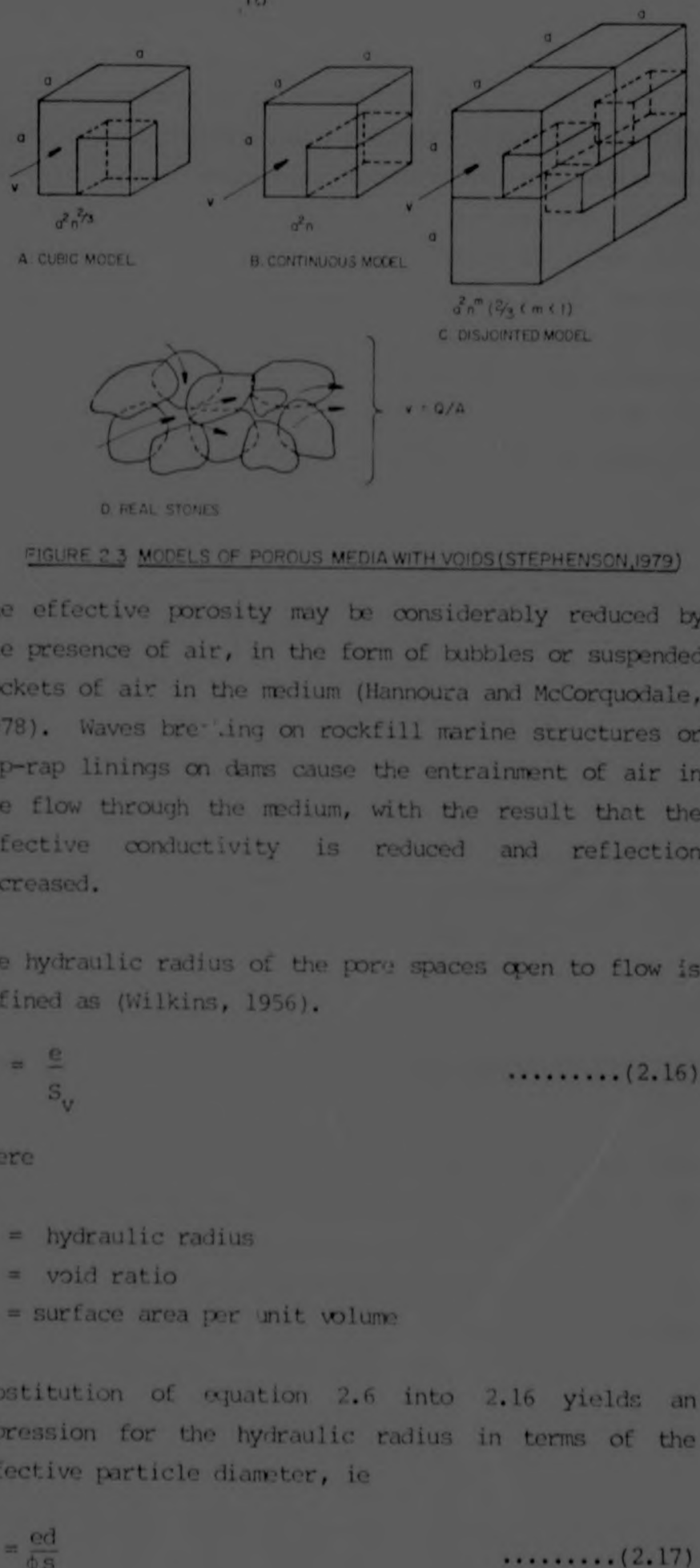


FIGURE 2.3 MODELS OF POROUS MEDIA WITH VOIDS (STEPHENSON, 1979)

The effective porosity may be considerably reduced by the presence of air, in the form of bubbles or suspended pockets of air in the medium (Hannoura and McCorquodale, 1978). Waves breaking on rockfill marine structures or rip-rap linings on dams cause the entrainment of air in the flow through the medium, with the result that the effective conductivity is reduced and reflection increased.

The hydraulic radius of the pore spaces open to flow is defined as (Wilkins, 1956).

$$m = \frac{e}{S_v} \qquad \text{.....(2.16)}$$

where

m = hydraulic radius
e = void ratio
S_v = surface area per unit volume

Substitution of equation 2.6 into 2.16 yields an expression for the hydraulic radius in terms of the effective particle diameter, ie

$$m = \frac{ed}{\phi s} \qquad \text{.....(2.17)}$$

It can therefore be said that for a given rockfill the dimensions of the flow path are represented by a characteristic length describing the size of the particles. The particle diameter d is taken to be the largest dimension on the least cross section of a particle (Figure 2.4). For a given shape and state of packing the void ratio is constant. The significance of this becomes apparent in the development of a permeability model for layered systems. Note the d is that of the effective stone size which is between the minimum and maximum size in Figure 2.4.

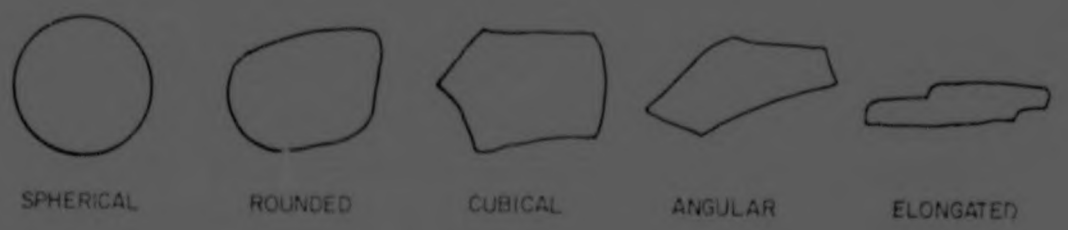




FIGURE 2.4 DEFINITION OF STONE SHAPE AND SIZE (STEPHENSON, 1979)

Using dimensional analysis (Yalin, 1971) or pipe flow analogy (Stephenson, 1979) the friction factor K is defined as:

$$K = \frac{idg}{v_v^2} = \frac{idgn^2}{v^2} \qquad \text{.....(2.18)}$$

and the Reynolds number R

$$R = \frac{v_v d}{\nu} = \frac{vd}{n\nu} \qquad \text{..... (2.19)}$$

Substituting equations 2.18 and 2.19 into 2.12 yields upon rearrangement

$$i = \frac{800\,\nu}{gd^2\,n}.v + \frac{K_t}{dgn^2}.v^2 \qquad \text{.....(2.20)}$$

or

$$i = av + bv^2 \qquad \text{.....(2.7)}$$

which is the Forcheimer equation and is applicable to the transitional region as well as laminar and turbulent flow.

Stephenson (1979) contends that the exponential flow equation had come into use merely because of the fact that the tests undertaken to substantiate this equation were conducted over a limited Reynolds number range. The Forcheimer equation therefore has the advantage of being applicable to a larger range of flow regimes as well as containing parameters that are constant for a particular medium, rather than being velocity dependent as is the case in the exponential equation.

2.2.2 Comparison of flow equations and conclusions

The study of the various flow equations revealed that the number of assumptions and generalisations increased in proportion to the level of sophistication applied in the theoretical derivation of the flow-headloss relationships. The physical parameters which to a varying degree affect the flow of water through granular media are:

- porosity of the medium, n
- a representative particle diameter or dimension, d
- roughness of the stone surface,
- shape of the particle, s
- surface area per unit volume, S_v

- surface area per unit volume, S_V
- hydraulic radius of the flow paths, m
- tortuosity of the flow path, T
- degree of saturation of the medium, S_r
- and the viscosity of water, ν

A change from laminar to turbulent flow in a particular medium will result in a change in the order of importance of the abovementioned parameters. This stems from the fact that the forces (and hence headloss) which predominate in the various flow regimes change from viscous forces for laminar flow to inertial forces in turbulent flow.

The definitions of the dimensionless parameters R and K vary from author to author, depending on which physical parameters were measured in tests, the empirical relationship between various parameters and the basic equations from which the friction factor/Reynolds number relationship was derived. In his review of previous research into headloss relationships Stephenson (1979) pointed out two possible sources of discrepancies in trying to correlate the various authors' experimental results:

(a) the definition of velocity: whether it is supposed to represent the gross velocity or velocity of flow through the pores, taking the porosity n into account (see equation 2.15); and

(b) the definition of the effective diameter d and the dominant size of stone which controls the permeability of a graded material.

Drawing on the work of previous investigators Rumpelt and Stephenson (1982) have concluded that the geometric

and flow path properties of a granular medium can be defined in terms of porosity, particle shape and effecive diameter (see equations 2.16 and 2.17), as opposed to for example, the use of the square root of the permeability (Arbhabhirama and Dinory 1973; Ward, 1964 and Ahmed and Sunada, 1969), which is calcualted indirectly from flow tests on particular media.

The derivation of the friction factor equation:

$$K = C_1/R + C_2 \qquad \text{.....(2.10)}$$

is based on analagous equations used in pipe flow: the Hagen-Poisovrille equation for laminar flow

$$i = \frac{h_f}{L} = \frac{32 \nu v}{gd^2} \qquad \text{.....(2.21)}$$

and the Darcy-Weisbach formula applied to turbulent flow:

$$i = \frac{h_f}{L} = \frac{\lambda v^2}{2gd} \qquad \text{.....(2.22)}$$

where λ = friction factor

Webber (1971) points out that λ is not a simple coefficient, but an overall coefficient which has to represent the combined effect of several variables, as is the case with C_2 in equation 2.10.

Laminar flow in coarse porous media is represented by the equation

$$i = C_1 \frac{\nu v_v}{gd^2} \qquad \text{.....(2.23a)}$$

which upon rearrangement

$$v_v = \frac{gd^2}{C_1 \nu} . i = ki \qquad \text{.....(2.23b)}$$

shows that a direct parallel can be drawn with the Hazen formula applied to Darcy flow where

$$k = f(d^2) = Cd^2 \qquad \text{.....(2.2)}$$

Multiplying equation 2.23a by dgn^2/v^2 results in

$$\frac{idgn^2}{v^2} = K = \frac{C_1 \nu n}{vd} = \frac{C_1}{R} \qquad \text{.....(2.24)}$$

which is the first term of equation 2.10.

Equations 2.18 and 2.22 are analogous to the equation proposed by Escande (equation 2.3).

$$v_v^2 = \frac{dg}{C_2}.i = Bi \qquad \text{.....(2.25)}$$

$$\text{But } K = \frac{idgn^2}{v^2} \qquad \text{.....(2.18)}$$

$$\text{Therefore } C_2 = \frac{idgn^2}{v^2} = K_t \qquad \text{.....(2.26)}$$

for turbulent flow.

Table 2.1 contains C_1 and C_2 values obtained from the data of previous investigations.

TABLE 2.1 : DATA FROM PREVIOUS INVESTIGATIONS

Source	Medium	$K = C_1/R + C_2$	
		C_1	C_2
Dudgeon (1966)	Marbles	312 - 791	1,8 - 2,3
Dudgeon (1966)	River Gravel	917 - 1150	2,6 - 5,7
Dudgeon (1966)	Blue Metal	625 - 962	5,4 - 8,3
Ahmed (1967)[a]	Sand	1045	4,4
Subba (1969)[a]	Sand	507	4,3
Subba (1969)[a]	Gravel	782	4,0
Sunada (1965)[a]	Marbles	384	2,6
Volker (1969)	Gravel	965	4,3
Arbhabhirama (1973)	Rounded gravel	641	1,4
Arbhabhirama (1973)	Angular gravel	444	2,2
Arbhabhirama (1973)	Sand	809	3,9
Leps (1973)	Gravel	-	3,0
Stephenson (1979)	Marbles	800	1,0
Stephenson (1979)	Rounded stone	800	2,0
Stephenson (1979)	Angular stone	800	4,0

[a] In : Arbhabhirama and Dinoy (1973)

Note: The values obtained above were derived from the published test results, and are thus independent of the equations used or assumptions made by the investigators in their interpretation of results.

The values of the turbulent friction factor ($C_2 = K_t$) show good correlation and all show the tendency of increasing in value with increasing angularity of the particles of the medium. The C_1 values show a considerably larger scatter and vary with the medium tested. A possible explanation for this scatter could be the difference in the definition of the particle diameter d. C_1 is proportional to d^2 and hence more sensitive to changes in the effective particle diameter than C_2.

TABLE 2.1 : DATA FROM PREVIOUS INVESTIGATIONS

Source	Medium	$K = C_1/R + C_2$	
		C_1	C_2
Dudgeon (1966)	Marbles	312 - 791	1,8 - 2,3
Dudgeon (1966)	River Gravel	917 - 1150	2,6 - 5,7
Dudgeon (1966)	Blue Metal	625 - 962	5,4 - 8,3
Ahmed (1967)[a]	Sand	1045	4,4
Subba (1969)[a]	Sand	507	4,3
Subba (1969)[a]	Gravel	782	4,0
Sunada (1965)[a]	Marbles	384	2,6
Volker (1969)	Gravel	965	4,3
Arbhabhirama (1973)	Rounded gravel	641	1,4
Arbhabhirama (1973)	Angular gravel	444	2,2
Arbhabhirama (1973)	Sand	809	3,9
Leps (1973)	Gravel	-	3,0
Stephenson (1979)	Marbles	800	1,0
Stephenson (1979)	Rounded stone	800	2,0
Stephenson (1979)	Angular stone	800	4,0

[a] In : Arbhabhirama and Dinoy (1973)

Note: The values obtained above were derived from the published test results, and are thus independent of the equations used or assumptions made by the investigators in their interpretation of results.

The values of the turbulent friction factor ($C_2 = K_t$) show good correlation and all show the tendency of increasing in value with increasing angularity of the particles of the medium. The C_1 values show a considerably larger scatter and vary with the medium tested. A possible explanation for this scatter could be the difference in the definition of the particle diameter d. C_1 is proportional to d^2 and hence more sensitive to changes in the effective particle diameter than C_2.

From the above comparisons it can be deduced with reasonable confidence that the equation of the form

$$K = C_1/R + C_2 \qquad \text{.....(2.10)}$$

is applicable for most practical purposes to the flow through coarse porous media. The generalised plot of this equation is given in Figure 2.5.

2.3 Mechanical properties of filter drains

The mechanical properties of filter drains need to be analysed so as to be able to predict the changes in permeability as progressively larger overburden loads are applied. It has been established (Blight and Caldwell, 1980 and Marsal, 1973) that single sized stone under load degrades to a greater extent than graded material. The consequences of degradation are a decrease in the particle size and a decrease in porosity, both contributing factors to a reduction in permeability.

An additional problem may be the clogging of the drain as more and more particles that have broken off the parent material are washed down the drain to be trapped and then broken down again. Finding a representative grading of the material is difficult in this case. Chapter 3 outlines theoretical, idealised models which represent the extreme cases in the segregation of materials.

2.3.1 Description of the grain skeleton

Statistical parameters have been utilised (Marsal, 1973) in the description of granular materials to determine dimensions and shapes of grains, grading, particle concentration and numbers of grain contacts. These properties are required primarily to establish what effect contact forces and particle breakage have on the compressibility and permeability of the filter drain.

From the above comparisons it can be deduced with reasonable confidence that the equation of the form

$$K = C_1/R + C_2 \qquad \text{.....(2.10)}$$

is applicable for most practical purposes to the flow through coarse porous media. The generalised plot of this equation is given in Figure 2.5.

2.3 Mechanical properties of filter drains

The mechanical properties of filter drains need to be analysed so as to be able to predict the changes in permeability as progressively larger overburden loads are applied. It has been established (Blight and Caldwell, 1980 and Marsal, 1973) that single sized stone under load degrades to a greater extent than graded material. The consequences of degradation are a decrease in the particle size and a decrease in porosity, both contributing factors to a reduction in permeability.

An additional problem may be the clogging of the drain as more and more particles that have broken off the parent material are washed down the drain to be trapped and then broken down again. Finding a representative grading of the material is difficult in this case. Chapter 3 outlines theoretical, idealised models which represent the extreme cases in the segregation of materials.

2.3.1 Description of the grain skeleton

Statistical parameters have been utilised (Marsal, 1973) in the description of granular materials to determine dimensions and shapes of grains, grading, particle concentration and numbers of grain contacts. These properties are required primarily to establish what effect contact forces and particle breakage have on the compressibility and permeability of the filter drain.

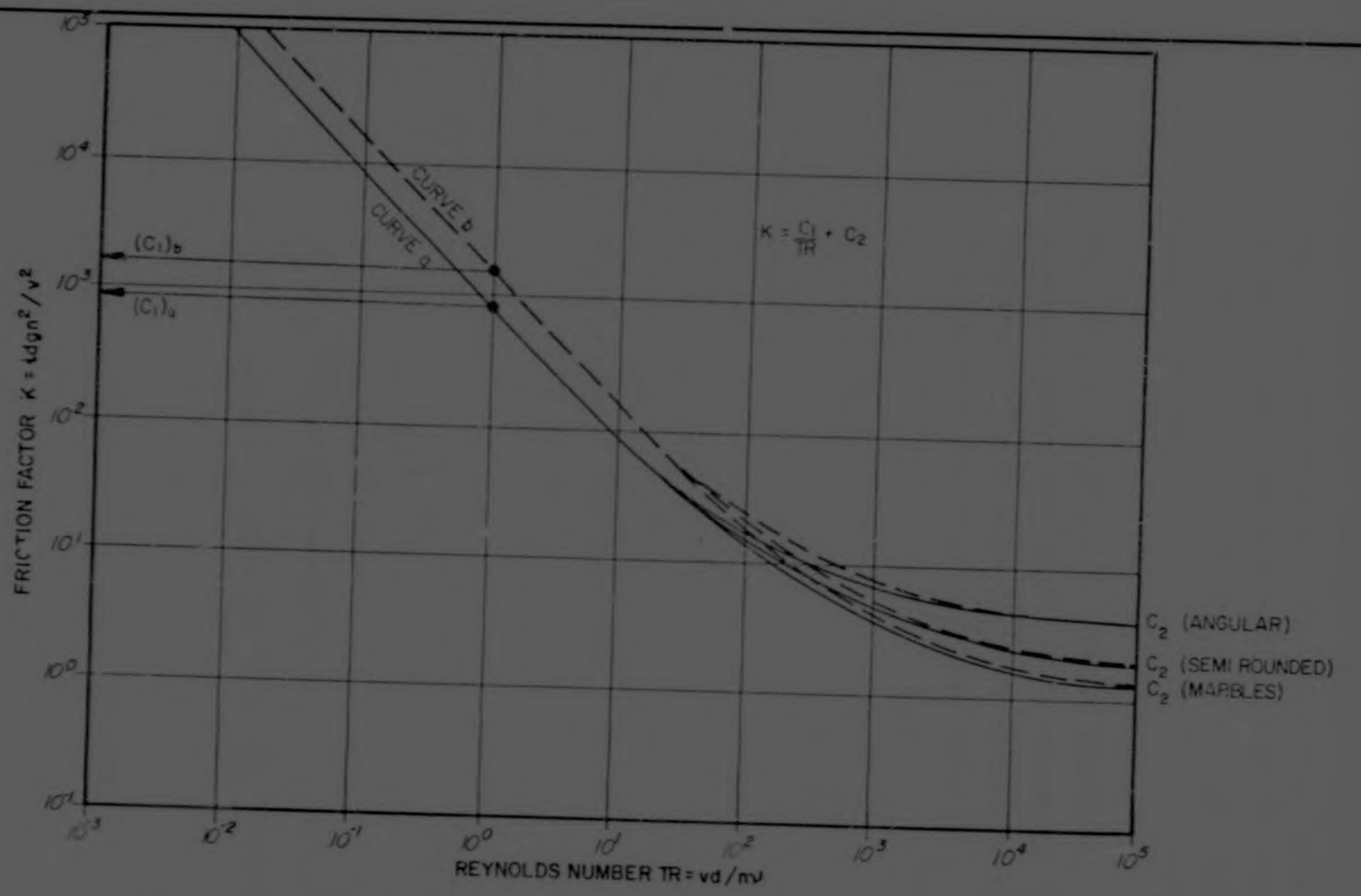


FIGURE 2.5 FRICTION FACTOR vs REYNOLDS NUMBER - GENERALISED PLOT

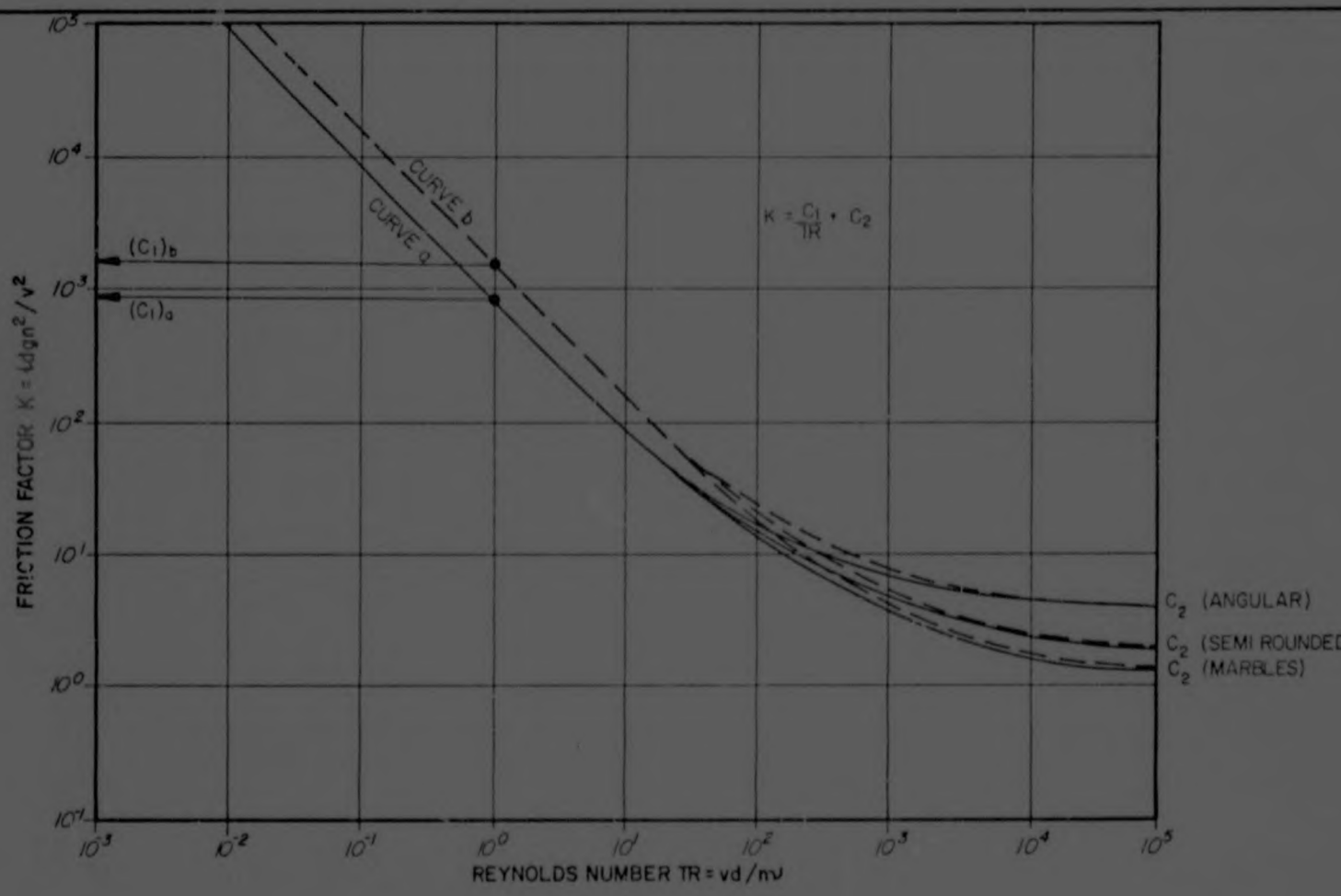


FIGURE 2.5 FRICTION FACTOR vs REYNOLDS NUMBER - GENERALISED PLOT

Section 2.3.5 deals with the physical properties and parameters used to describe a certain gravel in terms of its grading, grain size and shape factor using standard measuring procedures. Marsal (1973) calculates the number of grain contacts from standard descriptions such as grading and void ratio together with statistically formulated charts.

The concept of idle particles is mentioned. These are particles which make up the solid volume but do not participate actively in carrying the load, resulting in the definition of the structural void ratio e_s:

$$e_s = \frac{e + \psi}{e - \psi} \qquad \text{.....(2.27)}$$

where

e = void ratio
ψ = $\Delta V_s / V$
ΔV_s = volume of idle particles
V = total volume

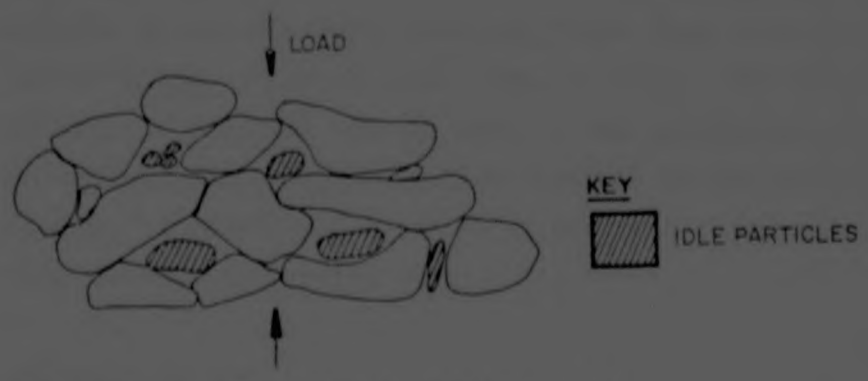


FIGURE 2.6 STRUCTURALLY IDLE PARTICLES

It is difficult to define the volume of idle particles which are effectively regarded as voids. From trying to

sketch these particles in two dimensions it can be intuitively seen that the presence of idle particles is more likely in a gap graded material. If a lot of fine material is present it will tend to fill the voids and become part of the structural matrix.

Marsal (1969a) discussed scale effects which occurred when choosing a representative sample. The most significant factors singled out in trying to model the prototype were:

- the defects in the particles, and
- the law of variation of the granular interaction, ie the contact forces

The number of interparticle contacts is a function of particle size.

Another scale effect on shear strength is the effect of the D/d_{max} ratio, where D = the minimum dimension of the specimen and d_{max} = the maximum particle size. Ratios of between 6 and 10 have been suggested, although values above 10 seem to be preferred, for example in the Aggregate Crushing Value Test (A.C.V) the ratio D/d_{max} = 11,4 (B.S. 812 - 67). No mention of wall or edge effects is made in the standards and it is assumed that these have been implied in the considerations. Section 2.4 contains a detailed discussion on wall effects in loading tests.

2.3.2 Particle forces

Gravel under load undergoes structural changes due to displacements, rotations and particle breakage. These actions depend on the particle forces and have been found to be a function of the grading index properties

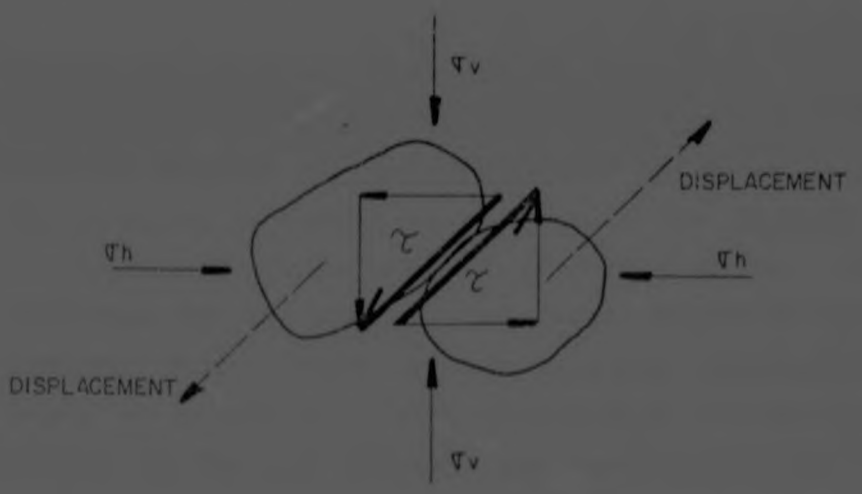
and void ratio of the gravel. The actions between particles are analysed using a probabilistic approach to establish the relationship between friction, granular forces and contact forces (Marsal, 1969b; 1973).

One of the results obtained from Marsal's investigations is that the magnitude of the contact force is dependent on the size of the grains. For example, assuming a resultant stress of one kilogram per square centimetre over the gross cross sectional area of a sample the average contact forces for various materials are computed (Marsal, 1973):

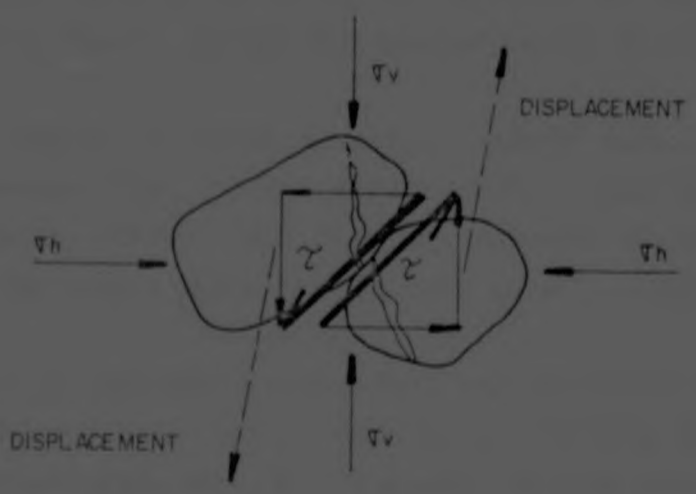
Medium sand	1 gram
gravel	1 kilogram
rockfill (d = 700 mm)	1 ton

Thus low stresses may cause breakage in a rockfill mass, whereas stresses several orders of magnitude larger are required to break the grains of a sand. This comparison can be considered as proof that scale effects have to be taken into account, full scale tests being the most preferable.

The friction force has the direction of the relative movement between two particles at a point of common contact. Consequently, the friction resistance developed in the granular body is a vector, its direction being connected to some average value of the relative movements at the contacts.



a) NO PARTICLE BREAKAGE : MOVEMENT PARALLEL TO INTERPARTICLE FRICTION



b) PARTICLE BREAKAGE : MOVEMENT NOT PARALLEL TO INTERPARTICLE FRICTION

FIGURE 2.7 MOVEMENT OF PARTICLES RELATIVE TO INTERPARTICLE FRICTION

The mean relative movement may be represented by means of the average grain path which is obtained from the strain as the material is loaded. Strains in the x and y directions cannot be measured unless a large scale triaxial test is performed. The effect of frictional resistance and its influence on the strength of a gravel can therefore not be found in a one dimensional compression test.

2.3.3 Particle breakage

Particle breakage is a complex process which varies from the formation of powder by crushing of the contact to the rupture of grains into two or more fragments. Many particles may be cracked, but their fragments remain together with little or no relative displacement. Depending on the grain size distribution and degree of compaction, the new fragments and particularly the fine ones, can remain idle, ie without participating structurally in the granular skeleton. Further breakage is retarded then as the average particle size becomes smaller with a corresponding decrease in the average contact forces, unless the applied stress is increased.

The degree of grain breakage depends mainly on the gradation (Lee, 1969; Marsal, 1973; and Blight and Caldwell, 1980); the crushing strength of the grains and the stress level (Blight and Caldwell, 1980).

It is of interest to note that the so-called aggregate crushing value, used in the Standard Methods of Testing Materials (RSA Dept of Transport), defines the crushing strength of gravels in terms of particle breakage, ie change in grading. Another method of describing particle breakage, in this case for products obtained from a crushing and screening plant, is the Flakiness Index.

In this case the quality of the gravel is described in terms of the shape it breaks down into.

Other quantitative measures of grain breakage have been proposed:

- Marsal (1973) defined a parameter B_g which is equal to the positive sum of the differences in fractional weight of each grain size fraction before and after crushing due to loading.

- Lee (1969) took the 15 percent grain size as parameter in recognition of its importance in soil filter design and thus defined particle breakage in terms of the so-called Relative Crushing Ratio d_{15i}/d_{15a} where d_{15i} is the 15 percent diameter before the test and d_{15a} the 15 percent diameter after the test.

2.3.4 Factors which influence grain breakage

Besides the gradation, particle size and stress level, extensively covered by the Lee (1969), the crushing strength of individual grains is dependent on some brittle fracture law.

The rock particles are generally brittle and have a compressive strength four or more times greater than their tensile strength. Fissures and voids may be present and thus influence the tensile strength even more. Stresses in a granular rock mass are transmitted through forces acting on limited areas of the grain surface. Joisel (in Marsal, 1973) presented a simplified analysis of failure based on the differences in the elastic moduli of the mineral components of the rock. An analogy with the results of this analysis can be drawn with the theoretical background to the Brazilian or cylinder splitting test applied to spheres discussed in Jaeger and Cook, 1976 (see Appendix B). If W is the diametral load at failure for a sphere of diameter d the tensile strength q_t is given by

$$q_t = kW/d^2 \qquad \text{.....(2.28)}$$

Jaeger found the constant, k, to range from 0,92 to 1,80.

The application of Griffith's energy theory of failure, and the assumption that the crack length is a function of the diameter, leads to the follcwing equation:

$$q_t \propto \frac{1}{\sqrt{d}} \qquad \text{.....(2.29)}$$

Therefore an empirical equation of the form

$$q_t = \eta d^{\lambda} \qquad \text{.....(2.30)}$$

is obtained, where η and λ are material parameters, with λ equal to -3/2 if equations 2.28 and 2.29 are combined.

Tests undertaken by Marsal have revealed that η is a complex coefficient in which the shape of the particle and the soundness and degree of alteration of the parent rock have to be taken into account.

In a comparison of results obtained from triaxial tets and oedometer tests, Marsal found stress conditions to be more favourable to the development of breakage in the triaxial tests because of a higher principal stress ratio (3 to 9) than in the oedometer tests (2 to 3).

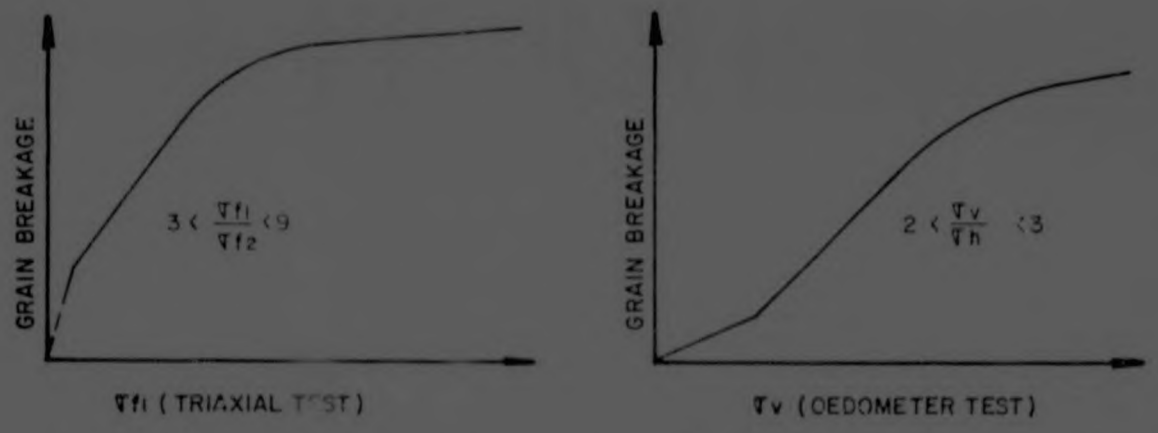


FIGURE 2.8 COMPARISON OF DEGREE OF GRAIN BREAKAGE FOR DIFFERENT FAILURE CONDITIONS (AFTER MARSAL, 1973)

A rubber, sand or foam lining inside the oedometer/permeameter will cause the grain breakage to follow a similar curve to that of the triaxial test at low loads. As the loads are increased and the particles are restrained fully by the walls of the testing cylinder, the grain breakage curve will follow that of the oedometer test.

2.3.5 Grading and grain breakage

One of the most important factors influencing grain breakage has been found to be the grading of the material.

Lee (1969) has investigated the degradation of filters under overb den pressures up to 4 MPa, but did not arrive at any concise conclusions besides the fact that the filter laws still held under these pressures. What should be noted however is the relative degradation when comparing the grading curves of two layers consisting of different sized particles. This illustrates the fact that particle breakage in gravel filters should not be considered in one layer (size) on its own. Note must be taken of the layer interaction as well as the varying rates of degradation with applied load, (Figure 2.9)

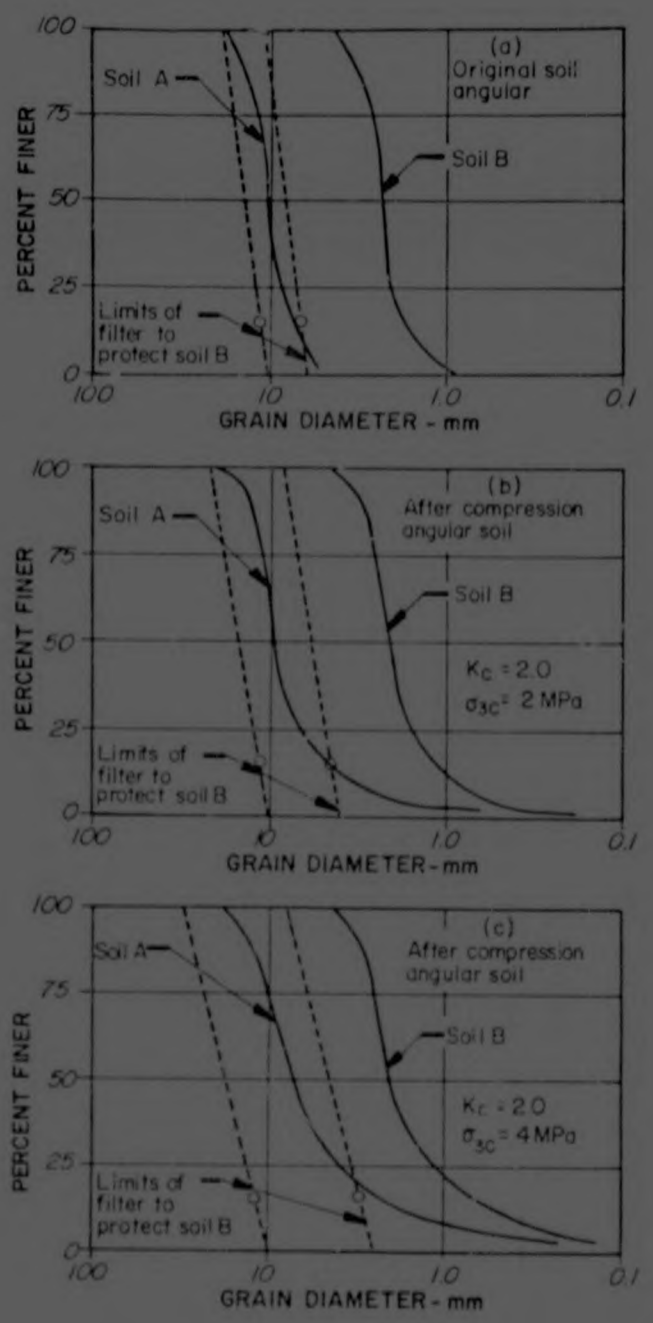


FIGURE 2.9 DEGRADATION OF FILTER AND SOIL UNDER LOAD (AFTER LEE, 1969)

The slope of the grading curve determines the amount of grain breakage. Graded materials (flat slope) degrade less than single sized (steep slope) materials. Although more idle particles may be present in a graded material, the overall effect is that there are more interparticle contacts between grains, thus the stress in the grains is reduced (see Fig 2.10).

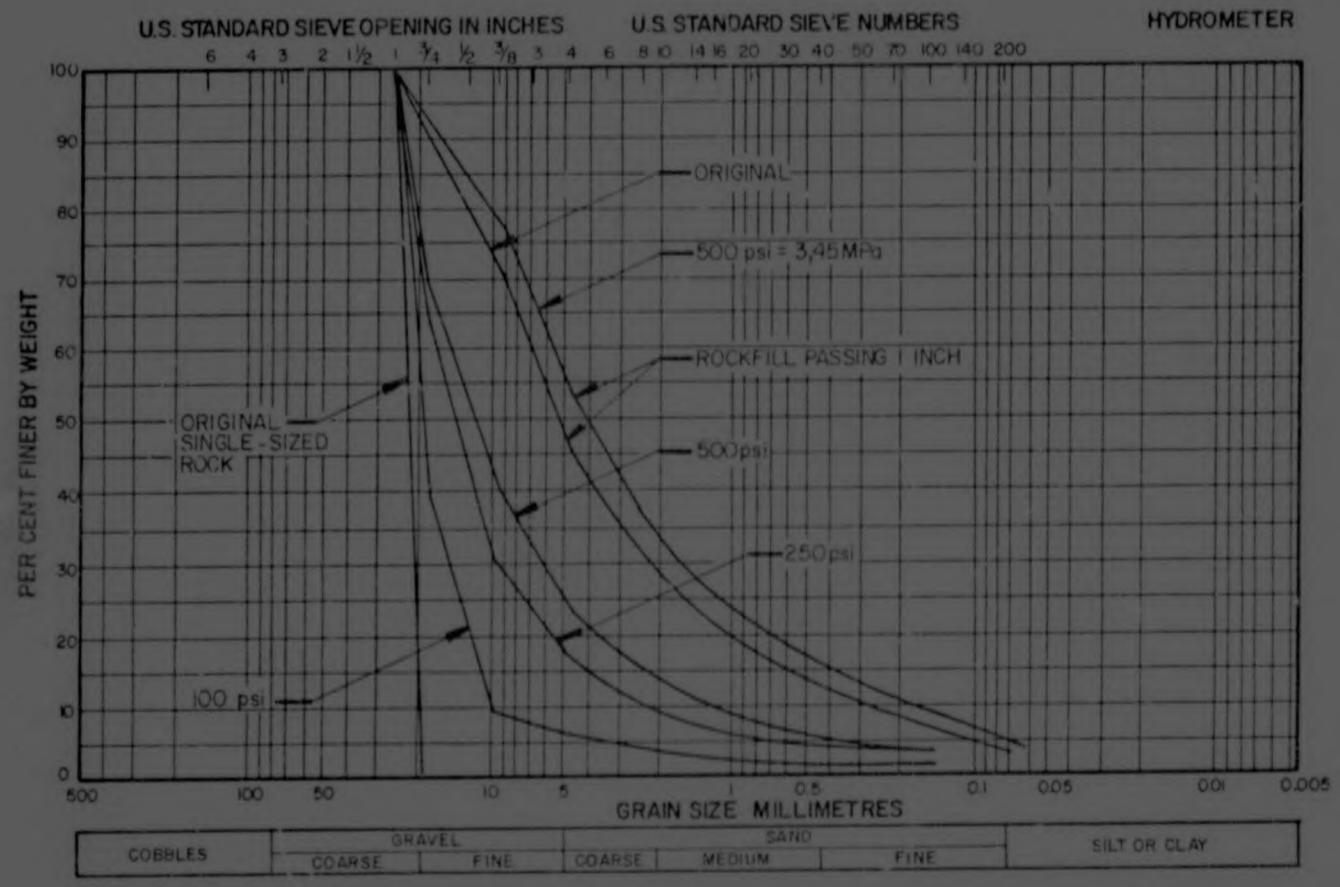


FIGURE 2.10 DEGRADATION OF SINGLE SIZED ROCK UNDER PROGRESSIVELY INCREASING STRESS COMPARED WITH DEGRADATION OF GRADED ROCK. (AFTER BLIGHT AND CALDWELL, 1980)

2.3.6 Particle size and grain breakage

In section 2.3.4 it was shown that the tensile strength of granular rock is inversely proportional to d^{λ} where $\lambda = 3/2$. This means that with increasing particle size a lower stress is required to break the particles. This fact has been verified experimentally by Lee (1969) and Marsal (1973).

A difference worth noting in Figure 2.11 is that Lee's crushing parameter considers one particle fraction only whereas in Marsal's B_g the fragmentation processes in all component fractions are taken into account. (B_g = positive sum of the differences in fractional weight of each grain size fraction before and after crushing due to loading). On inspection of Figures 2.9 and 2.10 it can be seen that most of the particle breakage takes place in the lower portions of the curves. This at first seems to contradict the relationships developed in Section 2.3.4 and shown in Fig 2.11. Alternatively, the conclusion can be drawn that where the larger diameter particles do fail, the resulting grains consist of large fragments with a lot of small broken off pieces and rock flour, ie d_{100} remains virtually unaltered as shown in the graph by Lee (1969) in Figure 2.12. The amount of local movement due to the fragmentation of a particular grain is greater than the average deflection of the medium under load. Therefore localised stress relaxation takes place.

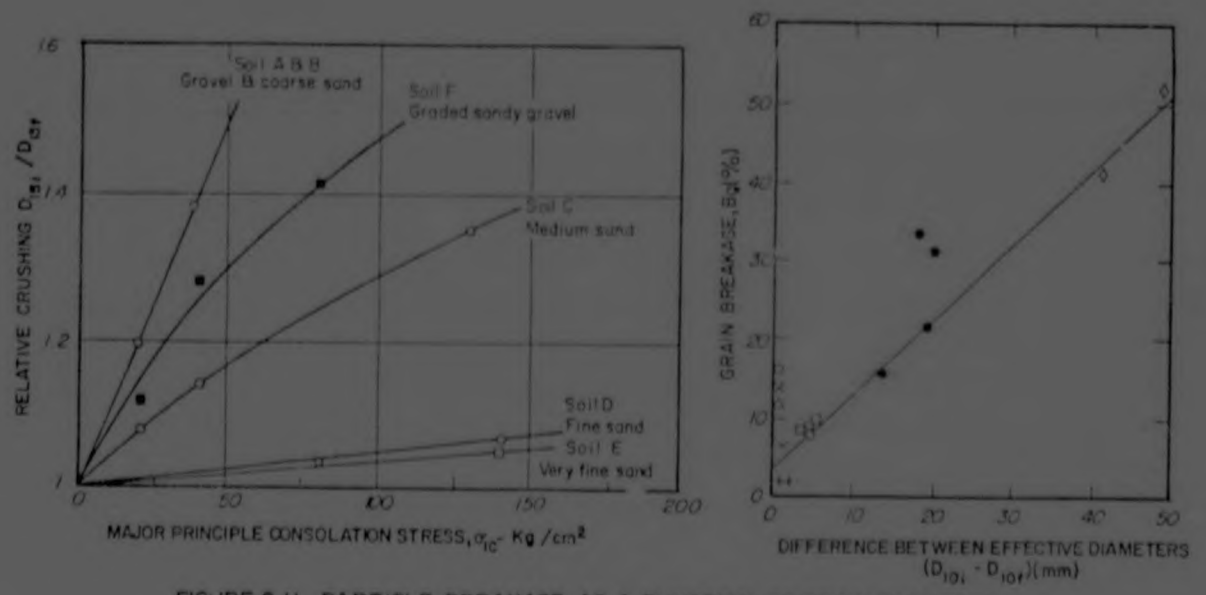


FIGURE 2.11 PARTICLE BREAKAGE AS A FUNCTION OF GRAIN DIAMETER
a) LEE (1969) : b) MARSAL (1973)

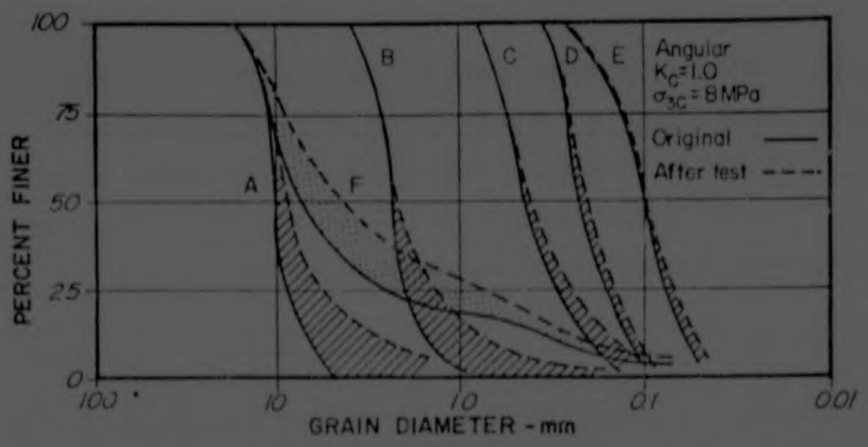


FIGURE 2.12 COMPARISON OF CRUSHING OF SOILS WITH DIFFERENT INITIAL GRAIN SIZES (AFTER LEE,1969)

2.3.7 Stress level and particle breakage

Because the nature of fracturing results in a large amount of relatively small particles being formed, breakage of grains continues with increasing stress. An alternative situation can arise in that a certain amount of damping of particle breakage occurrs as the material becomes a "graded" material once crushed under the first incremental load.

A certain amount of this damping is evident from the results of the tests conducted by Blight and Caldwell (1980). The plot of change in porosity and particle size with increasing stress is reproduced here as Figure 2.13.

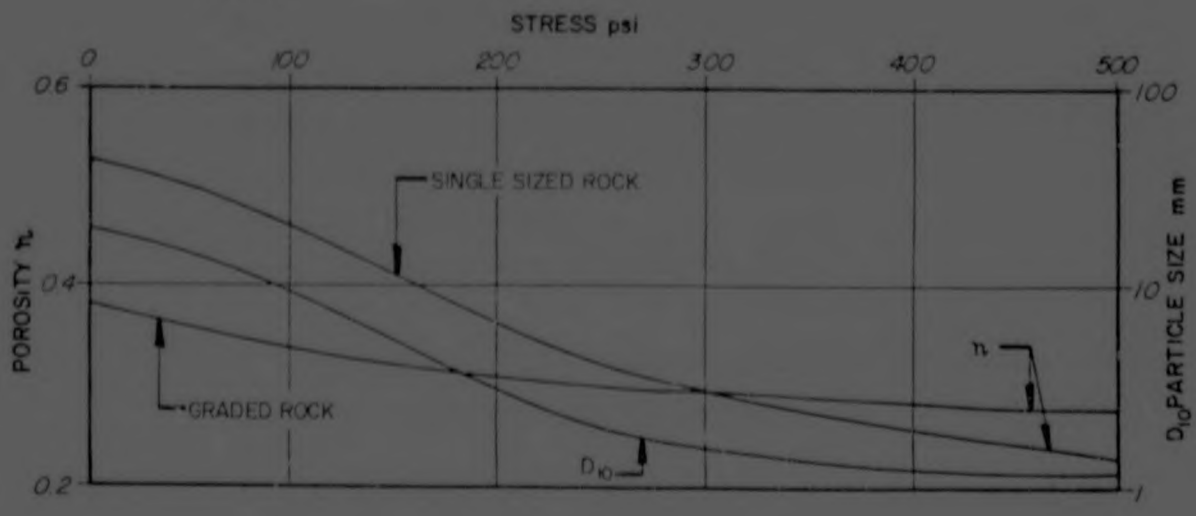


FIGURE 2.13 CHANGES IN POROSITY AND PARTICLE SIZE UNDER PROGRESSIVELY INCREASING STRESS FOR SINGLE SIZED AND AND GRADED ROCK (AFTER BLIGHT AND CALDWELL, 1980)

Particle shape also plays an important part in the breakage of grains at various stress levels. It is easier to break off small chips of rock from angular gravels than from subrounded pebbles, as shown in the experiments by Lee (1969) in Figure 2.14.

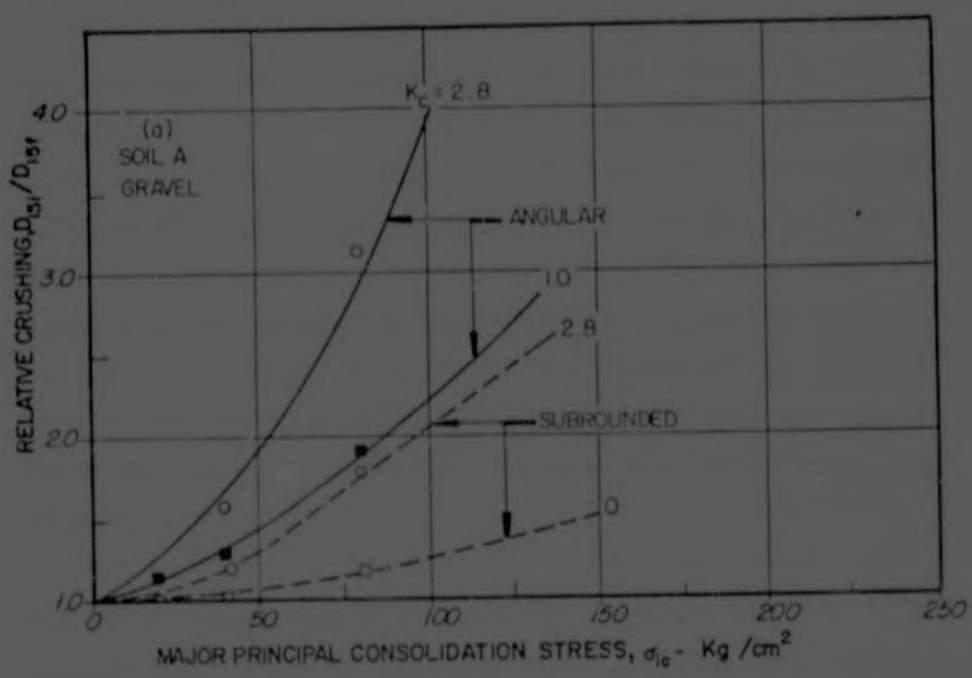


FIGURE 2.14 RELATIVE CRUSHING OF GRAVEL AT VARIOUS STRESS LEVELS (LEE, 1969)

2.3.8 Quantitative description of particle breakage

The parameters which affect the degradation of gravels under load are:

hardness and strength of parent rock,
degree of weathering and soundness,
void ratio, density,
grading,
shape: flakiness, elongation and angularity,
surface texture, and
abrasive resistance to deformation.

Unconfined crushing strengths are given for various rock types in textbooks and references, for example Leslie

(1969) and Stephenson (1979). Applied to gravels they have little significance on their own other than to create a basis of comparison between similar gravels composed of different parent rock material. The crushing strength of a gravel mass is greatly influenced by the abovementioned parameters. Rather than basing the strength of a gravel on the unconfined crushing strength of the parent rock it has been found that standard tests describing the overall crushing behaviour of gravels are more representative and useful. One such test is the Aggregate Crushing Value (A.C.V.) test in which a gravel sample is subjected to a stres of 23 MPa. The values assigned to a particular material are related to the amount of particle breakage determined by doing sieve analyses of the sample before and after crushing (Taylor, 1977).

The shear resistance of gravels depends on particle arrangement, shape and surface texture. The void ratio, density, grading indeces and shape factor can be utilised to model particle arrangement. The shape factor has been defined in various ways: eg Vesic (1969): particle sphericity equals the ratio of the projected area of the particle to the area of a circumscribed circle: or the angularity number, flakiness and elongation index used in concrete technology and design of asphalt pavements for an assessment of mechanical strength and workability. A measure of angularity or sphericity might also be gained by comparing grading curves obtained in sieve analyses using rectangular openings to curves obtained from analyses using sieves with circular openings.

3 THEORETICAL DEVELOPMENT OF THE FLOW EQUATION

3.1 Introduction

It was shown in the previous chapter that the headloss equations (equations 2.23 and 2.26) for coarse porous media are functions of the fluid viscosity, particle shape and roughness, the porosity of the medium and an undefined representative particle diameter. Flow tests undertaken by various researchers were invariably done on samples of uniform particle diameter. In most cases therefore the representative particle diameter was taken to be the mean particle diameter. No provision had been made for graded materials or for materials that were initially uniform, but then crushed under large overburden loads. It is also recognised that stratification of layers of different sized particles is an inevitable consequence of some construction techniques currently employed on rockfill embankments (Bertram, 1973).

Coarse porous media or rockfills can therefore be classified as being composed of

- single sized
- graded or
- stratified material

What distinguishes one material from the other when considering flow through the material is the effective particle diameter used in the flow equations. By means of mathematical modelling of the flow through these materials a rational definition of the representative particle size d as applied to either the laminar or turbulent flow equation was obtained. This investigation was necessary for the meaningful interpretation of the flow results before and after the crushing tests.

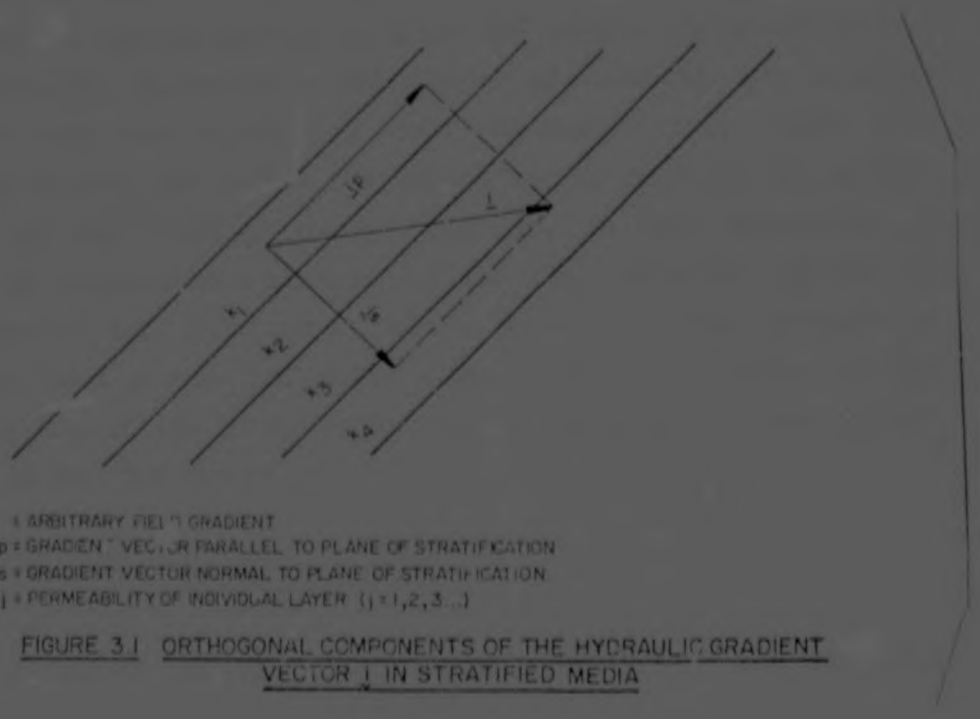
The approach adopted is analagous to the treatment of flow through layered soils in which equivalent vertical and

horizontal permeabilities are calculated by considering the flow behaviour in two orthogonal directions. Graded gravels are therefore represented by stratified media in which each layer consists of grains of a particular size. The layers of the stratified media are either parallel, perpendicular or inclined to the direction of flow. A method for the determination of the effective particle diameter for a randomly packed rockfill was developed and is presented here.

3.2 Flow equation applied to stratified media

Any arbitrarily orientated hydraulic gradient may be split into two component vectors, one parallel and the other orthogonal to plane of stratification, as shown in Figure 3.1. It will be assumed here that the layers are parallel to each other.

The headloss equations developed in the previous section assume in each case that the hydraulic gradient is parallel to the velocity vector, ie the material within each layer is homogeneous and isotropic.



$\underline{i}$ = ARBITRARY FIELD GRADIENT
$\underline{i}p$ = GRADIENT VECTOR PARALLEL TO PLANE OF STRATIFICATION
$\underline{i}s$ = GRADIENT VECTOR NORMAL TO PLANE OF STRATIFICATION
k_j = PERMEABILITY OF INDIVIDUAL LAYER (j = 1,2,3...)

FIGURE 3.1 ORTHOGONAL COMPONENTS OF THE HYDRAULIC GRADIENT VECTOR $\underline{i}$ IN STRATIFIED MEDIA

To be able to make use of this model the principle of superposition must be assumed to be valid. A comparison with flow through fissured rock may be made here in describing the principle of superposition as outlined in Snow (1965), Caldwell (1972) and Bear (1972) because of hydraulic continuity.

Snow (1965) describes the principle of superposition in fissured rock to apply in the following manner:

An imaginary field gradient of arbitrary orientation may be imposed across any mass transected by arbitrarily orientated, uniform continuous conductors. Real gradients on the conductors may be computed as projections of the field gradient. The flow on each may then be calculated according to its geometry, and since no mutual interference takes place, the total flow through the medium is the vector sum of the contributions of the individual conductors.

In the flow through layered media the principle of superposition is postulated here to apply as follows:

A field gradient of arbitrary orientation may be imposed across a parallel layered medium in which the strata are orientated in an arbitrary direction. The layers of material are distinguished from one another by their permeabilities. Real gradients within and across the layers may be computed as projections of the field gradient. The flow in each direction may then be calculated according to the flow equation applied to the particular direction. Since no mutual interferences or losses take place, the total flow through the medium is the vector sum of the contributions of the individual flow quantities in the two directions.

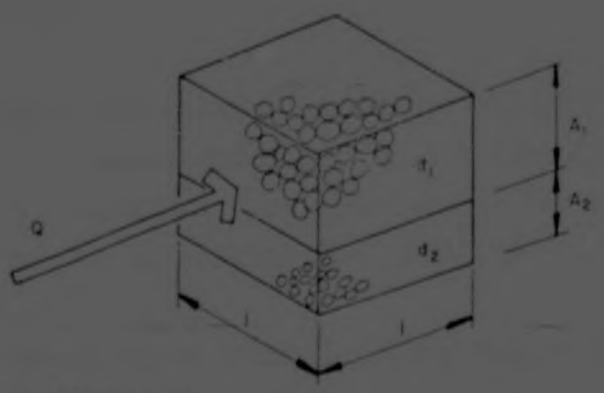
3.3 Development of the layered model

For a porous medium, flow is a function of the particle

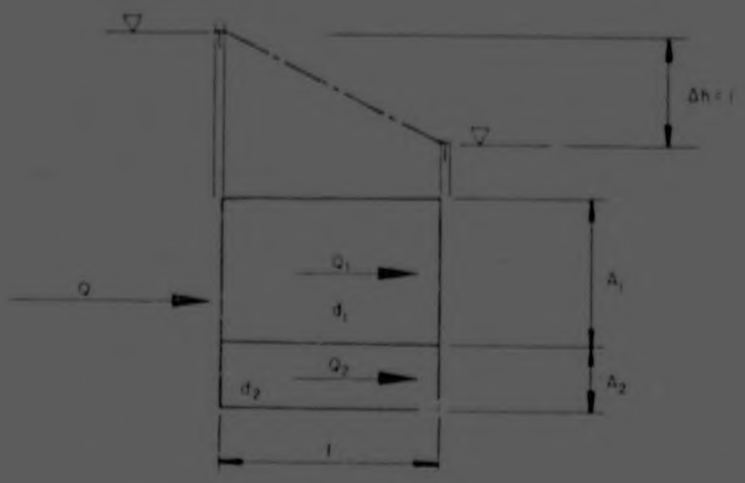
diameter d, porosity n and the turbulent friction factor K_t (or C_2), which depends on particle shape and roughness, (see equation 2.11). In the case of stratified media the assumption is made that K_t and n are constant for any diameter d. This assumption is the basis on which the parallel and series layered models are derived as functions of the effective particle diameter d. Each layer is assumed to consist of equally sized particles. The amount of layers per unit area or length is determined from the grading curve, where each size fraction by weight x_j is represented by a volumetric division of the same proportion. This follows from the assumption that the porosity is the same for all particle sizes.

3.4 Parallel layered model

The flow condition in the parallel layered model is illustrated in Fig 3.2.



a) ISOMETRIC VIEW



b) SECTION, SHOWING HYDRAULIC GRADIENT

FIGURE 3.2 PARALLEL LAYERED MODEL

The derivation of the effective diameter for the parallel layer model is based on the fact that:

- the hydraulic gradient is the same for all strata, and
- the total flow quantity Q is the sum of the flow quantities, Qj through the various layers.

3.4.1 Laminar flow

From equation 2.23a the partial flow quantity Q_j within a layer is found to be

$$Q_j = \frac{g\, d_j^2 n_j i_j A_j}{C_1 \nu} \qquad \text{.....(3.1a)}$$

$$\text{and } Q = \frac{g d_{PL}^2 n i A}{C_1 \nu} \qquad \text{.....(3.1b)}$$

where

d_{PL} = effective diameter for the parallel (P) layer model under laminar (L) flow conditions

Q_j = partial flow quantity, ie flow in layer j

$Q = \Sigma Q_j$ = total flow quantity

Referring to Section 3.4 and Figure 3.2, where

- $i = i_j$
- and $Q = \Sigma Q_j$

$$\frac{d_{PL}^2 g n i A}{C_1 \nu} = \frac{\Sigma d_j^2 g n_j i_j A}{C_1 \nu} \qquad \text{.....(3.3)}$$

reduces to

$$d_{PL}^2 = \Sigma d_j^2 \frac{A_j}{A} \qquad \text{.....(3.4)}$$

For $n = n_j$

C_1 = constant for all d

The layers of material consisting of the various sized particles have the same proportional cross sectional areas as the proportions by weight of the various stone sizes. This assumption can be made where the porosity of the layered medium equals the porosity of the individual layers.

Therefore

$$\frac{A_j}{A} = x_j$$

where

x_j = proportion by weight of stone size d_j

The equation (3.3) for the effective particle diameter for laminar flow in the parallel layer model can therefore be rewritten as:

$$d_{PL} = (\Sigma d_j^2 x_j)^{\frac{1}{2}} \qquad \text{.....(3.4)}$$

3.4.2 Turbulent flow

Upon rearrangement of the turbulent flow equation (equation 2.26), the partial flow quantity Q_j within a layer is

$$Q_j = \frac{(i_j d_j g n_j^2)^{\frac{1}{2}}}{C_2} A_j \qquad \text{.....(3.5a)}$$

and

$$Q = \frac{(i d_{PT} g n^2)^{\frac{1}{2}}}{C_2} A \qquad \text{.....(3.5b)}$$

where d_{PT} = effective diameter for the parallel (P) layer model under turbulent (T) flow conditions

Since C_2 is dependent on particle shape and roughness only, it can be assumed to be a cosntant applicable to all layers. By similar reasoning as that outlined in the previous sub-section, the expression for the effective diameter for the parallel layer model under turbulent flow conditions becomes

$$d_{PT} = (\Sigma \sqrt{d_j}\, x_j)^2 \qquad \text{.....(3.6)}$$

3.4.3 Transitional flow

Equations 2.20, 2,23a and 2.26 are combined to obtain the transitional flow equation of the following form:

$$i = \frac{C_1 \nu}{g d^2 n}\, v + \frac{C_2}{d g n^2}\, v^2 \qquad \text{.....(3.7)}$$

Even with the simplifying assumptions made in the previous cases, it is impossible to reduce the parallel layered flow equation under transitional flow into an explicit expression for the equivalent particle diameter. In order to be, by definition, the transitional flow equation, both terms of equation 3.7 need to be retained. Therefore

$$v = \frac{-n C_1 \nu + \sqrt{n^2 C_1 \nu^2 + 4 C_2 d^3 i n^2 g}}{2 C_2 d} \qquad \text{.....(3.8)}$$

For $Q = \Sigma Q_j$

$i = i_j$

The following equation has to be solved by iteration to obtain d_{PR}, the effective diameter for te parallel (P) layer model under transitional flow (R).

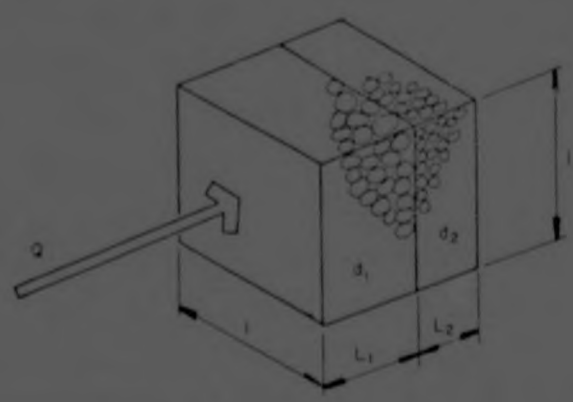
$$\frac{-1 + \sqrt{1 + C_3 d_{PR}^3}}{d_{PR}} = \Sigma \frac{(-1 + \sqrt{1 + C_3 d_j^3})}{d_j} x_j$$

where $C_3 = \frac{4C_2 i g}{C_1^2 \nu^2} = \frac{4C_2 i_j g}{C_1^2 \nu^2}$

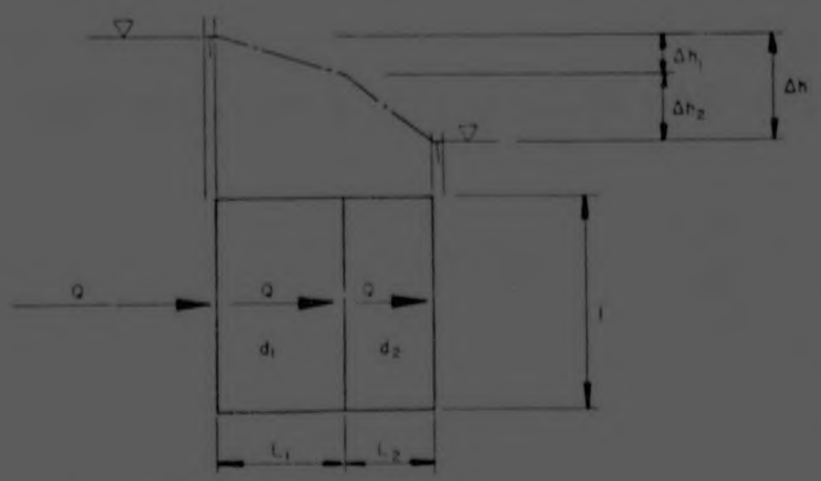
3.5 Series layered model

The series layered model is illustrated in Figure 3.3. The derivation of the effective diameter for the series layer model is based on the fact that:

- the total hydraulic headloss across the medium is equal to the sum of headlosses across each successive layer, and
- the total flow quantity Q is equal to the flow quantities Q_j through the various layers.



a) ISOMETRIC VIEW



b) SECTION SHOWING HYDRAULIC GRADIENT

FIGURE 3.3 SERIES LAYERED MODEL

3.5.1 Laminar flow

Equation 2.23a is rewritten in such a form that the hydraulic gradient is expressed as in Figure 3.3.

$$Q_j = \frac{g\, d_j^2\, n_j}{C_1 \nu} \quad \frac{\Delta h_j}{L_j} \quad 1 \qquad \text{.....(3.10a)}$$

and

$$Q = \frac{g\, d_{SL}^2\, n}{C_1 \nu} \quad \frac{\Delta h}{L} \quad 1 \qquad \text{.....(3.10b)}$$

Where d_{SL} = effective diameter for the series (S) layer model under laminar (L) flow conditions

Δh_j = headloss over jth layer of thickness L_j

Δh = headloss over j layers under consideration

Referring to Section 3.5 and Figure 3.3, where

- $Q_j = Q$
- $\Sigma \Delta h_j = \Delta h$
- $\Sigma L_j = L$, and

$$\frac{d_{SL}^2\, g\, n}{C_1} \cdot \frac{\Delta h}{L} = \frac{d_j^2\, g\, n_j}{C_1 \nu} \cdot \frac{\Delta h_j}{L_j} \qquad \text{.....(3.11)}$$

Rearranging (3.11) $\Delta h_j = \frac{d_{SL}^2}{d_j^2} \cdot \frac{\Delta h}{L} \cdot L_j$

and $\Sigma \Delta h_j = \Delta h \Rightarrow \Delta h = \Sigma \frac{d_{SL}^2}{d_j^2} \cdot \frac{\Delta h}{L} \cdot L_j$

$$1 = d_{SL}^2 \quad \Sigma \quad \frac{L_j/L}{d_j^2} \qquad \text{....(3.12)}$$

for $n = n_j$

C_1 = constant for all d

The layers of material consisting of the various sized particles have the same proportional lengths as the proportions by weight of the various stone sizes. This assumption can be made where the porosity of the layered medium equals the porosity of the individual layers.

Therefore

$$\frac{L_j}{L} = x_j \qquad \text{.....(3.13)}$$

Where x_j = proportion by weight of stone size d_j

The equation (3.12) for the effective particle diameter for laminar flow in the series layer model can therefore be rewritten as:

$$d_{SL} = \frac{1}{\sqrt{\Sigma x_j / d_j}^2} \qquad \text{.....(3.14)}$$

3.5.2 Turbulent flow

Upon rearrangement of the turbulent flow equation (eq 2.26), the partial flow quantity Q_j within a layer is

$$Q_j = \frac{(d_j g n_j^2 \cdot \Delta h_j)^{\frac{1}{2}}}{C_2} \cdot \frac{1}{L_j} \qquad \text{.....(3.15a)}$$

and $$Q = \frac{(d_{ST} g n^2 \cdot \Delta h)^{\frac{1}{2}}}{C_2} \cdot \frac{}{L} \qquad \text{.....(3.15b)}$$

for $n = n_j$

C_1 = constant for all d

The layers of material consisting of the various sized particles have the same proportional lengths as the proportions by weight of the various stone sizes. This assumption can be made where the porosity of the layered medium equals the porosity of the individual layers.

Therefore

$$\frac{L_j}{L} = x_j \qquad \text{.....(3.13)}$$

Where x_j = proportion by weight of stone size d_j

The equation (3.12) for the effective particle diameter for laminar flow in the series layer model can therefore be rewritten as:

$$d_{SL} = \frac{1}{\sqrt{\Sigma x_j / d_j^2}} \qquad \text{.....(3.14)}$$

3.5.2 Turbulent flow

Upon rearrangement of the turbulent flow equation (eq 2.26), the partial flow quantity Q_j within a layer is

$$Q_j = \frac{(d_j g n_j^2 \cdot \Delta h_j)^{\frac{1}{2}}}{C_2} \frac{1}{L_j} \qquad \text{.....(3.15a)}$$

$$\text{and } Q = \frac{(d_{ST} \, gn^2}{C_2} \cdot \frac{\Delta h)^{\frac{1}{2}}}{L} \qquad \text{.....(3.15b)}$$

where d_{ST} = effective diameter for the series (S) layer model under turbulent (T) flow conditions.

Since C_2 is dependent on particle shape and roughness only, it can be assumed to be a constant applicable to all layers. By similar derivation as that outlined in the previous section, the expression for the effective diameter for the series layer model under turbulent fow conditions is found to be:

$$d_{ST} = \frac{1}{\Sigma x_j/d_j} \qquad \text{.....(3.16)}$$

3.5.3 Transitional flow

Equations 2.20, 2.23a and 2.26 are combined to obtain the transitional flow equations of the following form:

$$i = \frac{\Delta h_j}{L_j} = \frac{C_1 \nu \quad V_j}{g d_j^{\,2} n_j} + \frac{C_2 \quad V_j^2}{g d_j n_j^{\,2}} \qquad \text{....(3.17)}$$

$$\text{and } i = \frac{\Delta h}{L} = \frac{C_1 \nu \quad V}{g d_{SR}^{\,2} n} + \frac{C_2 \quad V^2}{g d_{SR} n^2} \qquad \text{....(3.18)}$$

The summation of equation (3.17) equals (3.18). The assumption is made that the terms of the left had side of the equation may be equated to the corresponding terms on the right hand side. The equation for the effective diameter for the series layer model under transitional flow therefore is:

$$d_{SR} = \frac{C_4 + \sqrt{C_4^2 + 4C_4}}{2} \qquad \text{.....(3.19)}$$

Where

$$C_4 = \frac{1}{\Sigma (d_j + 1)\, x_j / d_j^2}$$

3.6 Application of effective particle diameter equations

To summarise the previous two subsections, the equations for the parallel and series layer models under various flow conditions are listed in Table 3.1.

TABLE 3.1 : EQUATIONS FOR THE EFFECTIVE PARTICLE DIAMETER

	Parallel model	Series model
Laminar flow	$d_{PL} = (\Sigma d_j^{\,2} \times j)^{\frac{1}{2}}$	$d_{SL} = \dfrac{1}{(\Sigma x_j / d_j^{\,2})^{\frac{1}{2}}}$
Turbulent flow	$d_{PT} = (\Sigma \sqrt{d_j} \times j)^2$	$d_{ST} = \dfrac{1}{\Sigma x_j / d_j}$
Transitional flow	$(-1+\sqrt{1 + C_3 d^3_{PR}}) / d_{PR} = \Sigma x_j (-1 + \sqrt{1 + C_3 d_j^3})/d_j$ $C_3 = \dfrac{4 C_2 i g}{C_1^2 \nu^2}$	$d_{SR} = \dfrac{C_4 + \sqrt{C_4^2 + 4C_4}}{2}$ $C_4 = \dfrac{1}{\Sigma (d_j+1) x_j / d_j^2}$

Before the Reynolds number is calculated it is not always immediately apparent which particle diameter should be used in calculations. The only method available is to estimate the Reynolds number, establish where (provisionally) the flow lies on the curve (Fig 2.5) and what equation from Table 3.1 should be used. With the corrected particle diameter thus obtained, the Reynolds number should be recalculated, to check the initial assumptions and to improve the degree of accuracy of calculations.

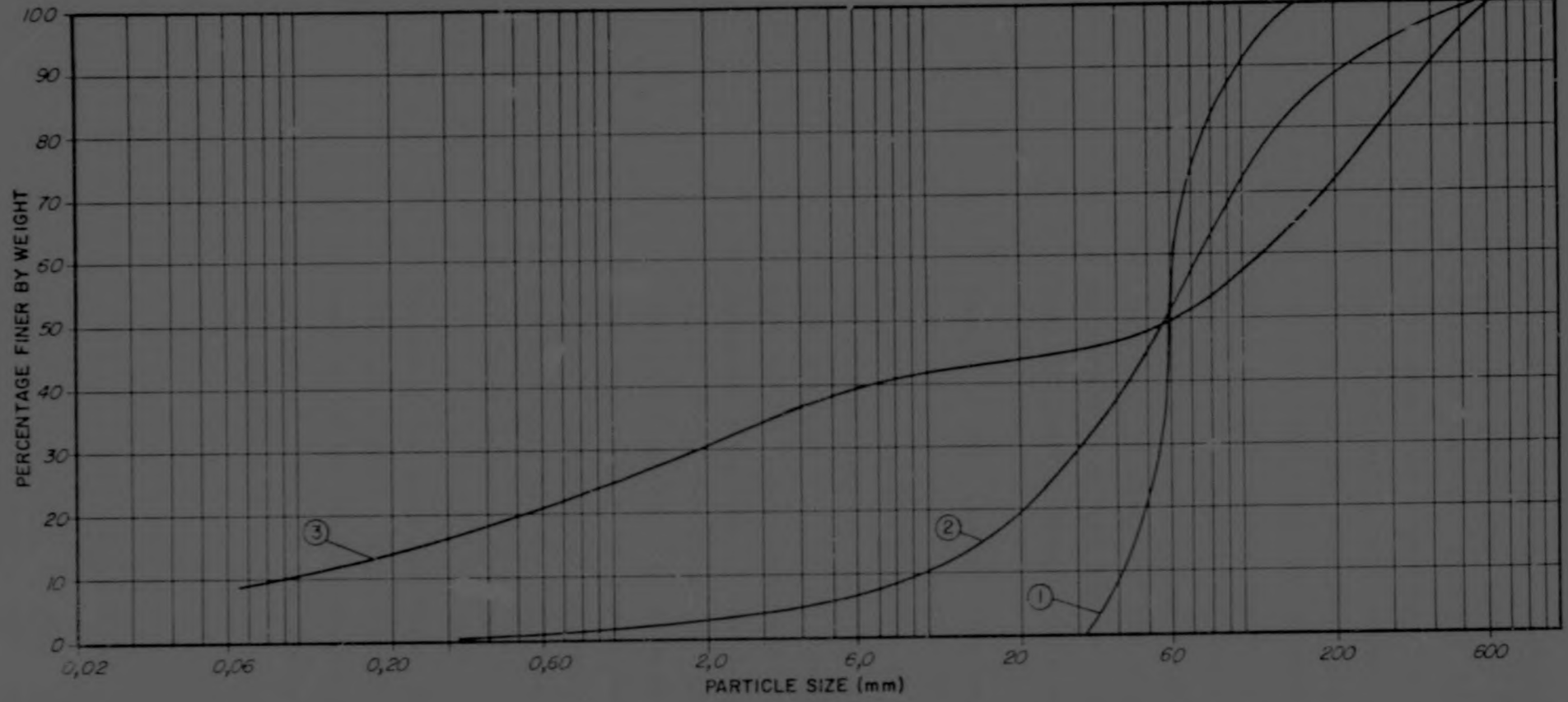
3.6.1 Effect of grading on permeability

The three materials whose grading curves are plotted in Fig 3.4 may be used as examples of how particle size and particularly grading influence the permeability if stratification is assumed. Table 3.2 shows the effective diameters of materials 1, 2 and 3 in the direction parallel to and across the strata, and compares these to the isotropic median particle size.

TABLE 3.2 : COMPARISON OF EFFECTIVE PARTICLE DIAMETERS

(mm)

Material	1	2	3
Description Coefficient of uniformity d_{60}/d_{10}	Uniform 1,5	Graded -1,5	Gap -1 200
LAMINAR FLOW: Parallel layers Isotropic d_{50} Series	 69 60 57	 131 60 5,4	 205 60 0,11
TRANSITIONAL FLOW: Parallel layers Isotropic d_{50} Series	 64 60 57	 67 60 5,4	 69 60 0,11
TURBULENT FLOW Parallel layers Isotropic d_{50} Series	 65 60 59	 69 60 16	 73 60 0,29



SILT	SAND			GRAVEL			COBBLES		
COARSE	FINE	MEDIUM	COARSE	FINE	MEDIUM	COARSE	FINE	MEDIUM	

DESCRIPTION

1 UNIFORMLY SIZED MATERIAL (e.g. STONE FOR HAND PACKING GABIONS)

2 GRADED MATERIAL

3 GAP GRADED MATERIAL (e.g. MINE DUMP ROCK, WAGENER 1980)

FIGURE 3.4 GRADING CURVES FOR VARIOUS ROCKFILL SAMPLES

It will be observed that with increasing d_{60}/d_{10} ratio (ie going from left to right in the table) the effective particle diameter increases in the parallel layer model and decreases in the series model. For graded and gap graded materials there is a dramatic decrease in the effective particle diameter when the series layer model is compared to the isotropic or parallel layer model. In other words, the series layer model could represent the case where the layering in a rockfill or gravel filter is caused by migration of the fines and blockage of the flow path to control the permeability of the medium. The above comments hold true for laminar transitional and turbulent flow.

Except in the laminar flow regime the parallel layer model is less sensitive than the series model to changes in grading and the presence of a large amount of fines. The permeability is directly proportional to the effective diameter squared for laminar flow (equation 2.23b) and to $d^{\frac{1}{2}}$ for turbulent flow (equation 2.25). Therefore a measure of the change in permeability may be gained from the range in particle diameters. The largest increase in permeability due to layering (parallel model) is approximately 12 fold while the greatest decrease in permeability (series model) is approximately 300 000 times for the materials of Fig 3.4 and Table 3.2.

To obtain a quick estimate of the effective particle diameter under transitional flow conditions, the parallel model can be compared to the turbulent case and the series model to the laminar case (exactly equal in this example).

3.6.2 Vector notation applied to layered media

The previous sections have shown that a flow-headloss equation may be obtained for layered media in which the particle size distribution and disposition relative to the flow direction will determine the directional permeability. In the absence of any discontinuities, flow channels or moving air bubble inclusions, the permeabilities parallel and normal to the direction of stratification may therefore be regarded as the two principal permeabilities. Flow through an arbitrarily orientated layered medium may therefore be resolved into component vectors parallel and normal to the stratification, as shown in Fig 3.1, ie:

$$\begin{bmatrix} i_p \\ i_s \end{bmatrix} = \begin{bmatrix} f(d_p) & 0 \\ 0 & f(d_s) \end{bmatrix} \begin{bmatrix} v_p \\ v_s \end{bmatrix} \qquad (3.20)$$

where i_p, i_s = components of hydraulic gradient parallel and normal to layers

v_p, v_s = Components of velocity parallel and normal to layers

$f(d_p)$ and $f(d_s)$ are the parallel layer and series layer expressions for laminar, transitional and turbulent flow as listed in Table 3.3.

TABLE 3.3 : EXPRESSIONS f(d) FOR EQUATION (3.20)

	Parallel	Series
Laminar flow	$\frac{C_1 \nu}{g n\, d_{pL}^2}$	$\frac{C_1 \nu}{g n d_{SL}^2}$
Transitional flow	$\frac{C_1 \nu}{g n\, d_{PR}^2} + \frac{C_2 \lvert v_p \rvert}{g n^2 d_{PR}}$	$\frac{C_1 \nu}{g n d_{SR}^2} + \frac{C_2 \lvert v_S \rvert}{g n^2 d_{SR}}$
Turbulent flow	$\frac{C_2 \lvert v_p \rvert}{g n^2\, d_{PR}}$	$\frac{C_2 \lvert v_s \rvert}{g n^2\, d_{SR}}$

Tensorial notation of anisotropic permeability can be utilised for the derivation of the effective equation for flow through an arbitrarily orientated system of layers.

It will be assumed here that the field gradient i is parallel to the co-ordinate system x axis as shown in Figure 3.5. The layers are inclined at an angle θ to the x axis and equation (3.20) holds for flow parallel and normal to the layers.

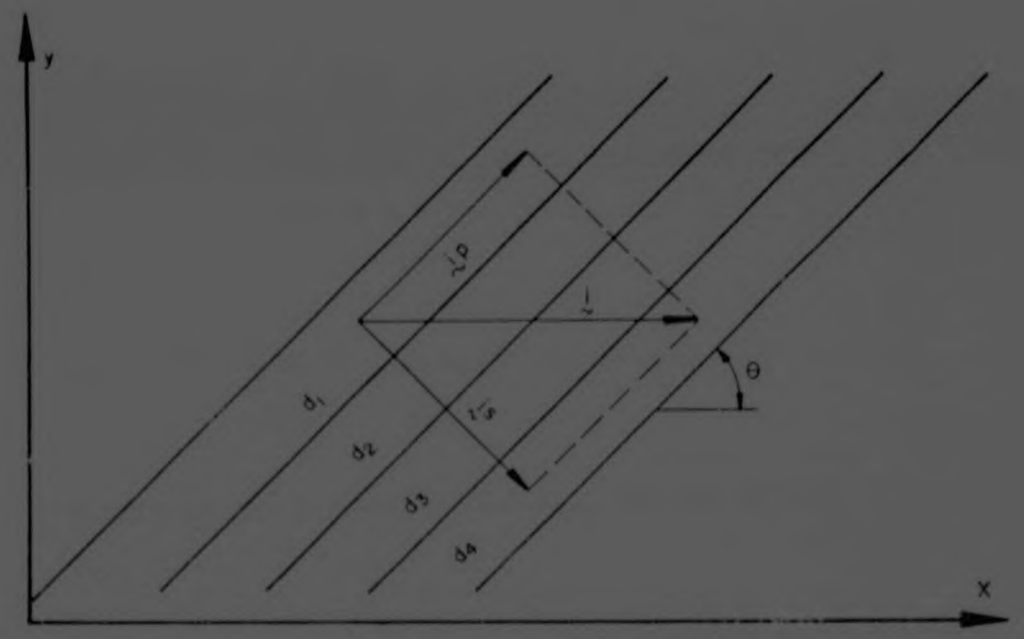


FIGURE 3.5 FLOW THROUGH INCLINED LAYERS

The method used to solve for the velocity in the x and y directions is as follows:

1 The effective particle diameter is found for the parallel and series layer model as outlined in previous sections and summarised in Table 3.1.

2 For the laminar, transitional and turbulent cases the general form of the flow equation can be written in matrix form as follows:

$$I = FV \qquad (3.21)$$

which is an abbreviated form of equation (3.20), and where I,V = gradient and velocity vectors with parallel and perpendicular components to the direction of stratification

F = square diagonal matrix with its elements listed in Table 3.3

3 If $I_{x,y}$ and $V_{x,y}$ are the gradient and velocity vectors with components in the x and y directions, the equation (3.21) may be written as:

$$L^{-1} I_{x'y} = F L^{-1} V_{x'y} \qquad (3.22a)$$

Where L^{-1} = the inverse of the transformation matrix L

ie $L = \begin{bmatrix} \cos\theta & -\sin\theta \\ \sin\theta & \cos\theta \end{bmatrix}$

and $L^{-1} = \begin{bmatrix} \cos\theta & \sin\theta \\ -\sin\theta & \cos\theta \end{bmatrix}$

Therefore the expression for $I_{x'y}$ can be written

$$I_{x'y} = L F L^{-1} V_{x'y} \qquad (3.22b)$$

Multiplying out and recalling that $i_y = 0$ (axes chosen to coincide with gradient direction) equation (3.22) can be written in the form:

$$\begin{bmatrix} i \\ o \end{bmatrix} = \begin{bmatrix} c^2 f(d_p) + s^2 f(d_s) & cs[f(d_p)-f(d_s)] \\ cs[f(d_p) - f(d_s)] & s^2 f(d_p) + c^2 f(d_s) \end{bmatrix} \begin{bmatrix} v_x \\ v_y \end{bmatrix} \qquad (3.22c)$$

Where i = hydraulic gradient imposed across medium (see Figure 3.5).

c,s = $\cos\theta$ and $\sin\theta$ respectively

v_x, v_y = velocity vector components in the x and y directions

Calculate $f(d_p)$ and $f(d_s)$ for the assumed flow regime and then solve for v_x and v_y by solving the two simultaneous equations in (3.22c).

Example: For material 2 of Table 3.2 calculate the flow velocity through the medium whose layers are inclined at 0° (parallel layer model), 30°, 60° and 90° (series model) to the imposed hydraulic gradient of 0,1.

Given: $C_1 = 800$, $C_2 = 4$, $n = 0{,}35$, $\nu = 1{,}05.10^{-6}$ m^2/s and $g = 9{,}81$ m/s. Assume transitional flow.

Solution:

$f(d_{PR}) = 5.45.10^{-2} + 49,68\ v_p$

$f(d_{SR}) = 8,390 + 616,40\ v_s$

Solve 0° and 90° first to get v_p and v_s

$v_p = 0,045$ m/s R = 8180)assume

$v_s = 0,008$ m/s R = 112)transitional

$f(d_{PR}) = 2,256$

$f(d_{SR}) = 13,097$

For $\theta = 30°$: Solve simultaneous equations:

$0,1 = ([\cos^2 30].2,256 + [\sin^2 30].13,097)\ v_x - ([\cos 30.\sin 30].10,841)\ v_y$

$0 = -([\cos 30.\sin 30].10,841)\ v_x + ([\sin^2 30].2,256 + [\cos^2 30].13,097)\ v_y$

ie $v_x = 0,035$ m/s or d = 42 mm

$v_y = 0,016$ m/s

For $\theta = 60°$ by similar calculation

$v_x = 0,017$ m/s or d = 13 mm

$v_y = 0,016$ m/s

The relative variation of flow velocity and effective particle diameter with increasing angle of inclination of the layers is illustrated in Fig 3.6. Note that for cases between parallel and series flow, there is flow in the y direction, ie the resultant velocity vector is not parallel to the gradient.

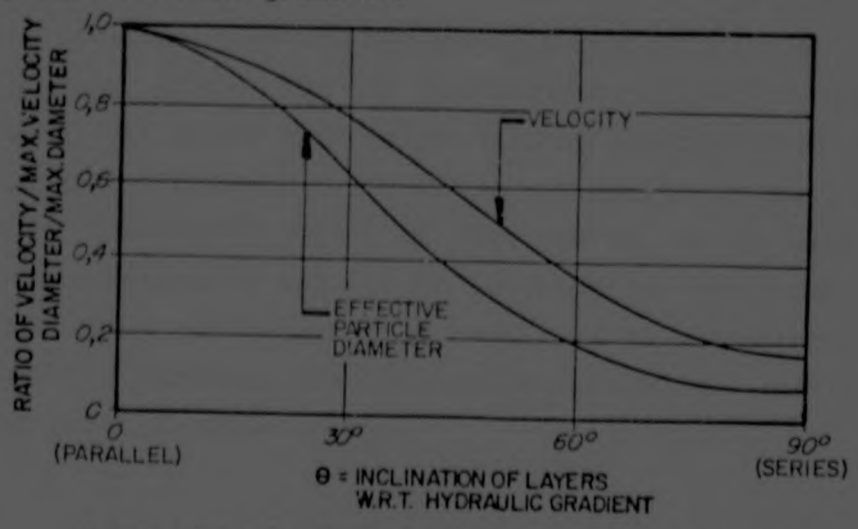


FIGURE 3.6 VARIATION OF FLOW VELOCITY AND EFFECTIVE PARTICLE DIAMETER WITH INCREASING θ (FROM CALCULATED EXAMPLE)

3.6.3 Randomly layered model

The models describing flow through stratified media may be considered to represent extreme cases in practice. Even if the material could be assumed to be stratified, the orientation of the layers with respect to the flow direction is not always constant.

A randomly layered model may be the way in which flow through material without stratification could be described. Random layering could be reproduced by means of randomly orientating the layers in time and space in a discretised model of the medium. It was shown in the example in Section 3.6.2 that the effect of altering the orientation of the stratification is to change the effective particle diameter as shown in Fig 3.6. Alternatively, the expected value or mean orientation may be used as a single value to be used in calculations.

The shape of the curve shown in Fig 3.6 depends on the grading of the material. Single sized materials will exhibit little variation in particle diameter with changing layer inclination. Large variations, probably best plotted on a logarithmic scale, can be expected with gap graded materials. No integration and only a small amount of manipulation is necessary to adopt this type of curve for use in Monte Carlo type sampling processes.

The inclination of the layers is a random variable with an equal probability of occurrence assigned to each value. It is for this reason that no integration of the curves in Figures 3.6 and 3.7 is necessary. In the case of a discretised model of the medium, a new random number between 0 and 1,0 is generated at each node or time step, multiplied by 90° and used to determine the particle diameter, and hence velocity, for that particular point in space or time.

Fig 3.7 illustrates a typical step of the sampling technique performed on one of the curves drawn from the example in Section 3.6.1.

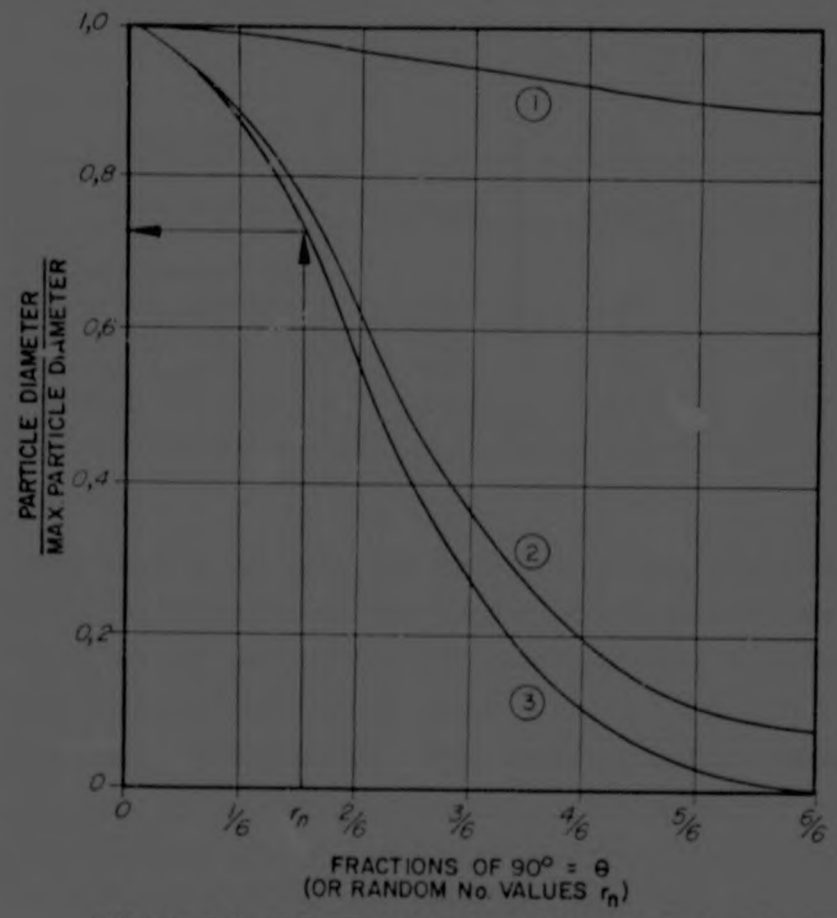


FIGURE 3.7 VARIATION OF EFFECTIVE PARTICLE DIAMETER WITH INCREASING θ FOR MATERIALS ①, ② & ③ USED IN MONTE CARLO SAMPLING TECHNIQUE

If the mean orientation of 45° is chosen to be representative of the entire sample, the effective particle diameters for the randomly layered model may be approximated by the values given in Table 3.4. The materials 1, 2 and 3 referred to are the same as those of the example in Section 3.6.1. The values are compared to the previously obtained values for the parallel, isotropic and series layer model under transitional flow conditions.

TABLE 3.4 : RESULTS OF SIMPLIFIED CALCULATION OF EFFECTIVE PARTICLE DIAMETER FOR THE RANDOM MODEL (mm)

Material	1	2	3
Description	Uniform	Graded	Gap Graded
Transitional flow			
Parallel layers	64	67	69
Isotropic d_{50}	60	50	60
Series layers	57	5,4	0,11
Random	60,5	25,0	20,0

Note that it is only for Material 1 that the effective particle diameter of the random model is approximately equal to the mean of the effective particle diameter for the parallel and series layer models. For the graded material (Material 2) the random model effective diameter is approximately equal to the geometric mean of the parallel and series layer effective diameters. It is for the gap graded material that the Monte Carlo technique is really necessary to determine the effective particle diameter for the random model.

4 DESIGN AND CONSTRUCTION OF EQUIPMENT

4.1 Introduction

The objective of the laboratory tests was to establish:

(i) the validity of the Forcheimer (or quadratic headloss) equation in the form given as $K = C_1/R + C_2$ (Chapter 2)

(ii) the validity of the layered media models (Chapter 3)

(iii) and what changes in permeability occur as a result of particle crushing and a decrease in the porosity of the medium

The ultimate aim of these tests was then to be able to provide practical means by which it may be possible to predict the throughflow characteristics of a gravel or rockfill medium subjected to a change in effective particle size and porosity.

It was recognised at an early stage that the flow and crushing tests would have to be performed on the rockfill in the same vessel. Disturbance of the sample could have caused segregation or layering and would in any event not be representative of the actual situation in which an initially uniform rockfill is crushed. Furthermore, valuable information on the ability of the rockfill matrix to retain the broken off particles and fragments would be lost. The major concern with gravel drains under large embankment loads is that the fragments migrate to downstream portions of the drains and then effectively clog the drain.

To do both the loading and flow tests, the testing apparatus would have to be a permeameter which could double as an oedometer. The rate of seepage in conventional oedometers is several orders lower than that through rockfill or gravels, so

that a "flooded" loading test would have been of little practical significance. In other words, it is impossible to calculate the permeability of a gravel or rockfill from a standard scaled up oedometer with any sensible degree of accuracy. It was decided, therefore, that flow studies would therefore not be made under load as this would have been difficult to set up in the laboratory. The rebound curve on unloading of gravels is sufficiently small to assume a negligible change in the degree of compression of the sample.

Therefore the sample, once the required load had been applied, was moved from the Heavy Structures Laboratory to conduct the hydraulic tests.

Research into the literature including test procedures set out in various standards revealed that the sample size for both the loading and flow test would have to be substantial. The sizing of the apparatus turned out to be an optimisation process of what was required (by extrapolation) from the standards and of available cylinders and presses. An upper limit on the size of the apparatus and sample was set by the criterion that the cylinder filled with rock would have to be able to be transported from the loading press in the Heavy Structures Laboratory to the sump in the Hydraulics Laboratory by means of the overhead gantry crane.

4.2 Design Criteria

4.2.1 General

The conflict in criteria for the apparatus used as a permeameter and oedometer is discussed in Section 4.4 which covers wall effects. The height to diameter ratio needs to be high for flow tests and low for loading tests. The available cylinders gave a height to diameter ratio ranging from 3 to 1,7 which falls within the

ratios of the plane strain equipment at the Rockfill Testing Facility of the university of California (Chan, 1969).

In compaction tests conducted by Wagener (1980) it was found that the maximum layer thickness for effective compaction is 300 mm. Although it is recognised that this figure pertains to different equipment and compaction methods, tests still have to be conducted to investigate whether there is a difference in the hydraulic properties of the material on samples loaded over a height of 1,0 m and 300 mm (i.e. height to diameter ratio of 1,7 and 0,5 respectively).

The dimensional and weight limitations for a practicable load and flow test apparatus were set by the winch of the largest hydraulic press in the University's Heavy Structures Laboratory and the capacity of 2 metric tonnes of the overhead gantry crane running to and from the adjacent Hydraulic Laboratory.

A system by which the gravel sample is suspended during the flow tests and supported during the loading tests had to be devised. Problems were foreseen with the manhandling of the equipment into position in the hydraulic press, which had to be addressed as a separate design exercise in itself.

4.2.2 Testing cylinder as loading cylinder

It was thought initially that some sort of provision would have to be made to lead at least a small quantity of water into the cylinder during the load tests if the full scale flow test cannot be done during loading. This would call for loading platens and supports designed in such a way that water could pass through

them. Because of the high drainage potential of the gravel, very insignificant changes in the loading characteristics of the material were anticipated for saturated tests so that the idea was eventually abandoned completely. If water had any lubricating effect in the rearrangement and compression of the rockfill or gravel it was considered adequate to wet the stone before the tests only.

The loading rig used would have to be able to apply fairly large loads to the sample, firstly because of the high stress range desired in the tests to simulate large embankments and secondly because of the large diameter of the sample to be stressed. Calculations revealed that the maximum load that could be applied to the sample would be of the order of 170 000 pounds (units used on the Macklow-Smith hydraulic press). In fact it turned out in the actual loading tests that the first signs of distress (bulging) of the cylinder started to occur at about 150 000 pounds. The tests were stopped at a maximum load of 160 000 pounds, which over the area of the stone is equivalent to a stress of 2,56 MPa. To perform tests at higher stresses and to reduce lateral deflection during loading, the present loading cylinder/permeameter will have to be stiffened.

4.2.3 Testing cylinder as permeameter

An immediate problem arising from the crushing tests was that piezometric readings could not be taken in the middle of the sample. Tappings would therefore have to be taken at the walls of the permeameter. The objective then was to compare the piezometer readings at a particular elevation within the sample with one test case which has the end positioned in the middle of the sample during the flow tests without any preload. From these

tests it was envisaged that a reasonable estimate of wall effects or the efficiency of the lining system could be made.

To obtain a wide range of hydraulic gradients the water was passed through the permeameter from bottom to top, cascading over the brim. The measurements required were differences in head, and therefore the entry and exit conditions were of little significance provided that the flow length within the sample and therefore between the piezometer points was a sufficient distance from the entrance and exit of the permeameter.

Because of the large diameter of the permeameter, full use of the Hydraulics Laboratory pumps had to be made to obtain flow rates of up to 30 l/s, thus covering all flow regimes. The higher flow rates made volumetric flow rate measurements impracticable at the time and it was therefore decided that a flow measuring device would have to be inserted in the delivery pipe. Modifications to the sump and the quick release valves would be required to make volumetric measurements of a pool disturbed intensely by the water cascading from the brim of the permeameter. The permeameter produced so much spray that an anti-splash screen had to be suspended around it to prevent the bottom half of the laboratory from becoming inundated.

4.3 Design and construction

4.3.1 Equipment required for flow tests

(i) Hydraulics laboratory

A flow circuit diagram of the equipment and facilities used in the flow tests is illustrated in Figure 4.1

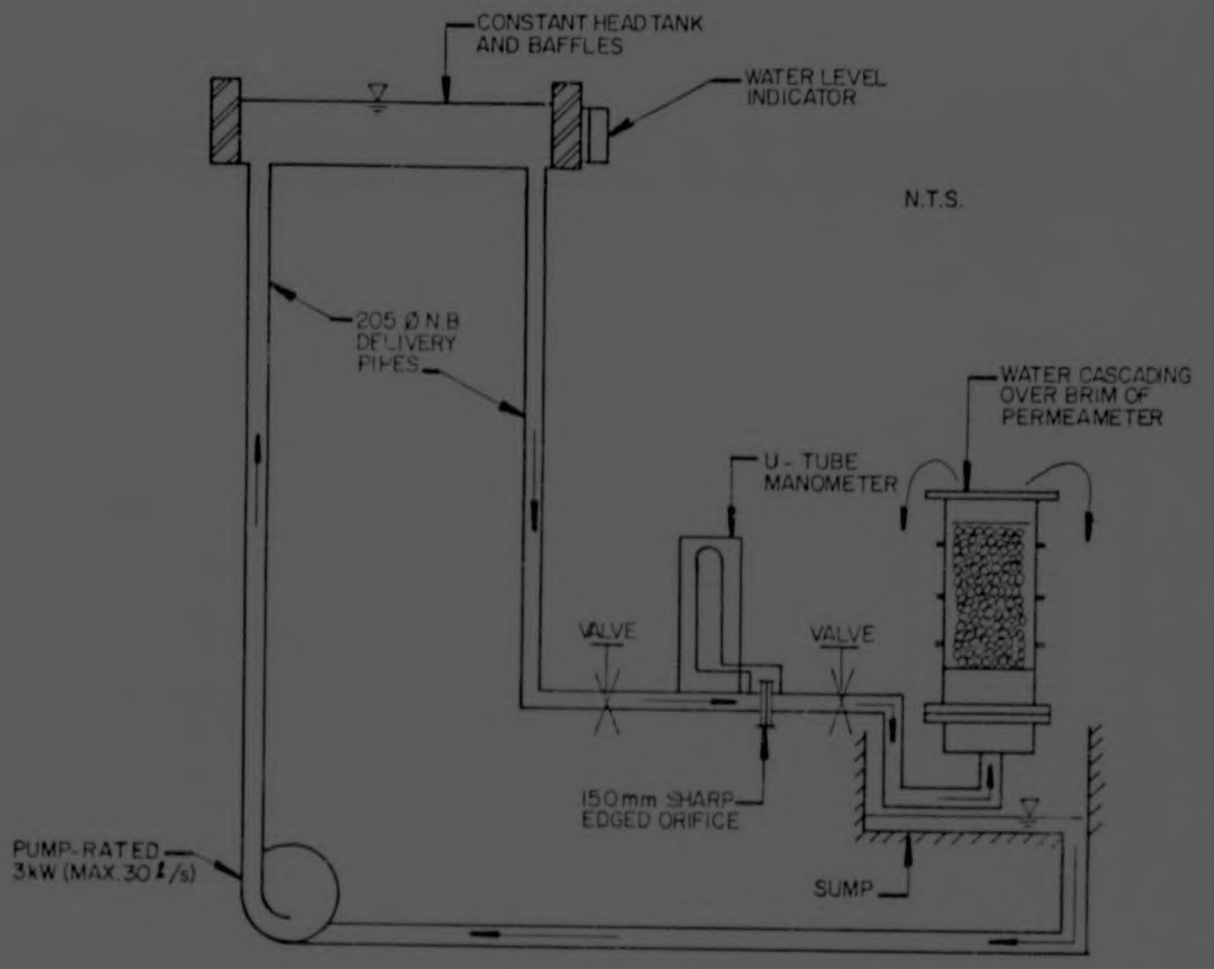


FIG 4.1 FLOW TEST CIRCUIT DIAGRAM

Access to the sump was provided by the overhead gantry crane. The delivery pipes to the permeameter were mounted on brick walls and connected to the equipment by means of a length of flexible pvc hosing. The flow rates were controlled by valves and monitored on a manometer taking readings on either side of a sharp edged orifice. The coefficient of discharge was obtained prior to the flow tests in calibration tests using volumetric flow rate measurements. The constant head tank with its baffles provided attenuation of any pump presssure surges and a constant static head. The level of the tank could be monitored by means of the dial level indicator outside the tank.

(ii) Permeameter

The permeameter consisting of cylinder plus base, lining, piezometer taps, delivery pipe and grid support for the sample is illustrated in Figure 4.2.

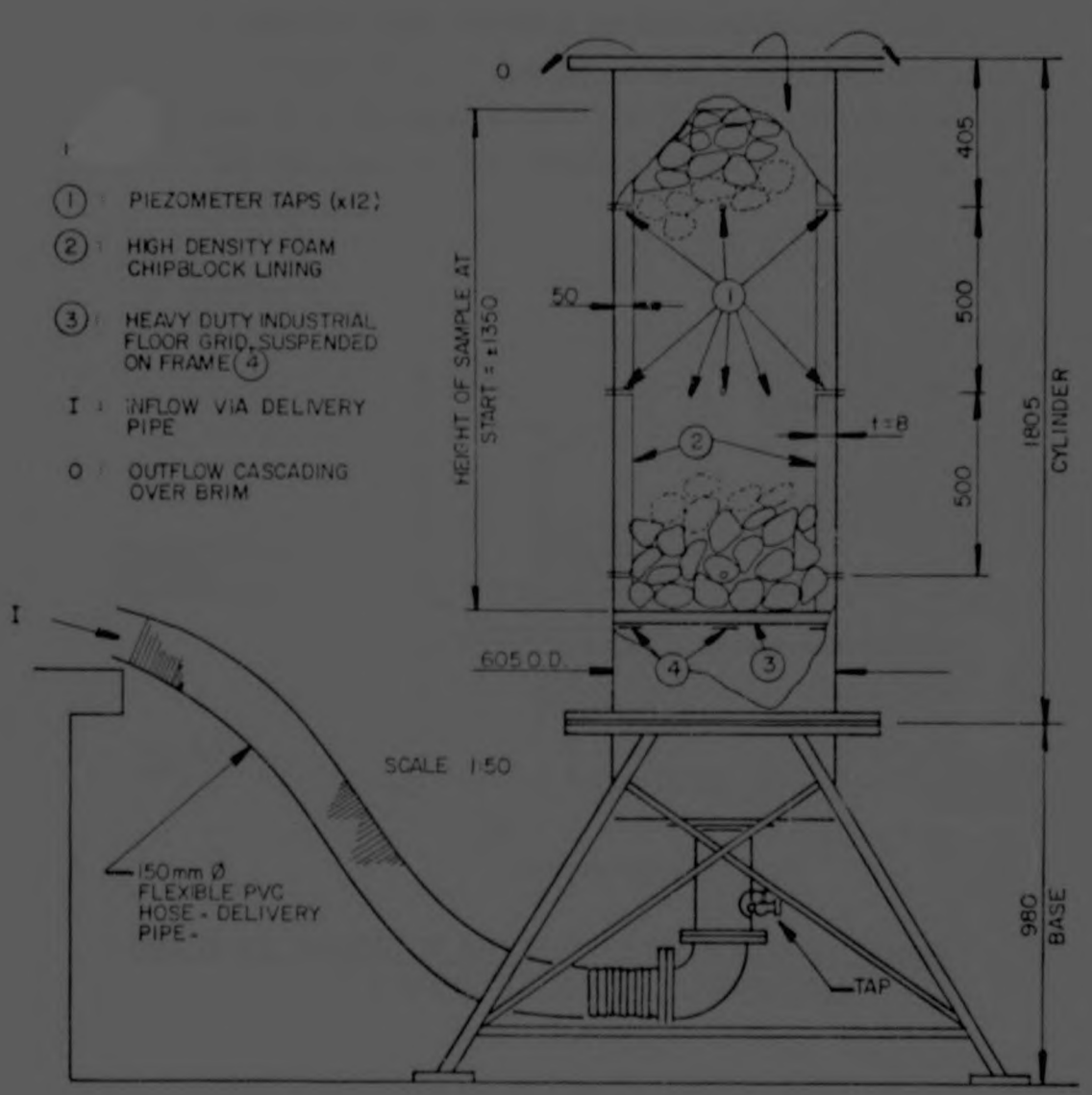


FIGURE 4.2 CYLINDER DURING FLOW TEST

The piezometer taps were specially turned and threaded to enable them to be screwed into the cylinder wall. Standard wall tap fittings were

either too long or had a thread with too long a pitch. During the load tests the portions of the taps protruding into the cylinder caused the taps to be either damaged or blocked. To remedy this, 8 mm thick plates should be welded onto the cylinder wall at the piezometer points and the piezometer taps attached to the cylinder as shown in Figure 4.3. The advantage here is that, should a blockage occur, the tap can be removed and replaced or the blockage freed and the tap reinserted.

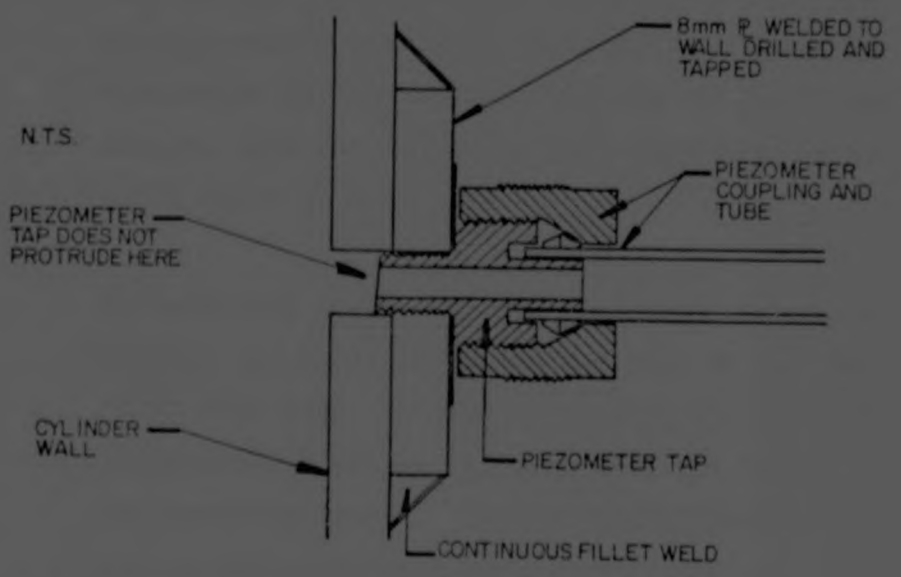


FIGURE 4.3 SUGGESTED ALTERNATIVE METHOD OF ATTACHING PIEZOMETER TAP TO CYLINDER WALL

In the initial tests pvc tubing was attached to the inside of the piezometer tap at one of the stations at each of the three heights. This

tubing was led to the centre of the specimen to enable a comparison between central and "wall" (ie. at the inside of the lining) readings to be made. The effectiveness of the lining as a measure against wall effects could therefore be evaluated.

(iii) Piezometer bank

Four piezometer taps were installed diagonally opposite each other on the cylinder in three groups at a vertical spacing of 500 mm between each group. By having the facility of four piezometer readings at each elevation a qualitative assessment of the fluctuations due to localised effects such as tortuosity and secondary turbulence could be made.

The mounting board for the piezometer tubes was plumbed and then clamped to the side of the constant head tank. In some flow tests the range in piezometric heads was greater than the length of the mounting board. Therefore the board would have to be raised at higher flow rates.

A plexiglass rule fitted to the board in a groove parallel to the tubes was used to read off the water levels in the tubes arranged in two groups of six on either side of a measuring tape, as shown in Figure 4.4. A large syringe (200 ml) was used to draw out air bubbles in the piezometer tubes before any readings were taken.

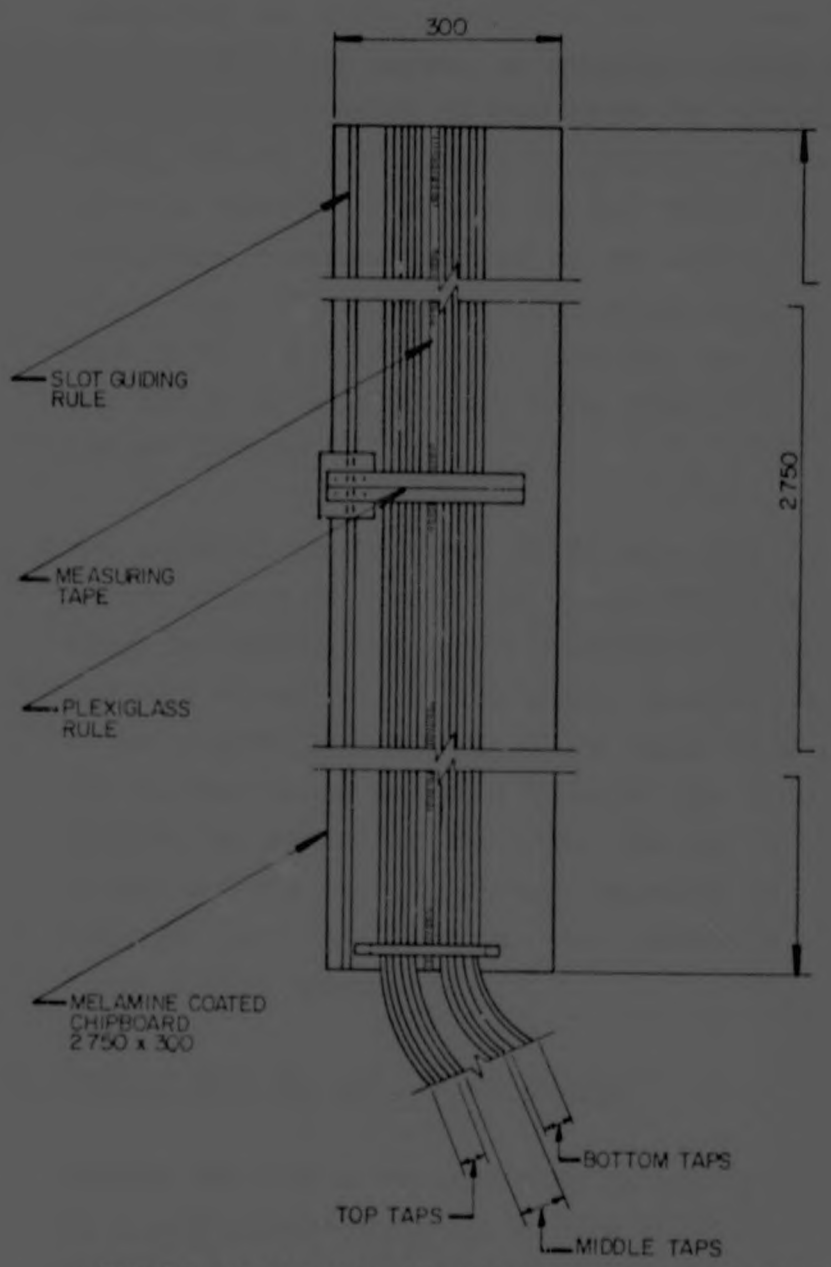


FIGURE 4.4. PIEZOMETER TUBES ON MOUNTING BOARD

4.3.2 Equipment required for loading tests

(i) Heavy structures laboratory

Because of the large size of the cylinder and the necessity to apply large loads to the specimen to obtain the required stresses to simulate conditions under large embankments, the largest hydraulic press available in the Heavy Structures

Laboratory was used. The press, manufactured by Macklow Smith, is capable of applying a force of 170 000 pounds, which is equivalent to approximately 750 kN, onto a specimen between a hydraulic ram housed in a sump in the floor and a stationary crosshead mounted on two 150 mm diameter ties. The amount of deformation in a load test is virtually unlimited. However, the specimen has to be unloaded while the cross head and ram are lowered.

The overhead gantry crane which runs along the entire length of the ground floor laboratories from the hydraulics to the structures sections was used extensively. This crane, together with a chain block suspended from the cross head of the Macklow Smith, was used to hoist the testing cylinder in and out of the press. The use of the cranes and the special harness attached to the cylinder for this purpose are described in Figure C.7 of Appendix C.

(ii) Testing cylinder and loading plates

Because the sample was suspended in the cylinder on a grid approximately 300 mm from the bottom it was found preferable to construct a pedestal through which the load is applied to the sample, rather than reinforce or support the grid by means of vertical plates. The loading plate and pedestal in the cylinder during a load test are illustrated in Figure 4.5.

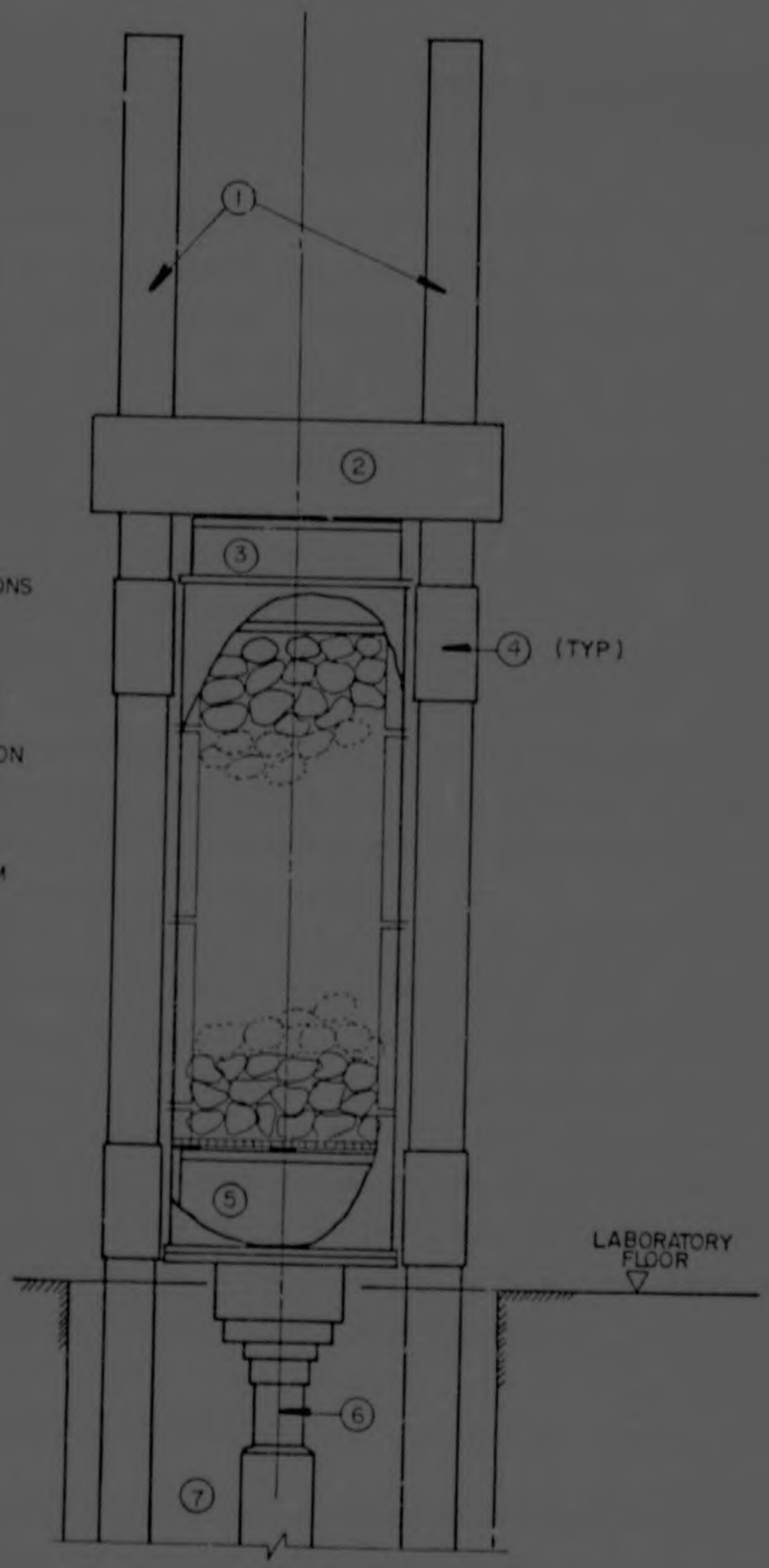


FIGURE 45 CYLINDER DURING LOAD TEST

4.4 Cylinder wall effects

4.4.1 Introduction

As it was anticipated that the loading and flow tests would be performed in the same testing cylinder with as little disturbance as possible, a literature search on the wall effects of both permeameters and large scale oedometers was undertaken. In standard soil mechanics tests for either permeability or compressibility, the dimensions of the testing device are chosen in such a way that end or edge effects are minimised. It became immediately apparent that the permeameter-oedometer would have to comply with conflicting requirements. To reduce entrance and exit effects in flow tests, the testing cylinder should be slender (ie low diameter to height ratio). To reduce the wall effects in loading and flow tests, the testing cylinder should be squat (ie high diameter to height ratio).

In addition to the dilemma presented above peculiar problems associated with testing of rockfills were reported on by Dudgeon (1967) and Marsal (1973). Dudgeon performed extensive tests with the purpose of determining the magnitude and extent of wall effects in permeameters. In tests to determine the plane strain characteristics of rockfill Marsal used several types of antifriction linings in the specimen mould.

4.4.2 Hydraulic considerations

The velocity distribution across an unlined permeameter was shown to vary as illustrated in Fig 2.15 in tests conducted by Dudgeon (1967). This causes the measured mean flow velocity in such a case to differ from that which would occur in an infinite medium under the same hydraulic gradient.

4.4 Cylinder wall effects

4.4.1 Introduction

As it was anticipated that the loading and flow tests would be performed in the same testing cylinder with as little disturbance as possible, a literature search on the wall effects of both permeameters and large scale oedometers was undertaken. In standard soil mechanics tests for either permeability or compressibility, the dimensions of the testing device are chosen in such a way that end or edge effects are minimised. It became immediately apparent that the permeameter-oedometer would have to comply with conflicting requirements. To reduce entrance and exit effects in flow tests, the testing cylinder should be slender (ie low diameter to height ratio). To reduce the wall effects in loading and flow tests, the testing cylinder should be squat (ie high diameter to height ratio).

In addition to the dilemma presented above peculiar problems associated with testing of rockfills were reported on by Dudgeon (1967) and Marsal (1973). Dudgeon performed extensive tests with the purpose of determining the magnitude and extent of wall effects in permeameters. In tests to determine the plane strain characteristics of rockfill Marsal used several types of antifriction linings in the specimen mould.

4.4.2 Hydraulic considerations

The velocity distribution across an unlined permeameter was shown to vary as illustrated in Fig 2.15 in tests conducted by Dudgeon (1967). This causes the measured mean flow velocity in such a case to differ from that which would occur in an infinite medium under the same hydraulic gradient.

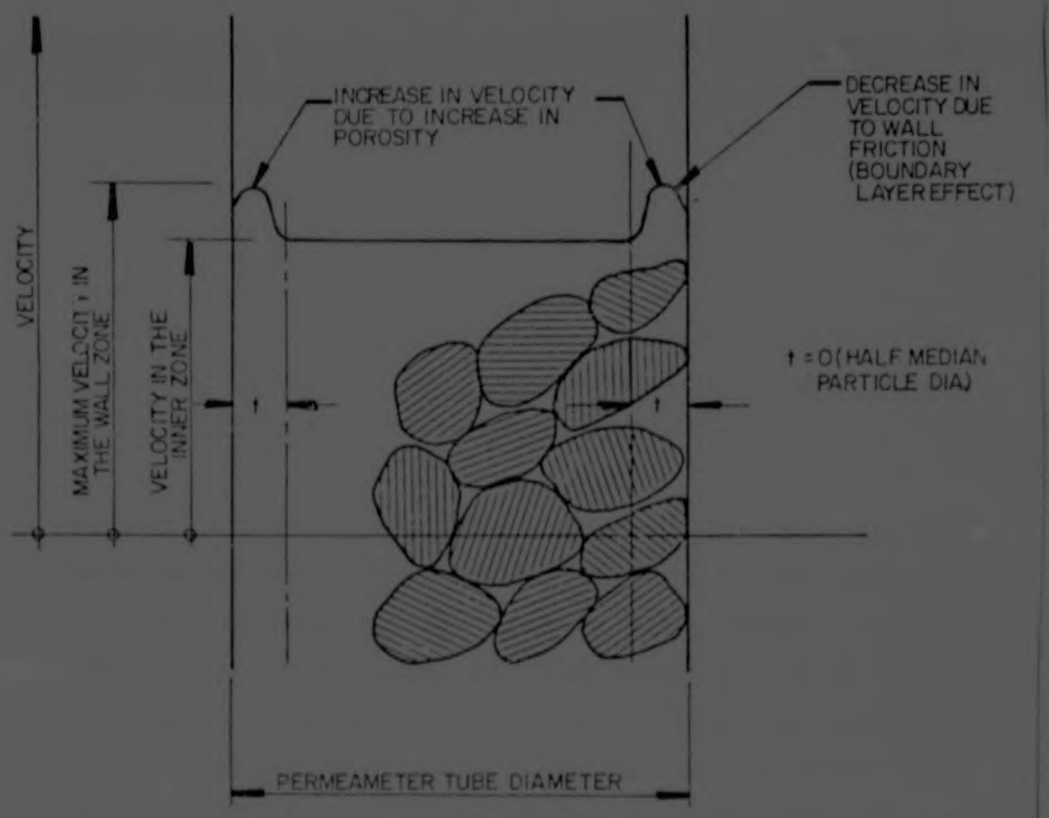


FIGURE 4.5 VELOCITY DISTRIBUTION ACROSS AN UNLINED PERMEAMETER (AFTER DUDGEON, 1967)

Porosity determinations by Dudgeon indicated that there is a zone of increased porosity near the walls of unlined permeameters in which gravels or rockfills are tested. By placing piezometer tubes at various distances from the outside wall of the permeameter, it was established that the extent of the zone of increased porosity is of the order of half a median particle diameter. Since velocity is dependent on porosity, a much higher than average flow rate occurs in this zone.

An equation yielding the ratio of mean velocity through the total area to the inner zone velocity was derived. This was done to establish the order of magnitude of measurement errors if piezometer readings were to be

taken from wall tappings only. For the transitional regime the ratio v_m/v_i was calculated by Dudgeon to be $\pm$ 1,06, where

v_m = mean velocity through the total area
v_i = velocity in the inner zone

This error turns out to be relatively small because the localised nature of the increase in porosity when viewed in relation to the entire cross section.

However, if the piezometer tappings are made in the permeameter wall, the localised effect of the increase in velocity takes on far greater significance. If no liner were to be used in flow tests of 16 mm (d_{50}) stone in a permeameter of diameter 572 mm, the ratio of velocity in the wall zone v_w to that in the inner zone v_i will be of the order of 2, (see Appendix A for calculations).

It was anticipated that difficulties would arise in the experiments if it were necessary to take pressure readings from the inner zone of the permeameter. Since the sample would be subjected to substantial loads, pressure readings at the central axis of the permeameter would have possibly been unreliable, regardless of the material of which the tubing was made. Reliable results may have been obtained from wall tappings in an unlined permeameter if the material were graded to a greater extent, ie the voids near the walls may have been filled with fines.

Recognising that the last was only half a solution in that it applied to special cases only, it was decided at that stage that the permeameter should be lined with

some suitable material. The effect of the liner would be to fill the voids in the wall zone, with the result that

- the area open to flow would be homogeneously packed, and

- pressure readings could be taken from tappings at the wall of the permeameter, thus obviating the abovementioned problems.

From the above considerations the minimum thickness of liner required was deduced to be half the median particle diameter of the largest particle size of the sample tested.

4.4.3 Mechanical considerations

The overall stress distribution across the cylinder when the gravel or rockfill is loaded is not uniform. Wall friction does not allow a true plane strain situation to develop (Marsal, 1973). From studies of oedometer tests on materials consisting of various sized particles, Lee (1969) concluded that if the diameter of the oedometer is more than 5 times the diameter of the largest particles, wall effects are negligible.

Opinions on the correct height to diameter ratio of the sample were also found to vary, because of edge effects and the maximum depth to which effective compression takes place. In the Rockfill Testing Facility of the University of California the plane strain equipment handles specimens where the height to width ratio ranges from 2,5 to 1,1 (Chan, 1969). Equipment developed by Marsal (1973) and Lee (1969) has a height to diameter ratio of 0,6 and 1,0 respectively.

Particle breakage will be reduced at the walls of unlined testing cylinders because of the reduction in the degree of particle packing near the walls of the cylinder. The result of this must be seen not only as distorting the overall particle breakage pattern but also in conjunction with the previously mentioned flow characteistics. No quantitative description (as in Dudgeon (1967) for flow tests) of wall effects under load has been found. It should be noted too that even with the standard A.C.V. (Aggregate Crushing Value) test (B.S.812) wall effects are not taken into account.

4.4.4 Possible solutions

The four criteria for the choice of a suitable lining material to overcome cylinder wall effects were recognised to be:

- Compatibility between hydraulic and mechanical considerations
- Effectiveness over half the median particle diameter
- Either durable or easily replaceable
- It must have a constant thickness

Cementing stones onto the inner surface of the cylinder would have been a suitable solution for overcoming the hydraulic edge effects. But once the specimen were to be loaded, the rough lining would have instigated excessive particle breakage at the walls, since the interlocking stones would be unable to move.

A rubber lining would have been suitable to overcome wall effects during loading, but would not have been

Particle breakage will be reduced at the walls of unlined testing cylinders because of the reduction in the degree of particle packing near the walls of the cylinder. The result of this must be seen not only as distorting the overall particle breakage pattern but also in conjunction with the previously mentioned flow characteistics. No quantitative description (as in Dudgeon (1967) for flow tests) of wall effects under load has been found. It should be noted too that even with the standard A.C.V. (Aggregate Crushing Value) test (B.S.812) wall effects are not taken into account.

4.4.4 Possible solutions

The four criteria for the choice of a suitable lining material to overcome cylinder wall effects were recognised to be:

- Compatibility between hydraulic and mechanical considerations
- Effectiveness over half the median particle diameter
- Either durable or easily replaceable
- It must have a constant thickness

Cementing stones onto the inner surface of the cylinder would have been a suitable solution for overcoming the hydraulic edge effects. But once the specimen were to be loaded, the rough lining would have instigated excessive particle breakage at the walls, since the interlocking stones would be unable to move.

A rubber lining would have been suitable to overcome wall effects during loading, but would not have been

penetrated sufficiently by the stones in order to overcome the hydraulic edge effects.

Marsal (1973) described the use of a sand layer which separates the specimen from the wall. The advantage of this method of lining is that the material is adequately restrained within the cylinder. The disadvantages are that specimen preparation would be cumbersome and time consuming and that the sand could be washed out during the flow tests unless contained in a membrane, which in turn is prone to puncturing.

The material eventually used in the flow and loading tests was a high density foam, which performed satisfactorily with regard to the abovementioned criteria.

5 EXPERIMENTAL PROCEDURE

5.1 Introduction

Since the emphasis in this investigational project had shifted largely to the development of the testing apparatus described in Chapter 4, the scope of the originally envisaged testing programme had reduced considerably. The tests in this project were performed on a single sample and may thus be described as prototype runs of a more extensive testing programme in which the objectives are more material (rather than equipment development) orientated. The experimental procedure may vary according to future requirements, but was executed in the way described here to demonstrate the feasibility of the testing apparatus as a means of determining the effects of heavy loads on the throughflow characteristics of rockfills and gravels. Many trial and "dry" runs were undertaken to test various aspects and components of the equipment, at which stage final modifications and adjustments were made before the proper testing was begun.

It was necessary to describe the material fully, so that later comparisons with other materials may be meaningful. Wherever possible, standard measures or tests were applied, so that the descriptions, although not fully applicable to the given problem, were at least accurate and not only qualitative. A further application of the standard tests or indices is their inclusion in specifications for construction and quality assurance.

The objectives of the tests performed may therefore be listed as:

(i) Examine the feasibility of the newly developed equipment for the determiniation of the effects of heavy loads on the through flow characteristics of rocks and gravels.

(ii) If the equipment works, determine which mathematical model best describes the flow conditions in rockfill and gravels.

(iii) Determine which physical characteristics of gravels and rockfills have a significant effect on their permeability under various loads.

5.2 Sample preparation

The sample used for the tests was drawn from approximately 1 tonne (metric) of -150 mm rockfill. The entire batch of rockfill was graded by means of a gauge, since sieves with openings greater than 50 mm are not easily obtained and difficult to use. The rock was obtained from a commerical quarry mining Halfway House Granites, with the physical properties listed in in Table 5.1. The test sample was composed of cobbles less than 150 mm and greater than 75 mm in diameter. "Diameter" is defined here as being the largest dimension on the smallest cross sectional area (see Figure 2.4) This dimension is the one which would control the passage through a screen if shaken for a long time. Besides the standard particle size analysis, the flakiness index was determined.

TABLE 5.1 : PHYSICAL PROPERTIES OF ROCKFILL TESTED

PROPERTY	Published value (Hippo quarries)	Measured value(s)
. Relative density	2,64	2,62 - 2,66
. Bulk unit weight-coarse (kN/m3)	12,9	13,0 - 14,4
. Texture (grain size)	coarse	coarse
. Aggregate crushing value	22,7	-
. 10 % Fact value (kN)	136	-
. % Silica content	72	-
. Flakiness index (%) (Before crushing tests)	-	37,2

To obtain a random distribution of differently sized particles the stone was mixed in manageable batches in drums and then tipped into the foam lined cylinder.

5.3 Calibration of measuring instruments

The 4 000 pound spring balance used for the preparation of the sample was calibrated in the tension test rig against standard weights.

The 150 mm diameter sharp edged orifice used for flow measurements was calibrated at various flow rates for various fluids in the U-tube manometer. By means of linear least squares regression analysis an expresssion converting difference in manometer height to flow rate was derived.

The calibration of the spring balance and orifice is described in detail in Appendix D.

5.4 Flow tests

The testing cylinder was hoisted into the sump at the end of the hydraulics laboratory and bolted onto the base. Water tightness between the base and cylinder was ensured by a rubber gasket. The piezometer tubes were then fastened onto the taps on the wall of the cylinder.

Below the sump the pump was then primed and started, then switched from star to delta configuration. The valves on the delivery pipes were then opened, the upstream one fully, the lower as required.

Once the flow through the system was established, the manometer taps were opened (otherwise the mercury or measuring fluid will disappear in the system).

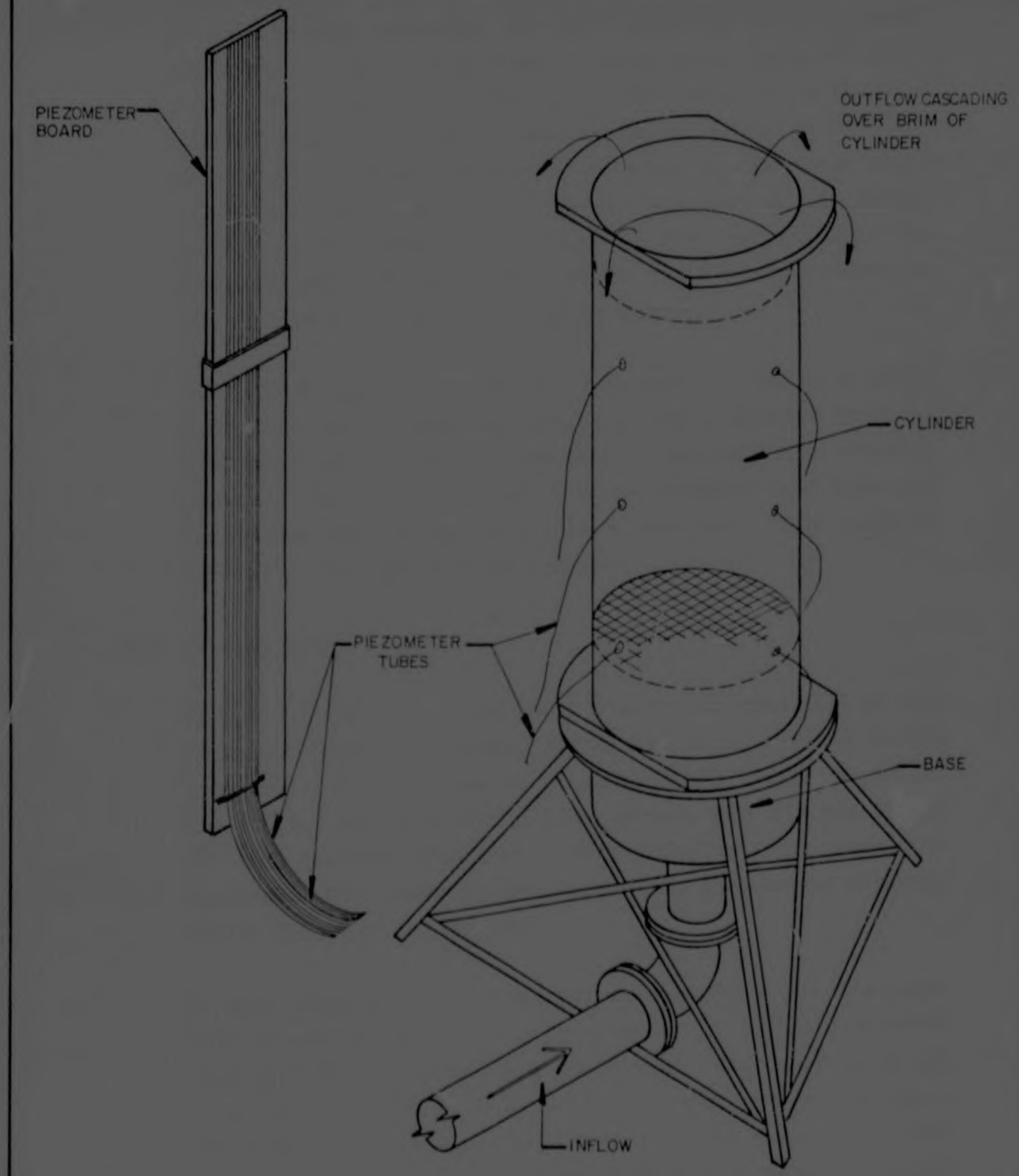


FIGURE 5.1 FLOW TEST SET-UP

Before any piezometer readings could be taken the piezometer tubes had to be de-aired. Because surface tension effects have a considerable influence on the tubes of 6 mm internal diameter, the de-airing process had to be done slowly and carefully. The de-airing was done by sucking the water in the piezometer tubes into a large capacity syringe until no more air bubbles were visible. Once this was achieved, the water level in the tube would have to be slowly restored to its static level. If the level were allowed to drop too quickly, the abovementioned surface tension effects would become evident in the air bubbles trapped in the water column.

The control valve in the delivery pipe was then set to a particular flow rate. Then the manometer and piezometer readings were taken for the various flow rates. Care had to be taken in observing that the flow rate from the constant head tank was not greater than the delivery rate to the tank. This could be checked on the dial level indicator.

5.5 Loading tests

Before the cylinder could be hoisted into position in the hydraulic press, the loading plates had to be attached to the apparatus. This was done by placing the top plates on top of the sample, attaching the lifting harness onto the top flange of the cylinder and then lifting the cylinder over the pedestal. Once lowered, the pedestal was then bolted onto the bottom flange of the cylinder.

A chain block of 2 tonne capacity was suspended from the cross head of the testing machine by means of a specially designed link made of flat steel bars and dowels. The cross head was then raised to its maximum height and the hook of the chain block attached to the second link on the lifting harness on the testing cylinder. A steel dowel used as a locating pin which matched hole in the centre of the pedestal was inserted into the centre hole below the cross head of the machine.

The cylinder assemblage was then lifted by the overhead gantry crane. When hoisted several centimetres above the ground, the chain block was used to draw the cylinder nearer to the machine. Once sufficient tension had been applied by the chain block, the tension from the overhead gantry crane was released. The cylinder was then suspended directly above the centre mark and set down onto the loading platen of the ram. The sequence of positioning (and removing, if looked at in reverse) of the cylinder is illustrated in Figure C.7 of Appendix C. Figure 5.2 shows the cylinder being lifted by both the chain block and the overhead gantry crane. To remove the cylinder from the press after the tests were complete the procedure described above was reversed.

Before the actual loading tests could begin, the crosshead had to be lowered onto the top loading plate, and the dial deflection gauges which stood on the floor next to the lower loading platen were zeroed. The Macklow Smith testing machine works on the principle of applying a constant rate of deformation until the load reaches a certain set value upon which the movement of the ram is either halted or the counterbalance moved out further and more load is applied. When this occurs a switch is tripped and this was used in the present tests as the signal that the desired load increment had been achieved. When this was done, the dial deflection gauges were read and the following load increment was subsequently added.

Substantial stress relief took place at times when larger particles began to break up and rearrange themselves. It then took quite a bit of deformation to produce an increase in the load applied to the specimen.

The amount of deformation in the last loading test was of such magnitude that the top loading plate was pushed into the cylinder and the sample had to be unloaded to insert spacers

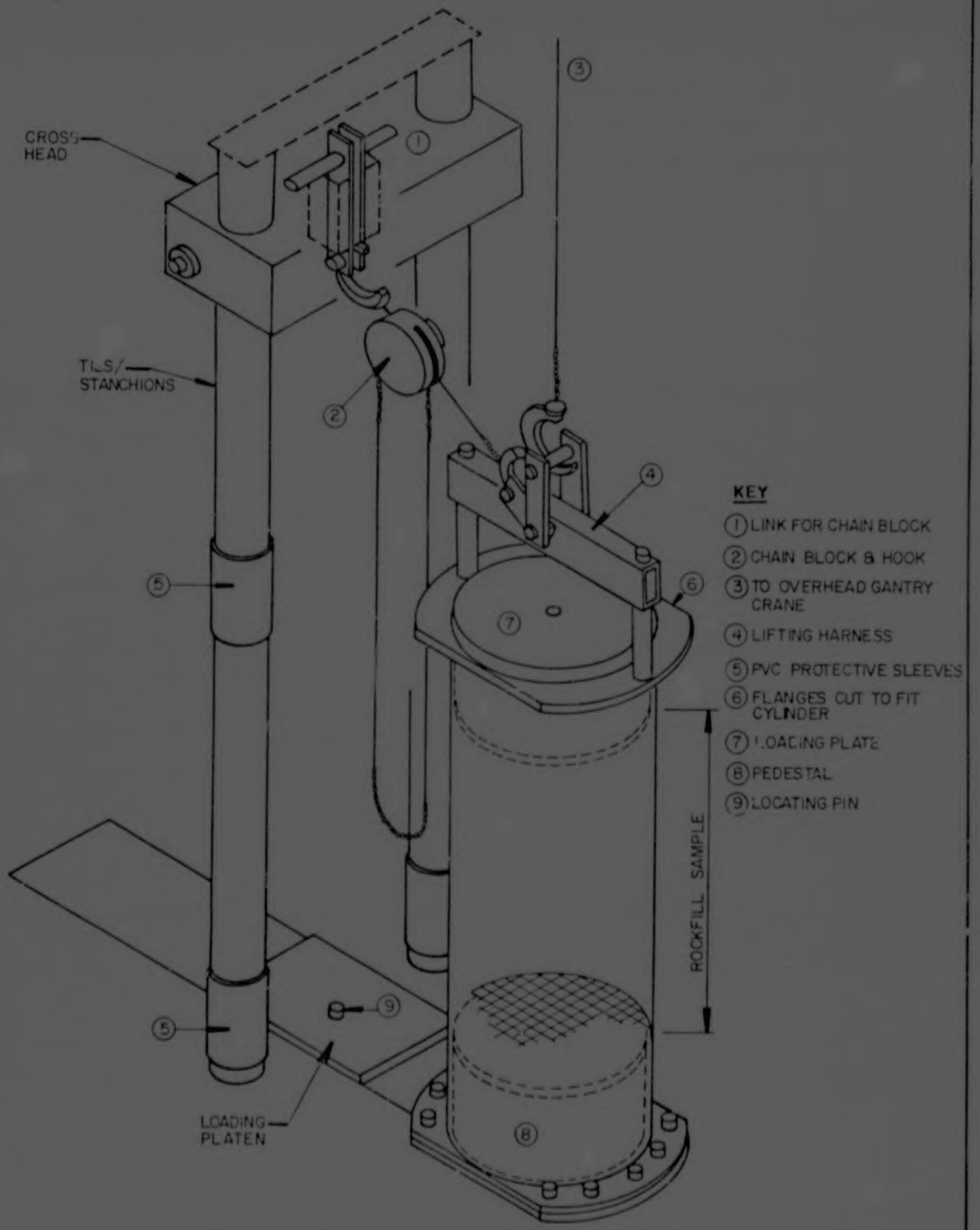


FIGURE 5.2 MANOEUVERING CYLINDER IN AND OUT OF PRESS

between the cross head and loading plate before further load (and hence deformation) could be applied.

The amount of rebound and hence the validity of the use of the permeameter in an unloaded condition was determined in the second load test. The load test set-up is illustrated in Figure 5.3.

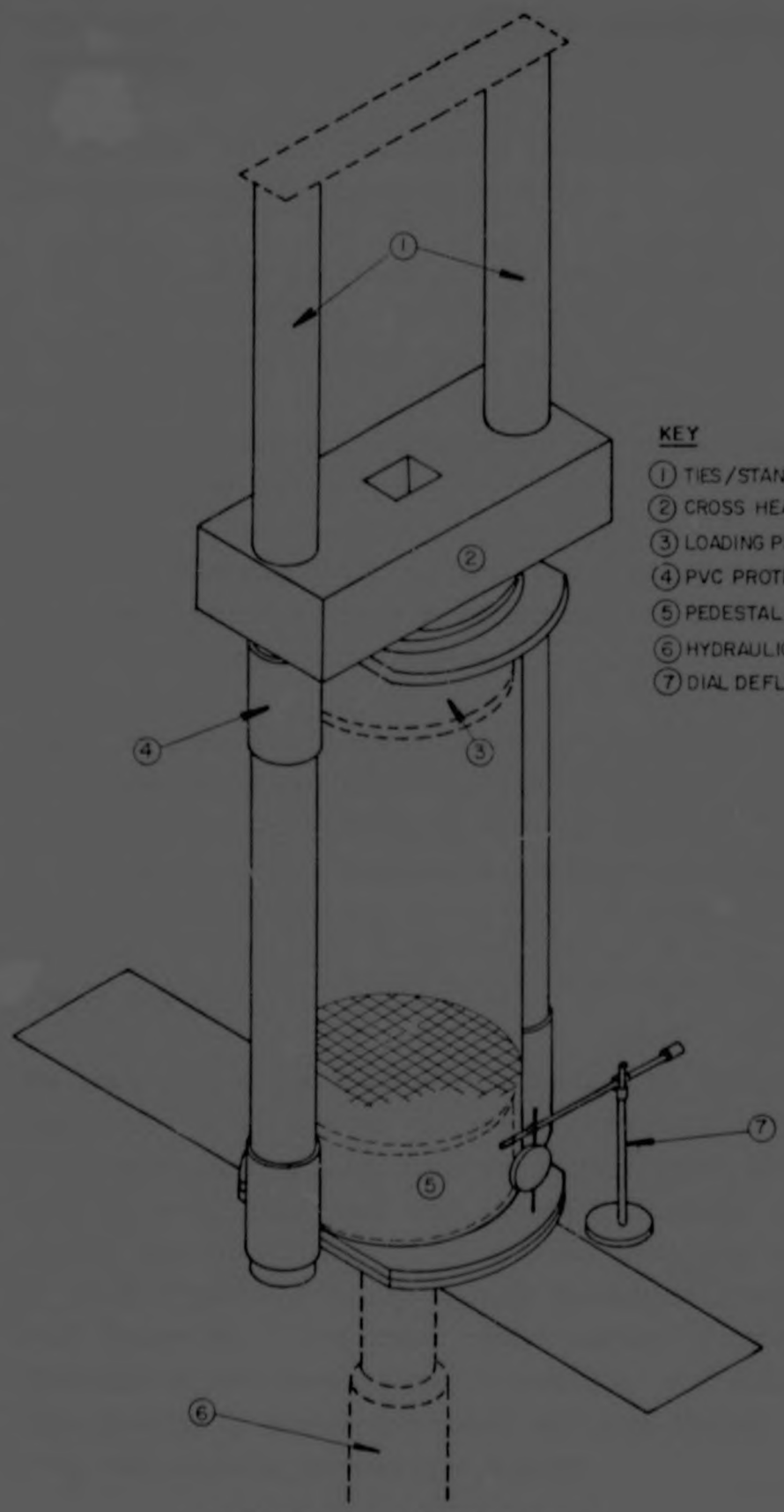


FIGURE 5.3 LOAD TEST SET-UP

6 TEST RESULTS

6.1 Introduction

In reporting on the test results reference is made again to the objectives of the tests. These were:

(i) To examine the feasibility of the equipment as a means for determining the throughflow characteristics of gravels and rockfills under load.

(ii) To determine which mathematical models best describe the flow and loading processes.

(iii) To determine which physical characteristics of gravels and rockfills have a significant effect on their permeability under various loads.

(iv) To provide a means by which it is possible to predict the reduction in permeability of a rockfill or gravel that had been subjected to large overburden stresses, resulting in a decrease in porosity and degradation of the particles.

6.2 Sample properties

The sample properties are listed in Table 6.1. The rock can be described as an angular to cubical coarsely crystalline, unweathered, hard granite from the Halfway House Series. It must be noted here tha' the standard flakiness index was applied here out of context, so that the relatively high value of 37,2% belies the fairly angular to cubical nature of the rock fragments. Comparison with standard descriptors is difficult in any event, since the particle size analysis was done manually by passing individual particles through a gauge - a far more exacting process than sieving.

TABLE 6.1 : SAMPLE DESCRIPTION

Property	Value/desciption
. Sample weight	411 kg
. Grading before and after loading tests	See figure 6.1
. Relative density	2,62 - 2,66
. Bulk unit weight (uncompacted)	13,0 - 14,4 kN/m^3
. Surface texture	Coarsely crystalline
. Particle shape	Angular to cubical
. Weathering	Unweathered
. Silica content	72%*
. Aggregate crushing value	22,7*
. 10% FACT value	136 kN*
. Flakiness index (before crushing)	37,2%

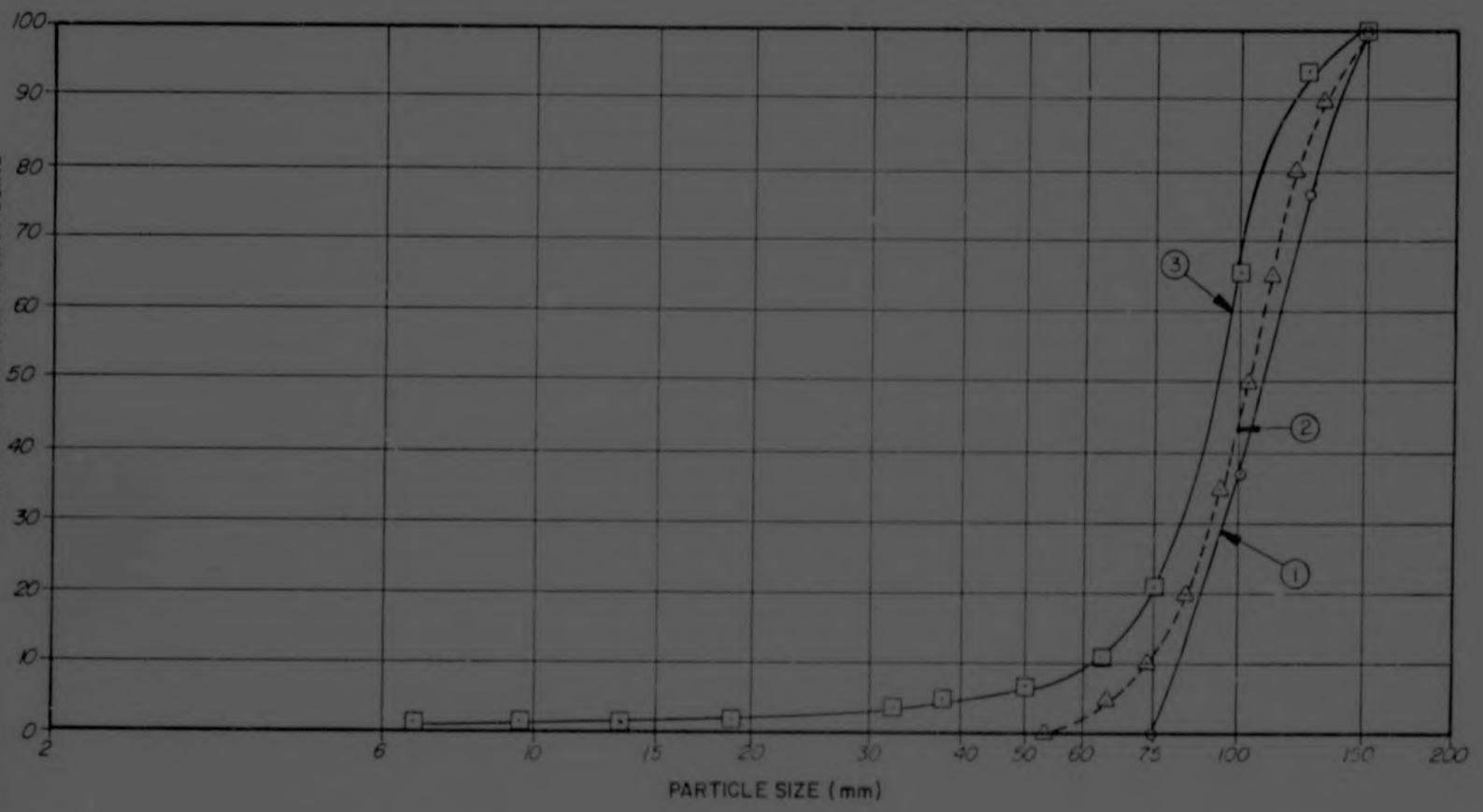
* Published values (Hippo Quarries Ltd)

6.3 Particle size analyses

A uniformly sized sample was chosen for the initial sample so as to get a substantial amount of particle breakage in the loading tets. With the degradation of the original material, an opportunity to test the flow models describing layered media presented itself. The effective particle diameter decreased substantially after the load tests. The grading curves before and after the load tests are shown in Fig 6.1. The change in effective particle diameter due to loading can be seen from Table 6.2 and Figs 6.2a and 6.2b.

TABLE 6.2 : EFFECTIVE PARTICLE DIAMETERS OF CRUSHED MATERIAL (mm)

		Parallel layer model			Series layer model		
Test No	Load applied (kPa)	Laminar	Transi-tional	Turbulent	Laminar	Transi-tional	Turbulent
1	0	98,48	95,63	95,65	91,14	91,21	92,88
2	667	99,06	95,67	95,69	89,07	89,19	91,86
3	3 556	82,72	76,60	77,19	40,17	40,46	62,15



KEY

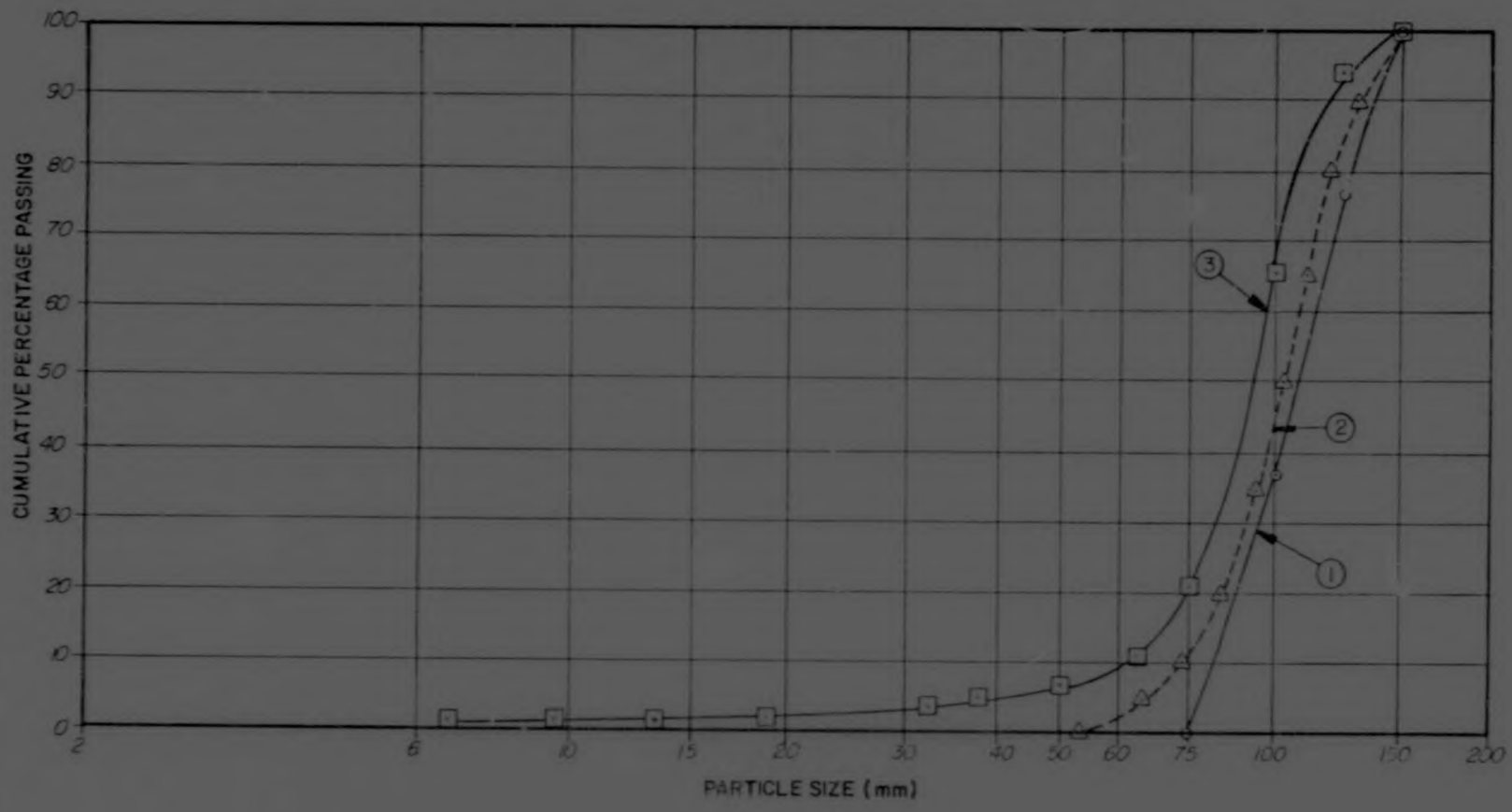
① GRADING BEFORE TESTS

② GRADING AFTER LOAD OF 667 kN/m^2 (ESTIMATE, SEE NOTE (1))

③ GRADING AFTER LOAD OF 3 556kN/m^2

(1) NOTE: ESTIMATE OF GRADING CURVE BASED ON EQUATION (2.30)

FIGURE 6.1 GRADING CURVES OF SAMPLE BEFORE AND AFTER LOADING



KEY

① GRADING BEFORE TESTS

② GRADING AFTER LOAD OF 667 kN/m^2 (ESTIMATE, SEE NOTE (1))

③ GRADING AFTER LOAD OF 3.556kN/m^2

(1)NOTE: ESTIMATE OF GRADING CURVE BASED ON EQUATION (2.30)

FIGURE 6.1 GRADING CURVES OF SAMPLE BEFORE AND AFTER LOADING

Author Rumpelt T K
Name of thesis Performance of filter drains under large embankment loads 1983

PUBLISHER:
University of the Witwatersrand, Johannesburg
©2013

LEGAL NOTICES:

Copyright Notice: All materials on the University of the Witwatersrand, Johannesburg Library website are protected by South African copyright law and may not be distributed, transmitted, displayed, or otherwise published in any format, without the prior written permission of the copyright owner.

Disclaimer and Terms of Use: Provided that you maintain all copyright and other notices contained therein, you may download material (one machine readable copy and one print copy per page) for your personal and/or educational non-commercial use only.

The University of the Witwatersrand, Johannesburg, is not responsible for any errors or omissions and excludes any and all liability for any errors in or omissions from the information on the Library website.